Norwegian University of Life Sciences
Faculty of Environmental Science and Technology
Department of Mathematical Sciences and Technology

Master Thesis 2016
30 credits

Analysis of discrepancies between simulated and actual energy production for a photovoltaic system in Norway

Ulrik Vieth Rør

Preface and Acknowledgments

This study is a master thesis in solar energy at the Norwegian University of Life Sciences as part of an engineering degree in Energy and Environmental Physics. The thesis originates from an initiative from Dr. Bjørn Thorud, senior counselor in Multiconsult. The study was conducted to investigate and analyze possible discrepancies between simulated energy with the software PVsyst, and produced energy for a photovoltaic (PV) system in south-eastern Norway. The PV system is a 375 kWp, and located at the roof of ASKO Øst in Akershus county, Norway. The study was carried out during the spring semester 2016.

There are a lot of people to whom I must show my gratitude for being able to conduct and complete this thesis. First of all I want to thank my two supervisors Dr. Espen Olsen and Dr. Bjørn Thorud. Bjørn Thorud helped me form the ideas on which this thesis is built, and Espen Olsen for enthusiastic guidance and motivation throughout the semester. I must also give my greatest appreciation and thanks to Stanislas Merlet for excellent and invaluable help with the simulation software PVsyst. Their knowledge and valuable advices have been much appreciated.

Furthermore I would like to thank Thor Christian TUV from FUSen for vital help and information about the PV system at ASKO. I would also like to thank Marius Brenden og Øystein Ruud-Hansen in ITAS and Signe Kroken for access to meteorological data recorded at ASKO and Ås respectively.

Finally, I would like to thank my family and friends for motivation and support during the work with this thesis. It has been five interesting and invaluable years.

In memory of Peter Holum Normann for inspiring the student community, and illuminating us about the importance and the future of solar energy.

Ås, May 11th, 2016

Ulrik Vieth Rør

Abstract

The purpose of this study was to investigate and analyze parameters that influence the discrepancy between simulated and actual energy production for a photovoltaic (PV) system in south-eastern Norway for the year 2015. The aim was to derive solutions for how simulation models should be designed and how to treat loss parameters, by analyzing and discussing possible causes and solutions for deviations. The simulation software PVsyst was used to simulate different scenarios in order to investigate how the different parameters influenced predicted energy production. To increase the coherency between simulated and produced energy is important in the planning phase of a PV system, and the establishment of a reliable PV system that will meet the required energy demand.

Meteorological (meteo) data from weather stations and satellite data was used as input meteo in PVsyst to investigate any potential differences. Satellite data sources were Meteonorm and Meteocontrol, while weather station data came from Ås and ASKO (Vesby). The PV system was carefully designed in PVsyst according to system configuration and layout. The potential loss parameters were estimated, based upon theory and analysis of climate data from the different meteo sources. Different simulation scenarios were conducted in PVsyst to analyze the accuracy of the different meteo data, and the influence of adjusting loss parameters.

Results show that the accuracy of Global Horizontal Irradiation (GHI) data is vital for the coherence between simulated and produced energy. The sources with the least deviation in irradiation data from the reference value, resulted in the closest estimate to produced energy. Satellite collected data underestimated GHI about 3-4 %, while meteo data from ASKO underestimated 0,6 % and Ås overestimated 1,8 %. Monthly Root Mean Square Deviation (RMSD) was almost 100 % greater for satellite data compared to data from ASKO, with a RMSD of $1647,18\ kWh$.

Individual adjustment of loss parameters improved the accuracy of the simulations. Reducing soiling levels for summer and increasing levels for winter improved the coherence the most. Including thermal loss according to module temperature increased heat loss from the modules, and resulted in monthly increase of predicted energy. A rough estimate of ohmic resistance reduced ohmic loss from 1,5 % at standard test conditions to 0,3 %. The impact of albedo on the simulation result was negligible. Combining the loss parameters improved the accuracy of the simulation and resulted in a consistent monthly overestimate, suggesting possible losses due to light induced degradation or higher soiling loss during summer.

Sammendrag

Formålet med dette studiet var å undersøke og analysere faktorer som påvirker avvik mellom simulert og faktisk produsert energi for et fotovoltaisk (PV) anlegg på Østlandet i Norge i løpet av 2015. Mulige årsaker for avvik og potensielle løsninger er blitt analysert og diskutert med et mål om å utlede retningslinjer for hvordan simuleringsmodeller bør bli designet, og hvordan tapsfaktorer bør bli behandlet. Simuleringsprogrammmet PVsyst er brukt til å simulere forskjellige senarioer for å undersøke hvordan forskjellige faktorer påvirker forventet energi produksjon. Økt nøyaktighet mellom simulert og faktisk produsert energi er viktig for god planlegging av et PV anlegg og for å sørge for at planlagt anlegg er pålitelig og vil møte tenkt energibehov.

Meteorologisk (Meteo) data fra værstasjoner og satelitter er brukt som bakgrunn for analyse i PVsyst, for å undersøke mulige forskjeller. Satelittdata er hentet fra Meteonorm og Meteocontrol. Værstasjoner i studiet er fra Ås og fra anlegget på Asko (Vestby). PV anlegget var nøye konstruert i PVsyst, basert på system informsjon og oppsett. Mulige taspfaktorer er estimert med bakgrunn i teori og meteo data fra de forskjellige kildene. Ulike senarioer var utført i PVsyst for å analysere nøyaktigheten til de ulike meteo kildene, samt påvirkingen av endrede tapsfaktorer.

Resultatet av studien viser at nøyaktigheten på innstrålingsdata er viktig for presisjonen mellom simulert og produsert energi. Meteo data kildene med minst avvik i innstrålt data fra referanse data resulterte i de beste energi simulerings estimatene. Satelitt data underestimerte innstrålingsdata mellom 3 og 4 %. Meteo data fra ASKO underestimerte 0,6 % , mens Ås data overestimerte 1,8 %. Kvadrert standardavvik til referanse verdi (RMSD) var 100 % større for satelitt data enn for data fra ASKO, som resulterte i en RMSD verdi på $1647,18\ kWh$.

Individuell justering av tapsfaktorer forbedret simulerings nøyaktigheten. Beregnet tap grunnet akkumulering av støv og andre avsetninger på sommeren og økt tap grunnet snø på vinteren økte treffsikerheten på simulering betraktelig. Termisk tap fra modulene beregnet ut i fra modul temperatur, økte varmetapet fra modulene og resulterte i økt forventet energi på månedlig basis. Et grovt anslag av kabelmotstand reduserte kabeltap ved standard test betingelser fra 1,5 % til 0,3 %. Justering av albedo hadde lite påvirkning på simulert energi, og er en faktor som er ubetydelig i PVsyst. En kombinasjon av tapsfaktorene forbedret nøyaktigheten på simuleringen, og resulterte i noe overestiemering av energi hver måned. Overestimeringen antyder muligheter for lys indusert nedbryting (LID) og større tap fra støv og andre avsetninger på sommeren.

Contents

Preface and Acknowledgments i
Abstract iii
Sammendrag v
Abbreviations xi

1 Introduction **1**
1.1 Background 2
1.2 Aim and Procedure 3
1.3 Structure of the Report 4

2 Theory **5**
2.1 Solar Energy and Radiation 5
2.1.1 Placement of the Sun 6
2.1.2 Types of irradiation 7
2.2 Air Mass (AM) 8
2.2.1 Standard Test Conditions (STC) 8
2.3 The Photovoltaic System 9
2.3.1 The module 9
2.3.2 The solar cell 10
2.3.3 The inverter 13
2.3.4 Performance ratio 14
2.4 Parameters Influencing Power Production from PV Modules 15
2.4.1 Tilt and Orientation 16
2.4.2 Temperature 17
2.4.3 Shading 19
2.4.4 Soiling 20
2.4.5 Array incidence loss (IAM) 21
2.4.6 Electrical efficiencies and losses 22

2.4.7 Mismatch losses 22
2.4.8 Degradation 23

3 Data **25**
3.1 Error and Uncertainty 26
3.2 Data Sources 26
3.2.1 ASKO 27
3.2.2 Ås - weather station 30
3.2.3 Meteocontrol 30
3.2.4 Meteonorm 30
3.2.5 NIBIO 32

4 Methods **33**
4.1 Google Earth 33
4.2 Matlab 34
4.3 PVsyst 35
4.3.1 Site and Meteo 36
4.3.2 Importing meteorological data 38
4.3.3 Albedo – settings: 40
4.3.4 Orientation 40
4.3.5 System 41
4.3.6 Applying system information in PVsyst 43
4.3.7 Detailed Losses 45
4.3.8 Horizon 46
4.3.9 Near shadings 48
4.3.10 Module layout 49
4.4 Further Procedure 50
4.4.1 Comparison 50
4.5 Estimation of Loss Parameters 50
4.5.1 Albedo 50
4.5.2 Soiling 51
4.5.3 Thermal loss - determining U-values 55
4.5.4 Electrical loss 55
4.5.5 IAM 57
4.5.6 Degradation 57

5 Results and Discussion **59**
5.1 Meteorological Data . . . 59
5.2 Scenario 1 and 2 Simulation Results and Errors . . . 63
5.3 Adjustment of PVsyst Parameters . . . 69
5.3.1 The impact of albedo . . . 72
5.3.2 The impact of soiling . . . 73
5.3.3 The impact of thermal loss adjustment . . . 76
5.3.4 The impact of ohmic resistance adjustment . . . 79
5.4 Combination of Parameters . . . 81
5.4.1 Combination scenarios with ASKO meteo . . . 81
5.5 Investigating Impact of New Information . . . 86
5.5.1 The combined scenarios on the Meteonorm data . . . 90
5.6 General Discussion . . . 92
5.7 Recommendations for similar simulation models in PVsyst . . . 95

6 Conclusion **97**

7 Further Studies **99**

Bibliography **103**

A Module and Inverter Information **107**
A.1 Modules . . . 107
A.2 inverters . . . 107
A.3 Cables . . . 107
A.4 Module Behavior . . . 107

B Simulation Results **118**
B.1 Scenario 1 and 2 Simulation Results . . . 118
B.2 Other Simulation Parameters and Results . . . 123

C Further Information **125**

Nomenclature

Abbreviations	Exploration
AC	Alternating current
AM	Air Mass
AR	Anti-reflective coating
Comb	Combination
DC	Direct current
eq	equation
FF	Fill Factor
GHI	Global Horizontal Irradiation
IAM	Incident angle modifier
LID	Light Induced Degradation
Meteo	Meteorological
MC	Meteocontrol
MN	Meteonorm
mono-Si	Monocrystalline Silicon
MPP	Maximum Power Point
MPPT	Max Power Point Tracker
multi-Si	Multicrystalline Silicon
PR	Performance Ratio
PV	Photovoltaic
RE	Relative Error
RMSD	Root Mean Square Deviation
S1	Scenario 1
S2	Scenario 2
SA	Sub Array
STC	Standard Test Conditions
TR	Transmittance Rate

Latin	Exploration
A	Area, m^2
Am	Module area, m^2
b_o	Material dependent reflection constant, -
E	Energy, kWh
F_{IAM}	Irradiation absorbed by a module, -
h	Solar height, -
J	Current, A
J_{MPP}	Current at maximum power point, A
Jsc	Short Circuit Current, A
I_{beam}	Beam irradiation, W/m^2
$I_{diffuse}$	Diffuse irradiation, W/m^2
I_{global}	Global irradiation, W/m^2
Im	Irradiation incident on a module, W/m^2
Iph	Photoelectric generated current, A
L	Length, m
P	Power, W
P_{DC}	Direct current Power, W
P_{in}	Irradiation Power incident on cell, W
P_{MPP}	Power at maximum power point, W
Rs	Series resistance, Ω
Rsh	Shunt resistance, Ω
Si	Silicon, -
$Tamb$	Ambient Temperature, K, - unless other is specified
Tm	Module/Cell Temperature, K , - unless other is specified
U	Thermal loss factor, $W/(m^2 \cdot K)$
Uc	Material dependent thermal loss constant, $W/(m^2 \cdot K)$
Uv	Wind thermal value, $W/(m^2 \cdot K)/(m/s)$
V	Voltage, V
V_{MPP}	Voltage at maximum power point, V
Voc	Open Circuit Voltage, V

Greek	**Exploration**
η	Cell efficiency, -
γ	Module tilt angle, -
λ	Constant, -
μ	Absorption coefficient of solar irradiation, -
v_v	Wind velocity, m/s.
ψ	Azimuth angle, -
ρ	Resistivity of conductor, $\Omega \cdot m$
θ	Irradiation incident angle on the module plane, W/m^2
θz	Zenith angle, -

List of Figures

1.1 ASKO East industry area - a closer look 2
1.2 ASKO location 3

2.1 The ecliptic plane 6
2.2 Placement of the Sun 7
2.3 Air mass principle 8
2.4 The PV system 9
2.5 Cell, moduel and array 10
2.6 The JV and PV curve 11
2.7 Ilustration of the one diode model 13
2.8 IV-curve and irradiation 15
2.9 Tilt and Azimuth 16
2.10 IV-curve and temperature influence 17
2.11 Shading of a cell 19
2.12 Array incidence loss 21

3.1 The Kipp & Zonen CMP 10 pyranometer at ASKO 27
3.2 Picture and Google Earth excerpt of the Ventur wind sensor 29

4.1 ASKO PV-system location 34
4.2 PVsyst project design menu 36
4.3 PVsyst excerpt of the tool "Tables and graphs" 39
4.4 Schematic layout of the system at ASKO 41
4.5 Defing the mdoule characterstics 43
4.6 PVsyst system information section 44
4.7 ASKO rooftop panorama picture 47
4.8 PVsyst horizon profile from ASKO 47
4.9 PVsyst 3D shading scene 48

4.10 Excerpt from PVsyst presenting the definition of module layout. 49
4.11 Snow data 52
4.12 NIBIO: Monthly and daily rainfall 53
4.13 Electrical layout 56

5.1 Yearly and monthly irradiation 60
5.2 Monthly mean temperature 61
5.3 Monthly mean wind speed 62
5.4 Simulated and received irradiation 65
5.5 Simulated and produced energy per month 66
5.6 Relative Error between simulated and produced energy at ASKO 68
5.7 Correlation and deviation plot: Scenario 2 69
5.8 PVsyst loss diagram for ASKO 70
5.9 ASKO S2 and albedo relative error 73
5.10 Impact of soiling adjustment on simulated energy 74
5.11 Relative Error for thermal loss adjustments 77
5.12 Ohmic resistance adjustment 79
5.13 Combined scenario 1: relative error 81
5.14 Combined scenario 1: Correlation plot 82
5.15 Comb-2 scenario: Relative Error 83
5.16 Comb-2 scenario: Correlation plot 84
5.17 Comb-3 scenario: Relative Error. 88
5.18 Comb-3: correlation plot 89
5.19 Relative Error for MN-Comb-1 and MN-Comb-3 91

A.1 IBC PolySol 250 CS data sheet, page 1 108
A.2 IBC PolySol 250 CS data seet, page 2 109
A.3 IBC PolySol 250 CS data sheet PVsyst 110
A.4 The Sungrow 20KTL inverter - page 1 111
A.5 The Sungrow 20KTL inverter - page 2 112
A.6 The Sungrow 30KTL inverter - page 1 113
A.7 The Sungrow 30KTL inverter - page 2 114
A.8 Cable characteristics. Page 1 115
A.9 Cable characteristics. Page 2 116
A.10 Module efficiency as a function of irradiation 117

B.1 ASKO meteo data S2 - Performance Ratio 119
B.2 ASKO S2 loss diagram - Experimental soiling 120
B.3 Metenorm S2 loss diagram 121
B.4 ASKO S2 loss diagram - new characterstics 122
B.5 Excerpt from PVsyst displaying the tilt and orientation of the modules. 123
B.6 PVsyst detailed losses 124

C.1 The order sheet available at Meteocontrol.com 126
C.2 The order sheet available at Meteocontrol.com 127

List of Tables

3.1 Kipp & Zonen CMP 10 - Specifications . . . 28
3.2 Campbell Scientific 110PV - specifications . . . 28
3.3 Campbell Scientific CS125 - specifications . . . 28
3.4 Ventus ultrasonic wind sensor - specifications . . . 28
3.5 FAGKLIM instruments . . . 30
3.6 LMT NIBIO instruments . . . 32

4.1 ASKO location details. . . . 36
4.2 PVsyst temperature values for ASKO . . . 37
4.3 Variables in meteorological data. . . . 38
4.4 PVsyst standard albedo values. . . . 40
4.5 ASKO system details . . . 42
4.6 Default loss parameters . . . 46
4.7 NIBIO monthly albedo values at Ås . . . 51
4.8 Soiling values . . . 54
4.9 Temperature settings used in PVsyst . . . 55
4.10 Ohmc detailed computation . . . 57

5.1 Scenario 1 and 2 yearly results . . . 63
5.2 Root mean square deviation between simulated and produced energy . . . 64
5.3 Soiling values: Experimental . . . 74
5.4 RMSD values for thermal loss scenarios . . . 76
5.5 Recommended soiling values . . . 96

B.1 Scenario 1 results . . . 118
B.2 Scenario 2 results . . . 119
B.3 Soiling values: Comb-3 - alternative . . . 123

Chapter 1

Introduction

The implementation of solar energy systems is rapidly increasing worldwide, and is an important transition into a renewable future. Solar energy offers a solution for many countries to achieve the 20 % renewable target set by the European UNION (2009) by 2020. In Norway, the use of solar energy applications has increased in the last decade, and is continuing to increase. The Norwegian consulting company Multiconsult reported to the international energy agency (IEA) that the total amount of energy produced from solar cells increased 10 % from 2014 to 2015 in Norway. The most noticeable growth in the use of solar cells was within private housing, with a four time increase in installed capacity (Multiconsult).

With increased investments in photovoltaic (PV) systems it is important to be able to predict and simulate produced power and energy from PV systems accurately. The challenge is to design a system that meets the required energy consumption, and is economically optimized, considering the variability of solar energy. Norway´s geographical location at higher latitudes composes a challenge to less solar irradiation being received compared to areas further south. According to PELLANDS et al. (2013) the accuracy of simulated PV energy depends on the quality of the weather forecast, and mostly irradiation data.

Previous studies have reported that simulated energy production deviates from actual energy production. A study conducted by Andersen (2014) concluded that simulation tools in most cases underestimated solar irradiation on a yearly basis and thus also predicted energy production. According to Øygarden Flæten solar irradiation is mostly underestimated in Norway due to the method of collecting data, namely the use of satellites that may underestimate solar irradiation by up to 10 %. Therefore, the quality of meteorological (meteo) data in simulation tools are essential for the accuracy of the model.

That being stated, it is of interest to investigate and analyze parameters causing the discrepancy between simulated and actually energy production, when utilizing simulation tools. Knowledge about parameters that influence the predicted and simulated energy can result in more accurate simulations. Higher precision can increase the reliability of the PV system to meet the energy demand, and can help in the planning and design process of a PV system.

1.1 Background

A PV system in Norway is used to conduct a study to analyze the deviations between simulated and actual energy production. The PV system is located in Vestby municipality, Akershus county, Norway. The system was installed 3/9/14 at the rooftop of one of the industrial buildings at ASKO Øst. ASKO stores and distributes food and other household goods all over Norway. The system is rated at 375 kWp and consists of 1480 modules over almost 2500 square meters. The installment of the system is a part of ASKO´s aim to become sustainable and climate–neutral by providing renewable energy for cooling storages and transport.

Figure 1.1: Excerpt from Google Earth showing a close caption of the industry area of ASKO Øst. The area marked in red is the location of the PV system. Excerpt is taken April 3rd, 2016.

The system is located on one of the tallest buildings at ASKO, making the location optimal in terms of receiving direct sunlight as shown in figure 1.1. There are no buildings in the vicinity of the system that can interfere with the sunlight. Figure 1.2 presents the location of the PV system in the south-eastern part of Norway.

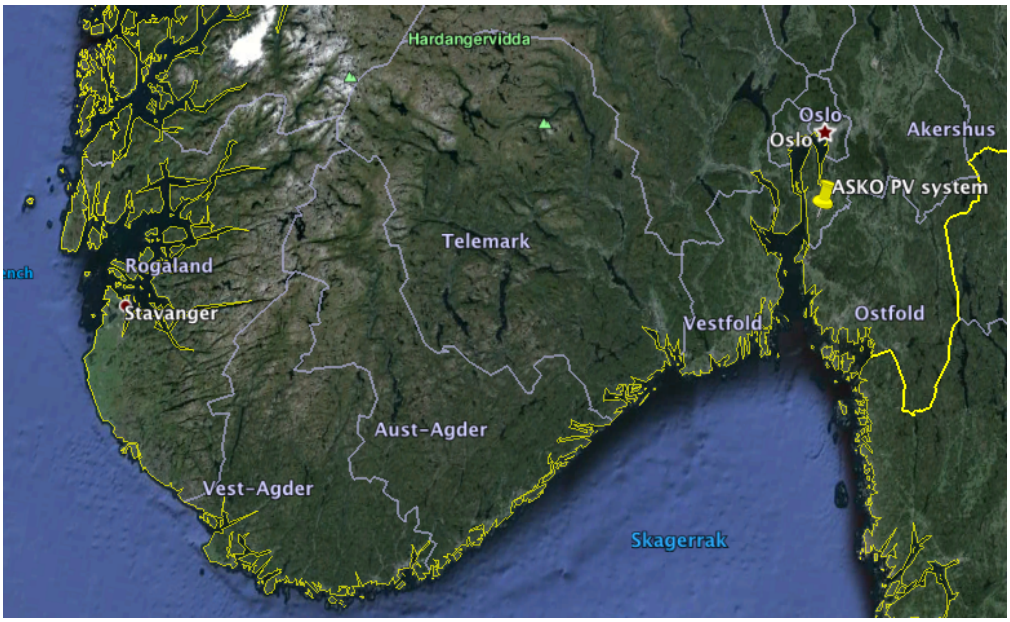

Figure 1.2: Excerpt from Google Earth presenting the geographical location of ASKO Øst. Excerpt is taken April 3rd, 2016.

1.2 Aim and Procedure

This thesis will investigate parameters that influence the discrepancy between simulated and the actual energy production. The reference is energy fed to the grid in 2015, which will be compared to simulated energy fed to the grid. The software PVsyst will be used as a simulation tool to conduct the study. Possible causes and solutions for deviations will be analyzed and discussed. The aim is to derive guidelines for more accurate simulations for similar systems in the future. To conduct the study, the following methodology will be applied:

- A short study of the four meteo data sets utilized in the study. Analyzing and comparing similarities and discrepancies between the data sets that consist of both satellite and weather station data.
- Designing the PV system in PVsyst accurately and carefully to achieve a good model for simulations.
- Simulating the created model with the meteo data from different sources and with different input parameters. The aim is to investigate how distinctive meteo data influence the simulation result.
- Analyzing the actual produced and simulated energy with the different meto sources.

Identify discrepancies, discuss and analyze possible adjustments of parameters to eliminate the discrepancies between the simulated and actual energy production.

- Individual adjustment of parameters that influence the simulation of energy.
- Creating a combined, optimal scenario with adjusted loss parameters, that more accurately simulates produced energy.

1.3 Structure of the Report

Chapter 2 provides the relevant and necessary theory in order to understand the study. This includes the physics of solar irradiation, energy production from photovoltaic systems and parameters influencing PV performance.

Chapter 3 describes the collection of the meteo data. The different meteo sources utilized in this thesis are described and the characteristics for their instruments are explained.

Chapter 4 explains the methodology of the conducted study. This includes an introduction to the software PVsyst, and presents the methods to investigate the influence of loss parameters.

Chapter 5 presents and discusses the assorted results of the study. The first part presents the results of analyzing the different meteo data, before the impact of different meteo data on the simulation result is presented. The second part presents the results of individual loss parameter adjustment and possible combination of parameters in order to increase simulation accuracy.

Chapter 6 summarizes and concludes the most important findings and results of the study.

Chapter 7 provides suggestions for further studies in this field of research.

Chapter 2

Theory

The necessary theory needs to be explained in order to understand and analyze the parameters causing discrepancy between simulated and actual energy production. The following chapter aims to clarify the relevant topics for the production of energy from photovoltaic (PV) systems and is of importance for understanding the work presented in this thesis.

2.1 Solar Energy and Radiation

The following section is short and concise, giving a brief explanation to the seasonal and daily variations in solar energy.

Solar radiation is caused by the Sun emitting waves. A fraction of these waves reaches earth, however the amount of radiation received by earth varies significantly. The Earth revolves around the Sun in an elliptical orbit (ecliptic plane), causing the distance between earth and the sun to continuously change as illustrated in figure 2.1. As a result, received radiation on Earth is constantly changing (Smets et al. (2016)). The Earth rotates around its own axis (equatorial plane) causing daily changes in received radiation and the tilt of the axis relative to the Sun causes seasonal changes (Chen (2011)). These changes are of major importance when estimating and forecasting yearly solar irradiation at a location.

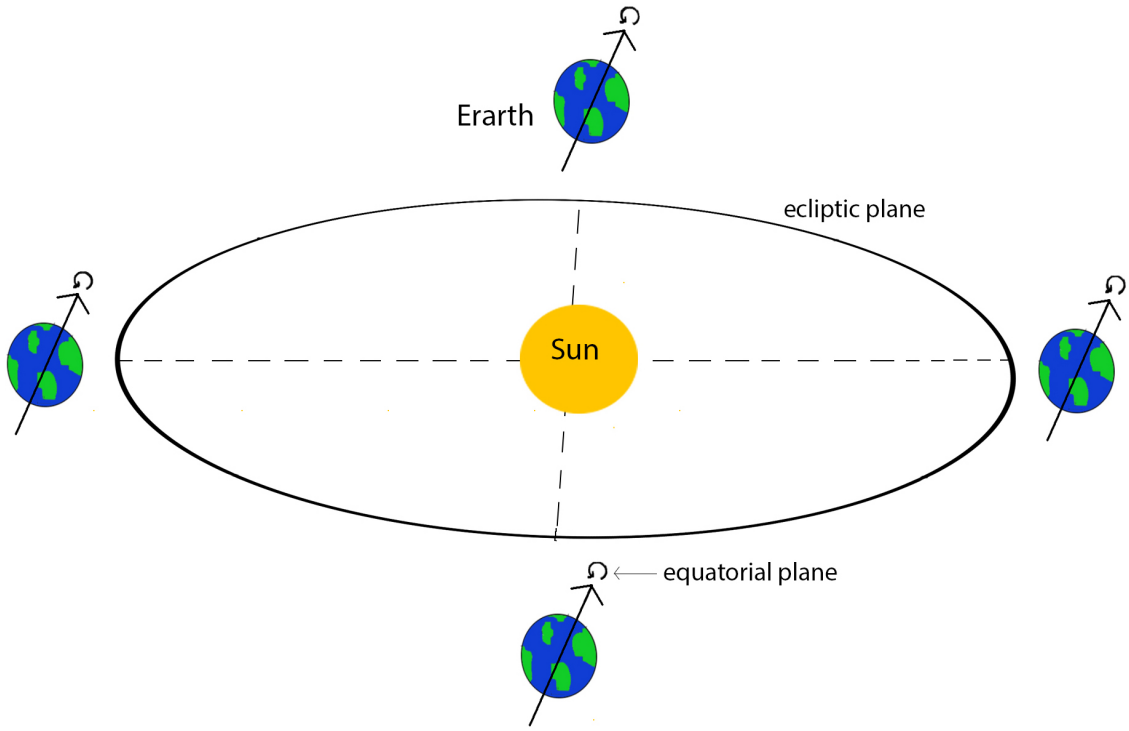

Figure 2.1: Illustration based on Iqbal (2012) showing the ecliptic plane as the Earth revolves around the Sun. The equatorial plane is shown by the arrow above Earth that shows a rotation of Earth around its own axis. The line through earth illustrates the tilt of the Earth.

2.1.1 Placement of the Sun

There are a number of terms and definitions used to describe the position of a body in the earth-sun sphere that are relevant for the the amount of received solar irradiation. The elevation describes the angular distance of the body with reference to the horizon and is denoted solar height h, in figure 2.2. The zenith angle is the compliment of the elevation angle, as it is the angle between the zenith and the body, and is represented by θz. Both these angles do therefore vary between 0 and 90 degrees, with sum of the two being 90 degrees. The azimuth angle, ψ, is the angle between the projectile of the body to the horizontal plane with respect to the south pole. South is referenced as zero, east as positive and west as negative. The azimuth angle thus varies between $\pm$ 180 degrees.

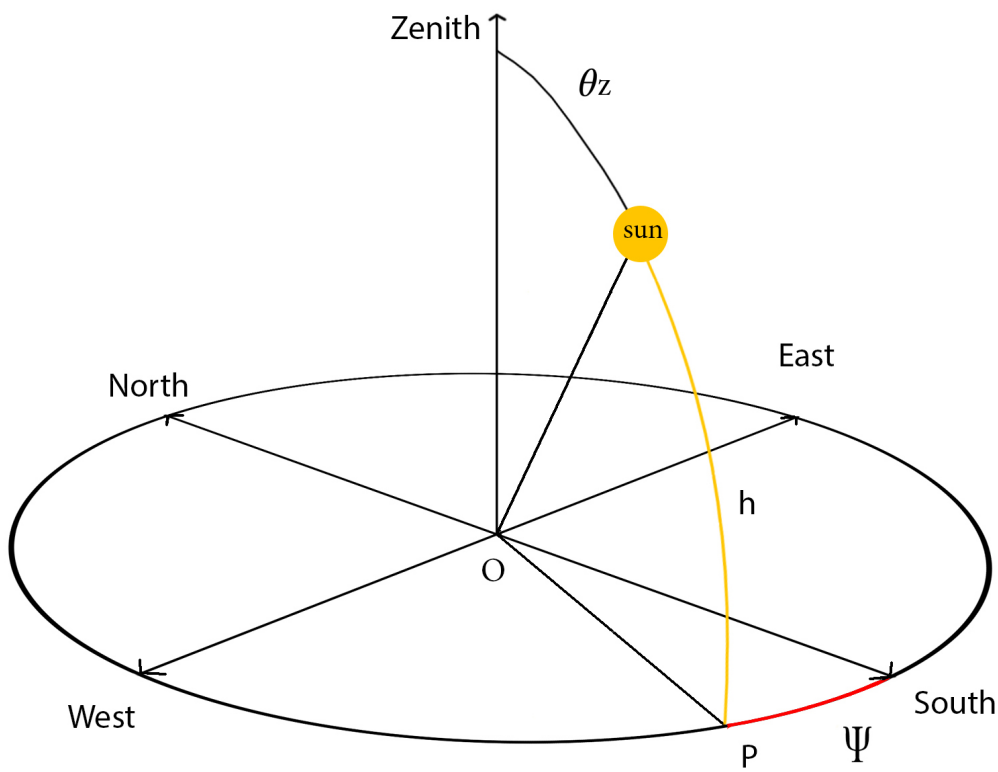

Figure 2.2: Illustration describing the placement of the Sun relative to that of Earth. The figure is inspired by Chen (2011).

2.1.2 Types of irradiation

The solar irradiation travels through the Earth´s atmosphere and may be partially scattered. The result is different ways to measure received irradiation. Solar irradiation is measured in power per unit area, usually W/m^2. The irradiation received at Earth´s surface is termed global irradiation, I_{global}. Further on in this thesis, Iglobal, may be denoted solar irradiation and *global horizontal irradiation* (GHI). The irradiation that travels through the atmosphere without interacting with the particles in the atmosphere is termed I_{beam}, and may also be referred to as direct irradiation. The irradiation that is absorbed and re-scattered or reflected is termed $I_{diffuse}$. Iglobal is the sum of the diffuse and the direct sunlight, as equation 2.1 shows.

$$I_{global} = I_{beam} + I_{diffuse} \quad \left(\frac{W}{m^2}\right) \tag{2.1}$$

2.2 Air Mass (AM)

The previous section described the motion and placement of the sun with respect to the earth. As the solar height changes (figure 2.2), the sunlight traveling through the atmosphere travels from different angles and thus have distinctive distances. The result is that the amount of interaction between the sunlight and particles in the atmosphere depends on the solar height. This is accounted for by the use of Air mass (AM) defined as $AM = \frac{ds}{dz} = \frac{1}{Cos(\theta z)}$, as explained in figure 2.3. Since the Sun is not at zenith (0 degrees, abbreviated AM1) during most parts of the day, the values of AM is in most cases greater than 1. The chosen standard value for air mass is AM1,5.

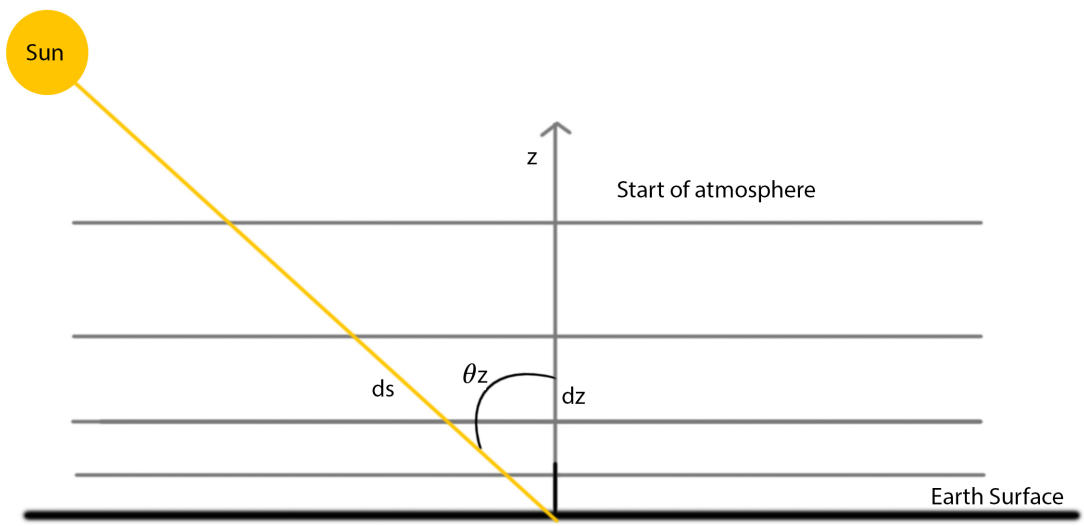

Figure 2.3: Illustration of air mass principle inspired by Chen (2011).

2.2.1 Standard Test Conditions (STC)

Air mass is part of the standardized test conditions for photovoltaic modules. Standard test conditions have been introduced to make uniform comparisons of modules from different manufactures. This is due to the different parameters that influence the energy production from a PV module. The test conditions are defined with the following parameters:

- Solar irradiation = 1000 W/m^2
- Ambient temperature: $Tamb = 25\ Celsius$
- AM = 1,5

2.3 The Photovoltaic System

Understanding the theory behind a photovoltaic (PV) system, is essential to optimize simulation with PVsyst to compare with produced energy from the actual system. PV systems may be grouped into grid connected systems and stand alone systems. This thesis studies a grid connected system, thus the emphasis will be on this system. A grid connected system is connected to the local electricity grid and has the advantage over stand alone system, where storage systems are also required. A PV system consists of several components that each has a role from the conversion of energy, to energy being delivered to the grid. The most important are the modules and the inverters (converts direct current (DC) to alternating current (AC)), as shown in figure 2.4.

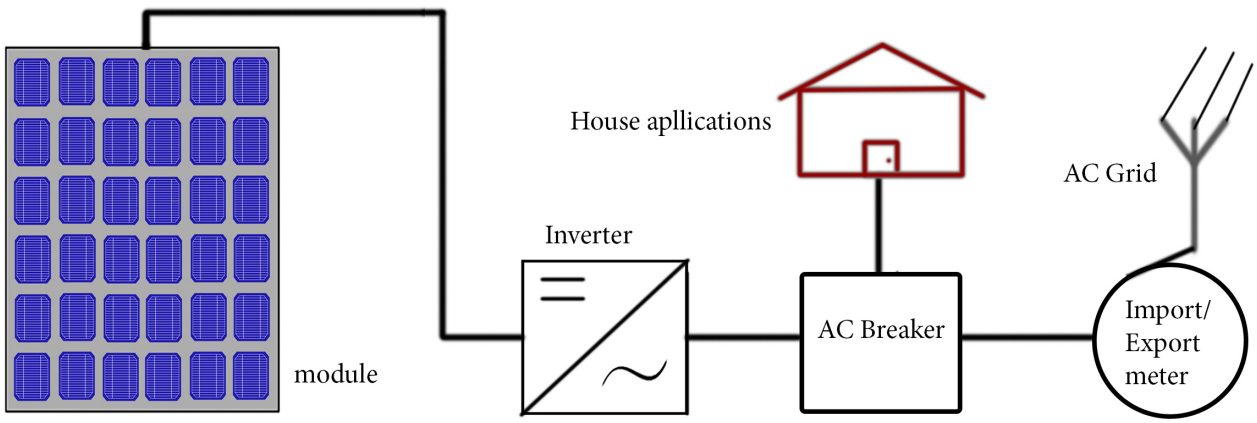

Figure 2.4: Illustration of a PV system including: module, inverter, AC breaker (delegates electricity), and an import/export meter (instrument to measure the flow of electricity in and out between the the grid and the PV system).

2.3.1 The module

A PV-system can consist of one or more arrays. Each array containing an assembly of solar modules (2.5). The modules are the most important element of the system (Nofuentes et al. (2011)). They may be connected in series called strings, or in parallel. An array is constructed to meet the requirements of demanded power. The modules are connected in strings (series) to obtain a higher voltage, as voltages is added when connected in series. Connected in parallel the current is increased, as currents in parallel are added.

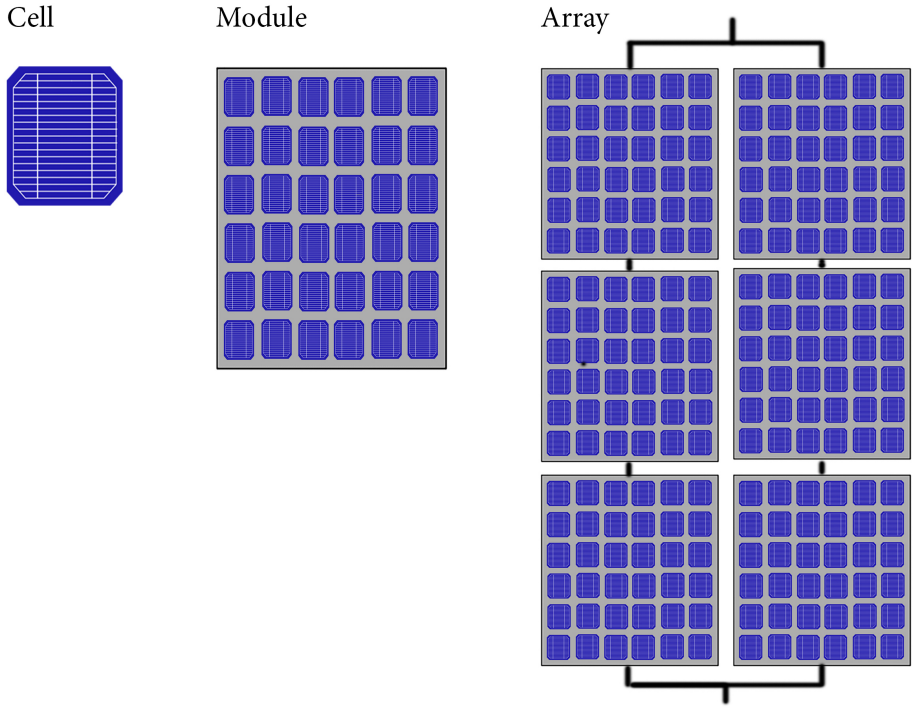

Figure 2.5: Illustration of a cell, module and array. Not to scale.

The module is a static current generator that converts solar radiation to electrical energy. Incident light on the surface of the module is absorbed by the material, known as a semiconductor, and generates a current, named the photovoltaic effect. The intensity of the electric currents is dependent on the intensity of the solar radiation (Chen (2011)). The modules typically consists of 60 cells in a string.

2.3.2 The solar cell

The solar cell is the smallest part of the module. The cell is developed as a semiconductor with the ability to emit electrons when light is incident on the surface. This effect is called the photoelectric effect and is the foundation for the photovoltaic effect. The cells are by 2016 primarily made by silicon wafers. Although there are other alternatives to silicon, silicon is found to be an abundant element on earth. Therefore, considering cost and efficiency, silicon is the most used material for semiconductors (Nofuentes et al. (2011)). Silicon wafers appear both as mono-crystalline silicon ($mono - Si$) and multi-crystalline silicon($multi - Si$). Mono-Si offers higher efficiency as the Si atoms are perfectly aligned, but also is the more expensive option. Multi-Si wafers have atoms aligned in different directions and have lower production cost as well as efficiency compared to mono-Si (Nofuentes et al. (2011)). Industrial modules have about 15-18 % - and 17-20 % efficiency for multi-Si and mono-Si respectively.

A silicon atom has 4 electrons in its outer (valence) shell, named valence electrons. The silicon semiconductor is made up by silicon atoms bonded together in a crystal lattice, where all atoms are surrounded by 8 electrons. To increase the conductivity of electrons in the semiconductor, each side of the silicon wafer is doped with foreign atoms. Most common atoms are Phosphorous and Boron, with 5 and 3 valence electrons respectively. Doping with Phosphorous creates an $n-type$ semiconductor material as available electrons are created in the crystal lattice. Doping with Boron creates a $p-type$ material, because silicon atoms in the p-type material can not create 4 covalent bonds. The results is a spare whole, where electrons can move freely. The combination of a p-type doped semiconductor material and a n-type semiconductor material creates a $p-n$ junction (Smets et al. (2016)).

The behavior of a solar cell may be characterized by an JV-curve (Smets et al. (2016)). The module operates at a unique direct current (J) and voltage (V) point that corresponds to a certain radiation and temperature value. This point lies on the JV curve, illustrated in figure 2.6.

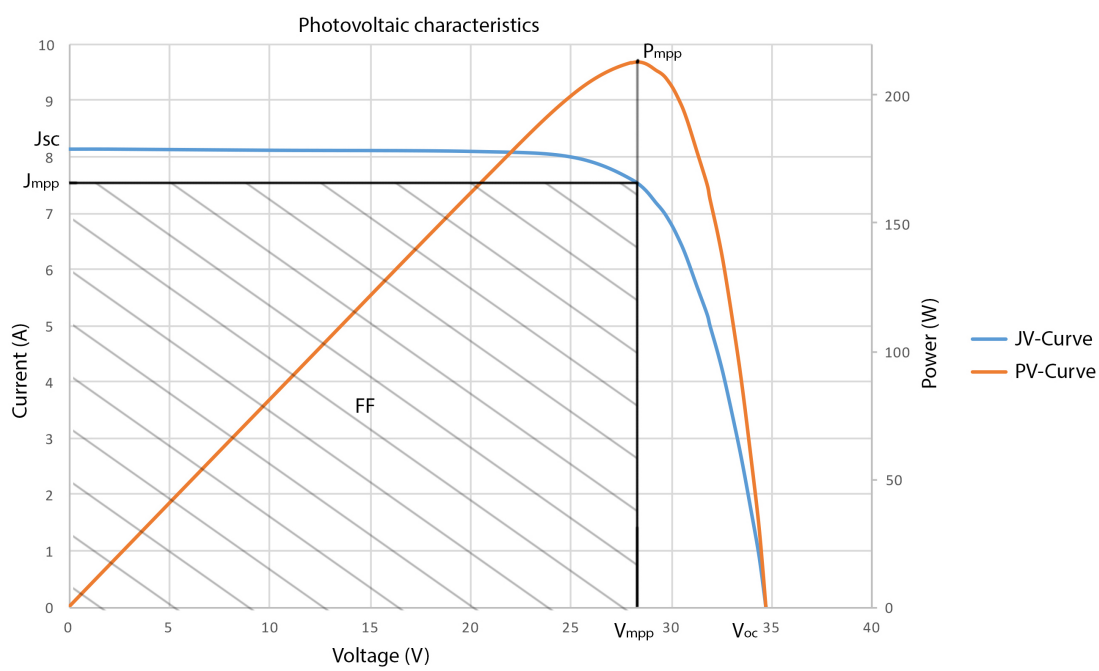

Figure 2.6: Figure of a JV curve and an effect (power) curve. The figure shows the points Jsc and Voc. Jsc is the short circuit current and is the maximum current from a cell, which occurs when the voltage is zero. Voc is the open circuit voltage and is the maximum voltage, which occurs when the current from the cell is zero. The marked area on the graph represents the fill factor (FF).

The power (P) – voltage curve (PV) is a function of the JV curve as the power is given by:

$$P_{DC} = J \cdot V \quad (W) \tag{2.2}$$

The optimal relation between current and voltage results in the maximum power point (MPP) shown in figure 2.6. The corresponding voltage and current are termed V_{MPP} and J_{MPP} respectively. The relation is described by:

$$P_{MPP} = V_{MPP} \cdot J_{MPP} = FF \cdot V_{oc} \cdot J_{sc} \quad (W) \tag{2.3}$$

In equation, 2.3 FF is the fill factor of the cell and is defined as the ratio of the maximum power delivered from the solar cell to the product of V_{oc} and J_{sc}, as shown figure 2.6. V_{oc} is the open circuit voltage and J_{sc} is the short circuit current, both presented in figure 2.6. As described earlier, modules in parallel increase the current, and in series increase the voltage. Each cell produce about the same amount of power, depending on the production of the cell. An IV curve for a module will have the same shape as that for the cell (2.6), and thus be a scalar of the cell (Smets et al. (2016)). The efficiency (η_m) of a cell can be calculated by:

$$\eta_m = \frac{P_{MPP}}{P_{in}} = \frac{FF \cdot V_{oc} \cdot J_{sc}}{I_m \cdot A_m} \tag{2.4}$$

I_m is an arbitrary irradiation value incident on a module (W/m^2) and A_m is the area of the module. P_{in} is the irradiation received on the cell (W).

FF, and thus in effect, the JV and PV curve is influenced by resistance in the cell, namely series resistance R_s and shunt resistance R_{sh}. The behavior of the solar cell is similar to that of a diode, as the p-n junction creates a diode (Smets et al. (2016)). An equivalent circuit can be drawn that describes the diode, R_s and R_{sh}, named the *one diode model*, as shown in figure 2.7.

I_{ph} is the current generated by the photoelectric effect. Low R_{sh} creates an alternative path for the current generated by the photoelectric effect and thus reduced output current of the cell. High R_s results in more power loss (explained in section 2.4.6) before output as it is dissipated in the series resistance. Generally, a high efficient cell at STC thus consists of a high shunt resistance and a low series resistance.

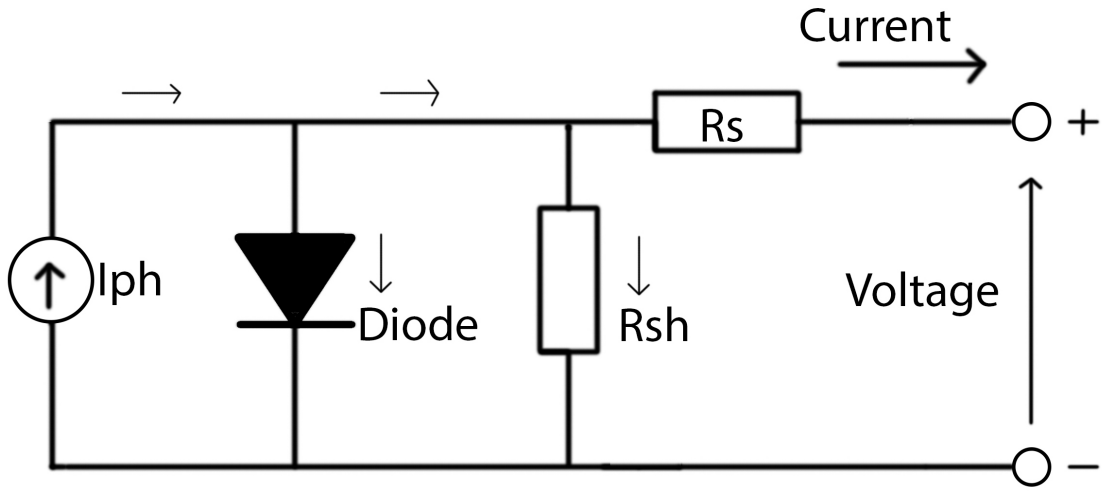

Figure 2.7: Illustration of the *one diode model*. I_{ph} is the photoelectric generated current from the cell. R_s and R_{sh} the series and shunt resistances respectively. The illustration is inspired by Smets et al. (2016).

This is just a brief explanation of the structure of solar cells and their materials. Further study may be conducted by the reader, but is not necessary for the thesis.

2.3.3 The inverter

This thesis emphasize explaining string inverters as the case study consists of string inverters. The inverter converts direct current (DC) generated by the PV modules to alternating current (AC), that can be fed to the grid, which utilizes AC. The inverter will adapt frequency and voltage to coordinate with the grid, according to Bernhard et al. (2012). The efficiency of the inverters are very high, and about 1-3 % of the energy is lost during the inverting of the current.

There are different types of inverters, each with their own specifications. Most common are the string inverter and the central inverter, although the relatively new micro inverter offers some great advantages (Lee and Raichle (2012)). The string inverter is used in systems with several strings per inverter and several modules in a string, thus resulting in a high voltage. The central inverter is typically used for larger systems with a higher power rating, and operates similar to the string inverter. String inverters are typically used for assemblies up to a 100 kWp while central inverters are used for systems above 100 kWp. Micro inverters are connected on each individual module and has some disadvantages and advantages over string and central inverters due to design. The micro inverter offers slightly lower efficiency compared to the string inverter and also has a higher acquisition cost (Bernhard et al. (2012)). The advantage of micro inverters

is their system performance when the system is influenced by shading, a concept that will be discussed later in the thesis. A study by Lee and Raichle (2012) explains how micro inverters provide a higher efficiency for a PV system compared to string inverters when the system is exposed to shading.

The system analyzed in this thesis consists of a string inverter. Further theory is thus limited to this inverter. As explained in the section above, each module delivers a current (J) and a voltage (V). A function of the inverter is to continuously track the MPP point with the purpose of the module to constantly operate at MPP. This function is named maximum power point tracker ($MPPT$), and allows the inverter to operate at MPP regardless of irradiation (Smets et al. (2016)), and maintain a high efficiency of the system. This function may be applied to a whole string of modules, thus optimizing the whole string the inverter is connected to. Some string inverters offers multiple MPPT that may track several operating conditions. This ability is useful with systems with multiple orientations.

2.3.4 Performance ratio

Performance ratio (PR) is a international measure to describe the degree of performance of a PV system (Reich et al. (2012)). PR is defined as the average system yield relative to the reference yield at STC and is calculated:

$$PR = \frac{E_{produced}}{E_{STC}} \tag{2.5}$$

PR is a good estimate to analyze how a system is operating in different time intervals. PR can therefore differ for each month and is a useful measure to compare for different systems.

2.4 Parameters Influencing Power Production from PV Modules

It is vital to understand how different parameters influence the performance of- and produced power by a PV system in order to alter parameter settings in the simulation tool.This includes: irradiation, tilt and orientation, temperature and wind, shading, soiling, array incidence loss, electrical loss, mismatch losses and degradation.

Irradiation is an essential part of the generation of power from a system. There is a strong correlation between the levels of irradiation and the resulting current and voltage produced in the cell. This relation is shown by equation 2.6 and in figure 2.8. The short circuit current (J_{sc}) produced by a module is proportional to the irradiation incident on the module (Smets et al. (2016)) by the relationship:

$$J_{sc} = I_m \cdot \lambda \quad (A) \tag{2.6}$$

where λ is a constant and I_m is an arbitrary irradiation value.

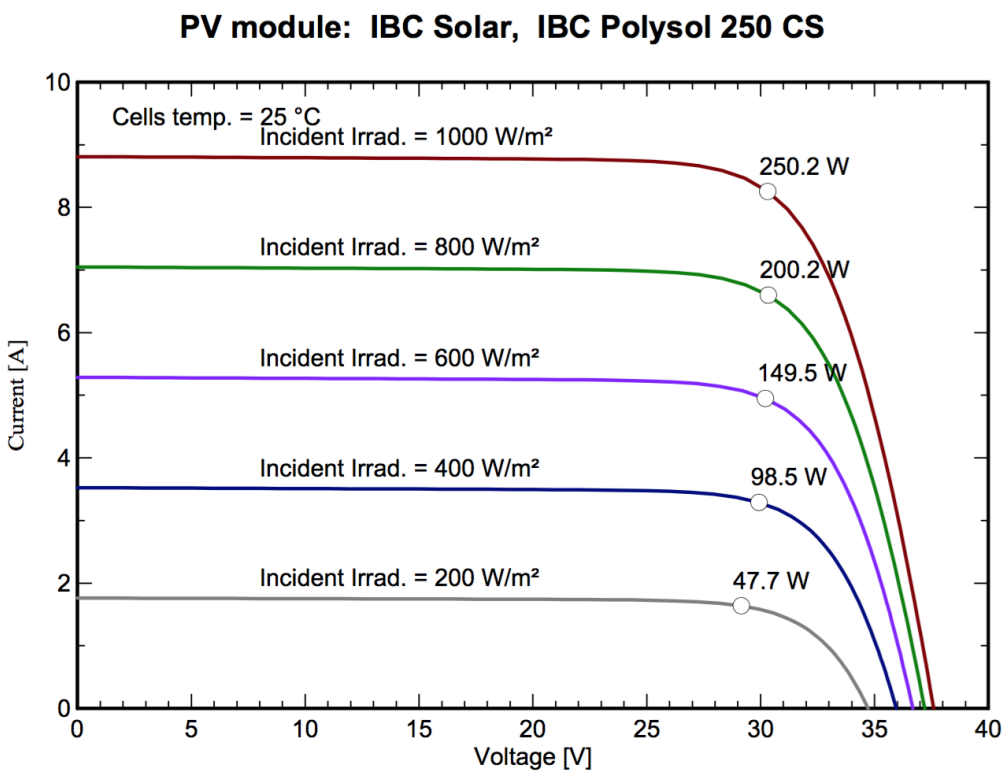

Figure 2.8: Illustration of how different irradiation levels influence the JV curve and thus the generated power. This is an excerpt from PVsyst executed for the IBC PolySol 250 CS modules used in the system at ASKO.

2.4.1 Tilt and Orientation

The performance of the PV system is dependent on the tilt and orientation of the system, because they influence the angle between the Sun and the module surface. As the current produced by a module is proportional to the incident irradiation, optimizing tilt and orientation is important. When the Sun is perpendicular to the module surface, the power incident on the surface is equal to that of the irradiation, and more current is generated. Figure 2.9 illustrates the theory of tilt and azimuth.

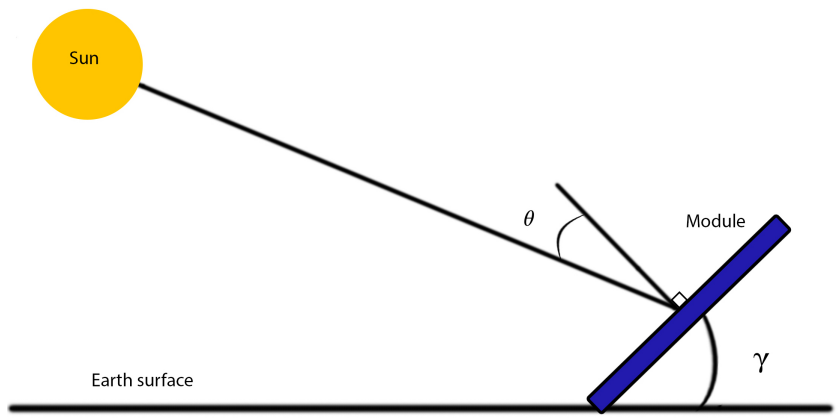

(a) Illustration of tilt.

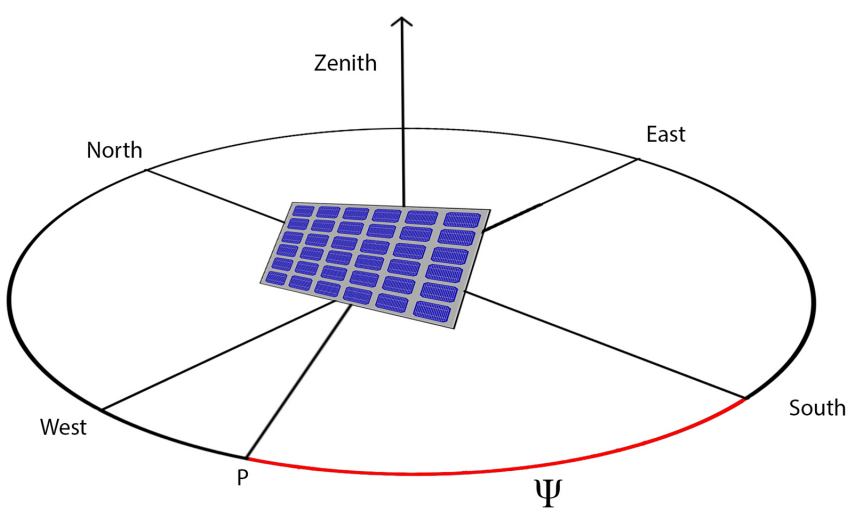

(b) Illustration of azimuth.

Figure 2.9: Illustrating the theory of tilt (γ) and azimuth (ψ). The tilt of the module is the angle between the module and earths surface. The azimuth angle is shown between point p and south.

2.4.2 Temperature

The ambient temperature of the PV system impacts the efficiency of the system. The impact is mainly on the the PV modules and their cells, primarily on the cell temperature (T_m), measured i Kelvin (K). Increased cell temperature results in a decrease of produced voltage and thus power supplied from a module, as illustrated in figure 2.10. The minor increase in short circuit current is outweighed by the more significant open circuit voltage drop. The voltage drop results in reduced power from the PV modules, shown by equation 2.2 in section 2.3.2.

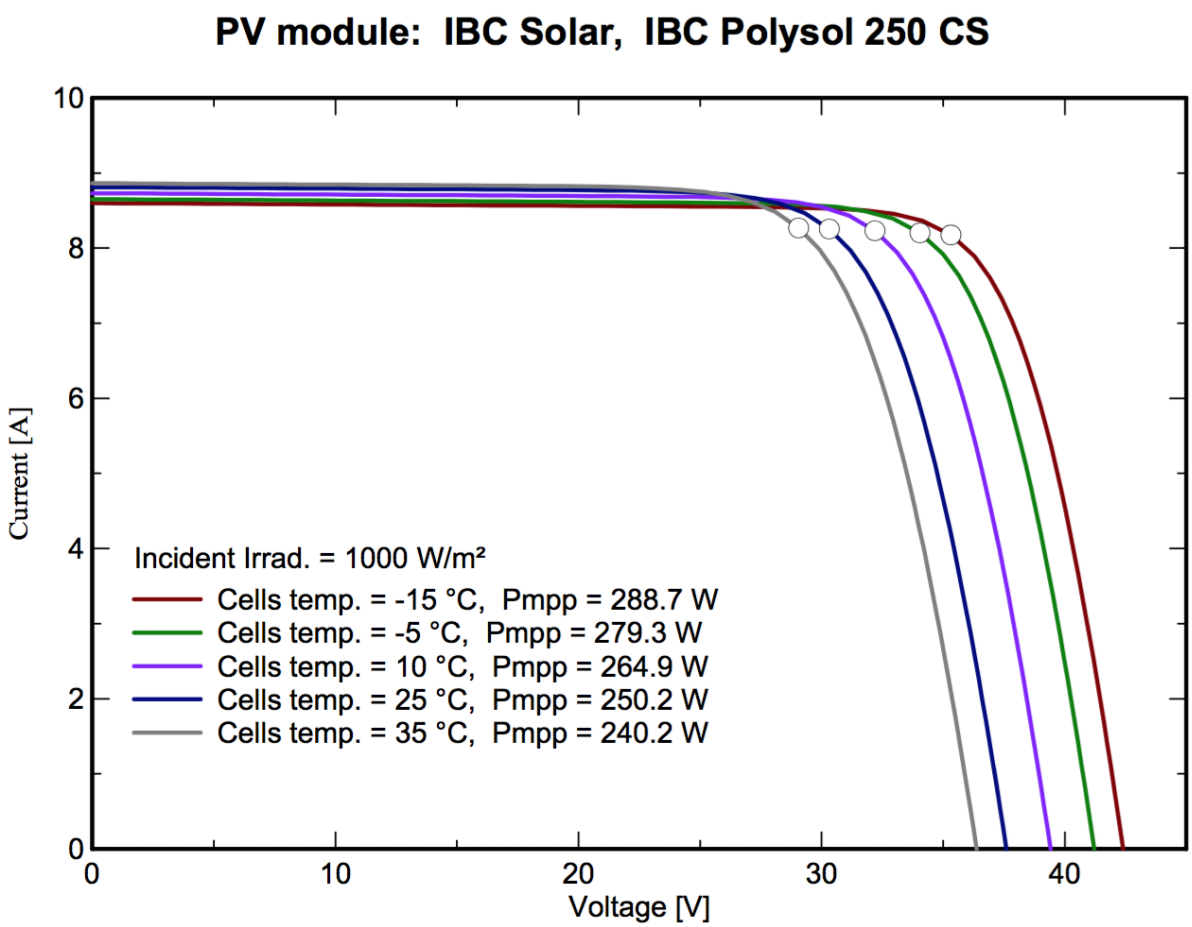

Figure 2.10: Excerpt from PVsyst of the CS 250 modules showing a shift in the JV curve with a change in temperature. Increased temperature reduces the voltage.

The excerpt from PVsyst (2.10) depicts the change in power output for different temperatures for the PV modules IBC PolySol 250 CS used in this thesis. The graph explains how the modules operate at a higher efficiency when the ambient temperature is low, thus increasing the overall efficiency of the system. Unfortunately, the increased efficiency does not compensate for the lower received irradiation during the winter half-year in Norway.

The influence of irradiation, wind velocity and temperature can be described with equation (2.7 and 2.8). The first is the thermal energy balance of the module, used in the PVsyst (2014) software.

$$U \cdot (T_m - T_{amb}) = \mu \cdot I_m \cdot (1 - \eta_m) \tag{2.7}$$

T_{amb} is the ambient temperature measured in Kelvin (K), while η_m is the efficiency of the module. μ is the absorption coefficient of solar irradiation. The U value is the thermal loss factor $W/(m^2 \cdot K)$ and is further elaborated in the equation below:

$$U = U_c + U_v \cdot v_v \tag{2.8}$$

In the equation above: v_v is the wind velocity in m/s, while U_v is the thermal wind value $(W/m^2 \cdot K)/(m/s)$. U_c is a material dependent constant measured in $W/(m^2 \cdot K)$. U values in the simulation software, PVsyst, is is related to the mounting of the system. Mounting is an essential part when evaluating and estimating heat loss. The closer the modules are mounted to the ground or roof the less air will flow behind the modules. The space behind the modules is often referred to as the air duct. The smaller the air duct and the longer the air path (length of string) the smaller the heat loss from the modules. The spacing between modules in series and strings plays an important role in airflow under and around the modules, and therefore also the heat loss.

Wind

Wind influences the performance of a PV module as the local wind creates a cooling effect on the module. The cooling effect is related to wind velocity and wind temperature as described in 2.4.2. Increased local wind velocities cause the module temperature to drop as the convective heat loss from the surface of the modules are greater at higher local wind velocities (Amin et al. (2009) and Smets et al. (2016)). The reduced module temperature further improves the module performance as described in figure 2.10 and equation 2.7. However, wind velocity is also related to the phenomenon of soiling, which impact the system performance and is discussed in the next section.

2.4.3 Shading

Shading of cells in a module may have a major impact on the power generated from a module. If a module is completely shaded power generation is diminished. If the module is partially shaded the current in the whole string the shaded cell is in, may be lowered to a minimum. As the current generated in a cell is proportional to the irradiation incident on the surface of the cell, reduced irradiation on one cell due to shading will significantly decrease the generated current. For cells connected in series, the current generated in the shaded cell will dictate the current flowing in the whole string. The resulting voltage generated in the unshaded cells may be dissipated in the shaded cell, leading to hot spot heating as illustrated in figure 2.11. Hot spot heating may cause injuries and damages on the cell.

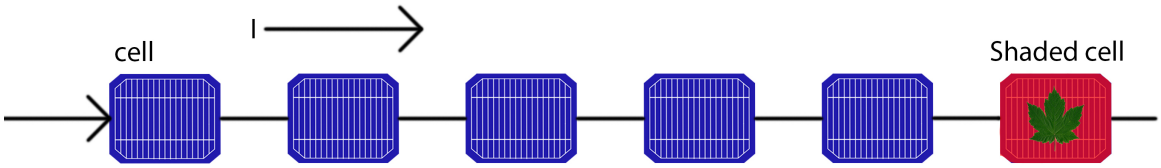

(a) A leaf shading the last cell.

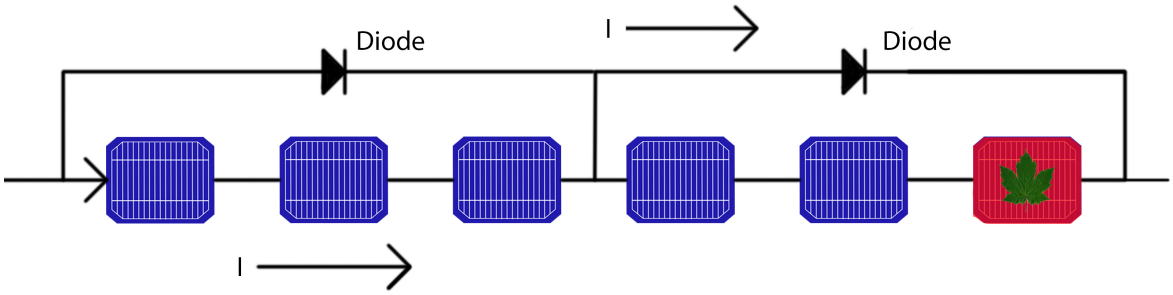

(b) The insert of diodes to bypass the shaded cell.

Figure 2.11: The upper figure illustrates the hot spot formations as a result of shading of a cell. This cell decreases the current in the whole string. The lower figure depicts the insert of a bypass diode to relieve the string of the shaded cell.

For a module consisting of 60 cells in series, a lot of power (high current from normal functioning cells and voltage generated by each cell) may be dissipated in the shaded cell. The module is hence equipped with bypass diodes. Normally 3 bypass diodes are used on one string, making 20 cells share one bypass diode (Smets et al. (2016)). The bypass diodes are connected in parallel over the cells and when the voltage from the unshaded cells become to high for a partially shaded cell the current will pass through the bypass diode instead of the shaded cell. The result is that the generated current in the string will be equal to that of a single, normal functioning,

cell and not dictated by the shaded cell.

A study conducted by Paraskevadaki and Papathanassiou (2011) investigated the impact of shading on multi-crystalline Silicon PV modules. Their study analyzed how materials with different transmittance rates (TR) covering parts of a module reduced the total power output. The study showed that a material with 28 % TR covering 17 % of the module area reduced power output to about 0,31 % of the unshaded value. For a material with 64 % TR covering the same area, the power output was reduced to about 68 % of the unshaded value.

2.4.4 Soiling

Soiling is the deposition of airborne particles on the surface of PV modules. In the context of this thesis, the airborne particles refer to both natural dust and soil particles, but also industrial particles as soot and carbon. Hence, soiling is influenced by the geographical site, mainly related to environment and weather conditions (Goossens and Van Kerschaever (1999)). The accumulation of dust and other airborne particles on the surface of PV modules reduce the performance of the PV system as solar irradiation being absorbed by the modules is reduced. Low-tilt systems are particularly prone to soiling according to Alet et al. (2014). The reasons being that more dirt may accumulate for lower tilt angles, and that the effect of natural cleaning through rainfall will be less efficient for low-tilt systems. If the system experience frequent precipitation the dust and soil on the modules are more likely to be naturally cleaned. Studies conducted by Caron and Littmann (2013) show that as little as 0,5 mm of rainfall is sufficient to naturally clean modules in areas with lighter soiling rates. Snowfall may also clean the modules, but it also may cover the modules completely and eliminate power generation. If the snow partially slides of the system, it will experience shading as described in section 2.4.3 above.

Snow and frost may be counted as soiling particles. Snow covering modules can completely diminish power production. Frost has the same capability. Frost consists of ice particles that deposits on the surface of the PV modules when the temperature is sub zero. Snowfall can be accounted for, but partial snow covering modules and frost on the PV surface are difficult measures to quantify. Not only in terms of amount of snow and frost, but also in terms of shading area. Frost and snow have different transmittance rates (TR) that impact the shading levels differently, as explained in section 2.4.3.

2.4.5 Array incidence loss (IAM)

Array incidence loss describes the decrease of solar irradiation reaching the surface of the PV modules, with respect to irradiation under normal conditions, due to reflections increasing with the incidence angle (PVsyst (2014)). The term for this loss is IAM, for Incidence Angle Modifier. IAM is an optical loss occurring when the solar angle of incidence on the surface of the PV modules is greater than zero. The concept of IAM is illustrated in figure 2.12.

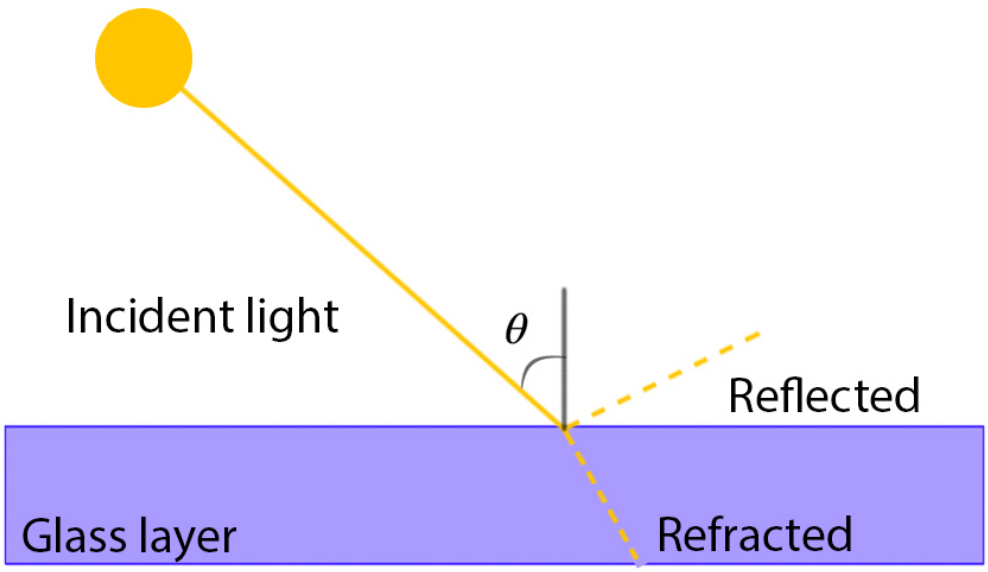

Figure 2.12: Illustration of the IAM effect. Incident light on the module may be: absorbed, reflected or refracted. The result is that (for most angles) the absorbed light intensity is not equal to the incident light intensity on the module.

For systems that does not track the direct beam incidence angle (orientation and tilt), the incidence angle will in most cases be greater than zero. Therefore, such systems are more prone to be affected by array incidence losses, which is the case for the system at ASKO. IAM depends on several factors, some of the more important being latitude, received irradiation and tilt of the modules. A study done by Martín and Ruiz (2005) derived an annual reflection loss of 5,31% with a 10° tilt angle at a latitude of 59,5°, which corresponds to Oslo. This study may be used as a reference for analyzing IAM loss in PVsyst. The PV modules at ASKO are mounted in two different orientations. This may potentially contribute to less total incidence loss as all the modules will not experience the same angle of incidence at all times.

The optical losses can be reduced by the use of anti-reflective (AR) coating on the surface of the protective layer (glass) of the PV modules as shown by a study by Perers et al. (2015). The CS

250 modules used in the case study are not equipped with an AR coating. The IAM loss can be calculated with the following equation:

$$F_{IAM} = 1 - b_0 \left(\frac{1}{cos(\theta)} - 1 \right) \tag{2.9}$$

F_{IAM} is the irradiation absorbed by the module, adjusted for the optical loss due to reflection increasing with the incidence angle on the plane, θ. b_0 is a material dependent constant, measured to be 0,05 for Silicon crystalline modules with a glass layer without AR coating (PVsyst (2014)). Equation 2.9 relates to a parametrization called ASHRAE, which the model used for IAM loss in PVsyst.

2.4.6 Electrical efficiencies and losses

The PV modules generate DC current that, before being converted to AC current in the inverters, are transported by cables from the modules to the inverters. The system will therefore experience Ohmic resistance loss in the cables. The loss is in form of power (W) as currents travels in the conductor (cables) and can be calculated by:

$$P = J^2 \cdot R \tag{2.10}$$

The resistance, R, of the conductor may be calculated with the following formula:

$$R = \frac{\rho \cdot L}{A} \tag{2.11}$$

Where, ρ is the resistivity of the conductor material measured in ($\Omega \cdot meter$), L is the length of the cable (m) and A is the cross section of the cable (m^2).

2.4.7 Mismatch losses

Mismatch losses are due to solar cells having different characteristics and electrical abilities. As explained in section 2.4.3 the cell with the lowest current will dictate the current in the whole string. A mismatch of cells or modules occur when cells or modules with different characteristics (IV curves) are connected together. The cell with the lowest generated current will reduce the generated power in the other cells in the string. Mismatch loss in a PV system is mist evident between modules. The mismatch loss may be reduced by grouping modules with similar characteristics together, although no modules are identical in a real scenario.

2.4.8 Degradation

The total power delivered from a system will decrease with the time the modules have been exposed to sunlight. There are degradation losses due to the first exposure of light and due to aging. The phenomenon of degradation due to light exposure is named LID, for light induced degradation of the cell performance. The efficiency of the modules suffers from degradation the first days they are exposed to illumination before they reach a stable level. The degradation value may lie between 1-3% (PVsyst (2014)). The LID loss is not included as a default loss parameter in PVsyst as it is not sufficiently established.

Aging is a result of weather and time impacting the performance of the system, both internally and externally (Smets et al. (2016)). Aging include factors as cracks due to thermal stress, hail, hot spot, mismatch and by pass diode failure. These factors may also results in damaged cells that performs poor compared to normal operating conditions and results in lower generated current. Over time modules can suffer from encapsulation failure leading to yellowing of the module surface.

Chapter 3

Data

The techniques used to measure or estimate meteorological (meteo) data in a particular place at a certain time are vital for the accuracy of a simulation. Besides solar irradiation, parameters such as wind and temperature are important for the power production of a PV-system (as explained in section 2.4.2). In this section, the measurement instruments and methods used to collect data utilized in the thesis will be explained. Thus, it may be other and perhaps more efficient methods of measurement. There are two methods to measure and estimate data, namely terrestrial measurements and satellite measurements.

The first method is based on ground equipment used in weather stations. Different types of ground equipment and the purpose of the equipment is shown below:

- A pyranometer: Measure irradiation
- Anemometer - Measure Wind
- Thermometer - Measure Temperature

The second method is based on the use of satellites. Solar irradiation is estimated by using satellite images of cloud cover and applying a radiation model (Honsberg and Bowden (2014)). The temperature is estimated by measuring radiation values in different wavelengths that are converted to temperature values using mathematical models.

3.1 Error and Uncertainty

The source of the data used for forecasting introduces statistical uncertainties. That is, the error and uncertainty is directly linked to the quality and collection of the data. Most of these errors are related to instrument sensors and their construction (Younes et al. (2005)). The two different methods of collecting data described in the section above introduce different error related to the method itself. Some important factors for quality of data are related to:

- Type of instrument
- Quality control of instrument
- Instrument placement
- Calibration
- Maintenance

This section will explore the factors mentioned above for all instruments described in the thesis, as well as it may be described with the given information. For the data to be accurate and reliable for modeling, the weather stations have to be located in the vicinity of the system. The further away the location of the system is from the weather station, the more unreliable will the data become. That is due to local climate patterns, topography etc. Some examples are different cloud cover and obstacles that reduce or change wind direction.

Satellites have problems separating clouds from snow covered landscape. One of the reasons is that Norway is located at a high latitude. That makes satellite measurement less reliable due to low incident angle. According to Younes et al. (2005), the use of ground measurements are more reliable compared to the use of satellites to estimate weather data.

3.2 Data Sources

Meteo data collected from the case study at ASKO is used as reference values for modeling in this thesis. Meteo data from other sources, introduced in the next section, are compared to the reference values to establish possible discrepancies. The previous section described the introduced error from the meteo data and is thus important for understanding possible uncertainties in forecasting models. Deviation between meteo data from the different sources can result in deviation between simulated and produced energy.

3.2.1 ASKO

The collection of meteorological data at ASKO is done by ITAS - Scanmatic Instrument Technology AS and is accessed with permission from the companies Brenden and Ruud-Hansen from ITAS and Tuv from FUSen. The information about the equipment is given by ITAS.
Instruments have been installed at the roof in the area where the PV system is installed. As this is data gathered at the location of the system, it should be the most accurate and reliable data. The weather sensor system at ASKO is equipped with:

- Kipp & Zonen CMP 10 pyranometer
- Campbell scientific 110PV surface thermistor
- Campbell scientific CS125 air temperature sensor.
- Ventus ultrasonic wind sensor

The Kipp & Zonen CMP 10 pyranometer measures global irradiation. A picture of this device is shown in figure 3.1 below. Measurements are made every 5th second and is stored as an hourly average value. The sensor has an accuracy of 7 to 14 µV/W/m2 as shown in table 3.1.

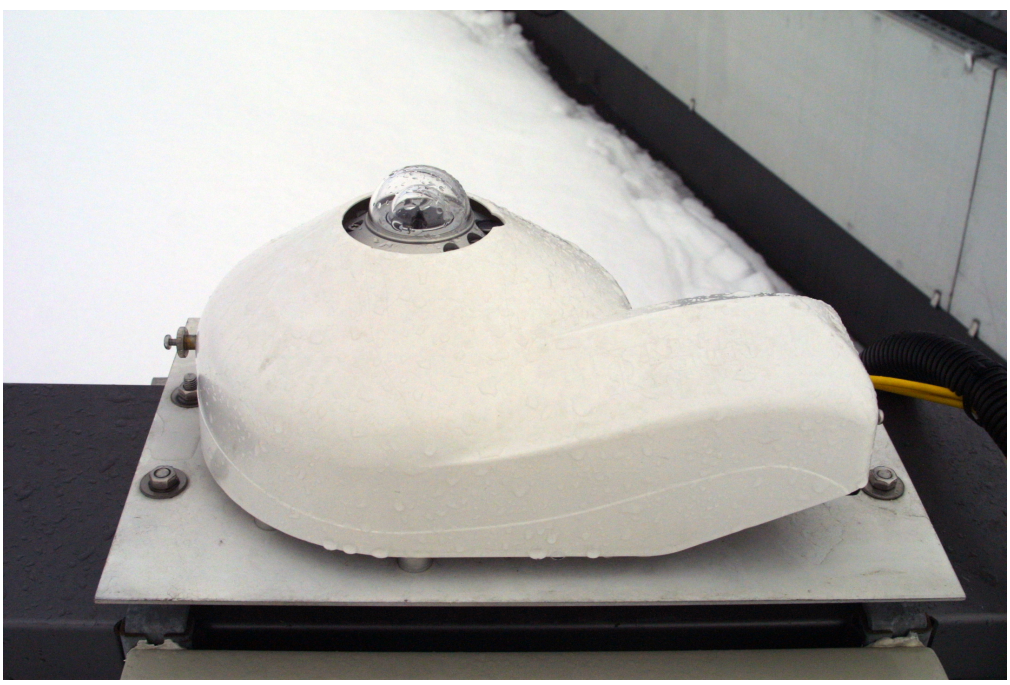

Figure 3.1: The Kipp & Zonen CMP 10 pyranometer at the rooftop at ASKO. This pyranometer is placed almost in the center of the system and is located about 30 cm above the surface of the modules.

Table 3.1: Specifications for Kipp & Zonen CMP 10 pyranometer

Measurement	Measurement range	Resolution	Accuracy
Global Horizontal irradiation	285 - 2800 nm	0,01	7 - 14 µV/W/m2

The Campbell scientific 110PV surface thermistor measures the surface temperature of solar cells. Table 3.2 below shows the specification of the sensor. Measurements are taken every 5th second and the data is stored as an hourly average value.

Table 3.2: Specifications for Campbell Scientific 110PV surface thermistor.

Measurement	Measurement range	Operating range	Accuracy
Surface temperature	-40 to +135 °C	-50 to +140 °C	±0,2 °C at -40 to +70 °C ±0,5 °C at +71 to +105 °C ±1 °C at +106 to 135 °C

The Campbell scientific CS125 measures air temperature and air humidity. Measurements are made every 5th second and stored as hourly average values. The specifications for the CS125 sensor are shown in table 3.3.

Table 3.3: Specifications for Campbell Scientific CS125 air temperature/humidity sensor. RH is short for relative humidity.

Measurement	Measurement range	Resolution	Accuracy
Air temperature	-40 to+70 °C	0,01	±0,3 % at +25°C ±0,4 % at +5 to +40 °C ±0,9 % at -40 to +75 °C
Air humidity	0 to 100 % RH	0,01	±2 % in the range 10 to 90% RH at +25 °C ±4 % in the range 10 to 100% RH at +25 °C

The Ventus ultrasonic wind sensor measures wind velocity and wind direction. Measurements are made every 5th second and stored as hourly average values. Table 3.2.1.2 shows the specifications for the sensor.

Table 3.4: Specifications for the VENTUS ultrasonic wind sensor

Measurement	Measurement range	Resolution	Accuracy	Unit
Wind speed	0 to 75	0,01	± 0,2	m/s
Wind direction	0 to 359,9	0,01	<2	°

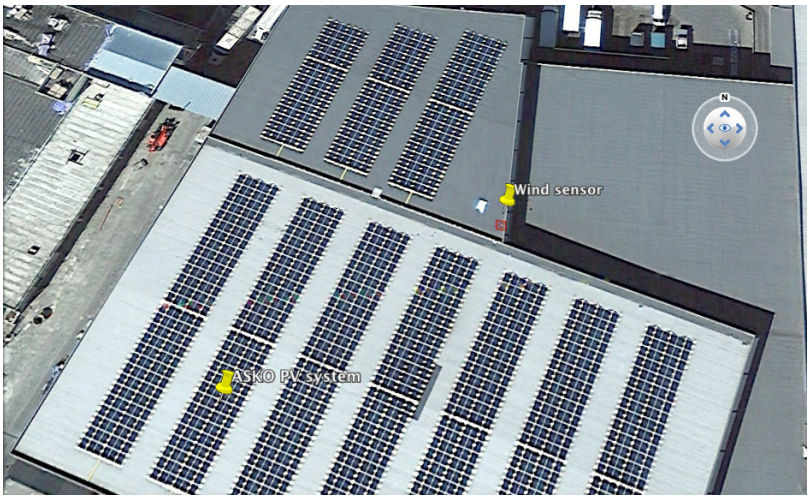

(a) Excerpt from Google Earth

(b) Picture taken at location

Figure 3.2: Picture of the wind sensor and excerpt from Google Earth showing the placement of the sensor. It is located right next to the end of the roof and may therefore experience wind turbulence. The excerpt is taken April 19th, 2016.

Figure 3.2 shows the Ventus ultrasonic wind sensor and its placement on the roof. The placement is not optimal as it might introduce uncertainty related to plausible wind turbulence resulting from wind directions between north and east hitting the wall beneath the sensor and then being directed upwards interfering with wind at the sensor height.

3.2.2 Ås - weather station

Meteorological data from Ås is collected from the field station FAGKLIM, maintained by NMBU. Data are measured every tenth second and stored as mean values every ten minutes. Data is provided by engineer Signe Kroken at NMBU.

Global irradiation is measured with a pyranometer of instrument type, Eppley precision pyranometer. Air temperature values are measured with a PT100 thermometer 2 meters above the ground. The wind velocity is measured using a Windmaster ultrasonic anemometer by Gill instruments. The data is collected 10 meters above the ground and measures both the velocity and the wind direction.

Table 3.5: Specifications of the instruments used at the FAGKLIM station located in Ås-

Instrument type	**Function**	**Unit**	**Uncertainty**
Eppley precision	Pyranometer	W/m^2	about 10 %
PT100	Thermometer	°C	about 0,1 °C
Windmaster ultrasonic	anemometer	m/s	0-20 m/s: 1,5 %, 20-35 m/s: 1,5 %, 35-60 m/s: 3 %

3.2.3 Meteocontrol

Data from Meteocontrol (MC) is collected by the use of satellites and is provided by the University of Oldenburg (Egger). Meteocontrol does not offer wind data, and temperature data had to be bought. Irradiation data was provided by University of Oldenburg without charge, and is the only used parameter from MC. The relative root mean square error is given to be 14,5 % and 3,6 for hourly and monthly values respectively. The information regarding data from MC is added in appendix C.1 and C.2.

3.2.4 Meteonorm

Meteonorm´s (MN) database includes 8325 weather stations and five geostationary satellites. Solar irradiation is based on normalized values from the time period 1991-2010, while temperature and wind speed on the time period 2000-2009. Data for a site of interest is derived by interpolation between different stations to best fit the site. MN allows calculation of synthetic hourly values by using a stochastic model (algorithm) based on the monthly values (Remund and Kunz (1997)). Data from MN introduces a range of errors due to the data being normalized,

interpolated and synthetically generated. The most influential parameter in Norway has been the amount of weather stations. MN´s database currently includes 4 stations measuring irradiation, while there are several more in Norway´s neighboring country Sweden. Until 2016 there were no irradiation station in the vicinity of Oslo, whereas the database now includes a station at Ås, as shown below. The station at Ås is by far the closest station to the system at ASKO and will thus constitute the most significant part of the interpolation value.

Irradiation interpolation locations with distance from the system at ASKO:

- Ås (8 km)
- Karlstad (156 km)
- Borlaenge (280 km)
- Skagen Fyr (206 km)
- Goteborg- Save (211 km)
- Bergen/Florida (313 km)

Uncertainty of yearly values:

- Gh = 3 %
- Bn = 6 %
- Ta = 0,8 °C

3.2.5 NIBIO

The Norwegian Institute of Bioeconomy Research (NIBIO) is one of Norway´s largest research institutes. Agrometeorology Norway (Landbruksmeteorologisk Tjeneste - LMT) is a service by NIBIO providing meteorological data collected from weather stations located around Norway. NIBIO has one station at Ås, which is located next to the FAGKLIM station and has been operating since 1991 (Lmt.nibio.no). All data is measured 2 meters above the ground and the instruments used are presented in table 3.6, according to information from Lmt.nibio.no. NIBIO data collected for this thesis constitute of measurements of: albedo, rainfall, snow-depth. Additionally, wind data recorded by NIBIO is supplied from Ås, as the wind data recorded by FAGKLIM at Ås is absent from January to July.

Table 3.6: Specifications of the instruments used at the LMT NIBIO station located in Ås-

Instrument type	**Function**	**Unit**	**Accuracy**
Genor	Rainfall	mm	± 0,1 mm, operating range down to -30°C
Cambell Scientific SR50A	Snow depth	cm	± 1cm
Vector/Friedrics	Anemometer	m/s	NA
Albedo instrument NA	Measure albedo	Unitless	NA

Chapter 4

Methods

This chapter describes the methodology for conducting the thesis and explains the tools used during the project. The methodology is a major part of the this thesis as it revolves around creating the PV system situation as accurately as possible in the simulation software. In order to conduct a thorough and accurate project in PVsyst the simulation software must be explored and learned. Furthermore, the system at ASKO must be investigated and known to detail for accurate re-construction in the simulation software.

4.1 Google Earth

Google Earth is a mapping software with access to map, satellite images and geographical information all over the world. The software is useful in the planning phase of the project, localizing and evaluating the site. Roof area for a PV system may be located and distances to buildings nearby that may shade the system can be roughly estimated. Google Earth does allow the user to evaluate projects without field work or to prepare for field work more efficiently. Google Earth was used to calculate the azimuth of the building the PV system is mounted on. Figure 4.1 shows a compass overlay with 5-degree intervals marked, which makes it possible to read of how many degrees the building turns away from south (0 azimuth). From the figure it can be determined that the building has an azimuth of 20 degrees. As the module lie in two different orientations, both parallel to the building, the resulting orientations are 110 degrees and negative 70 degrees.

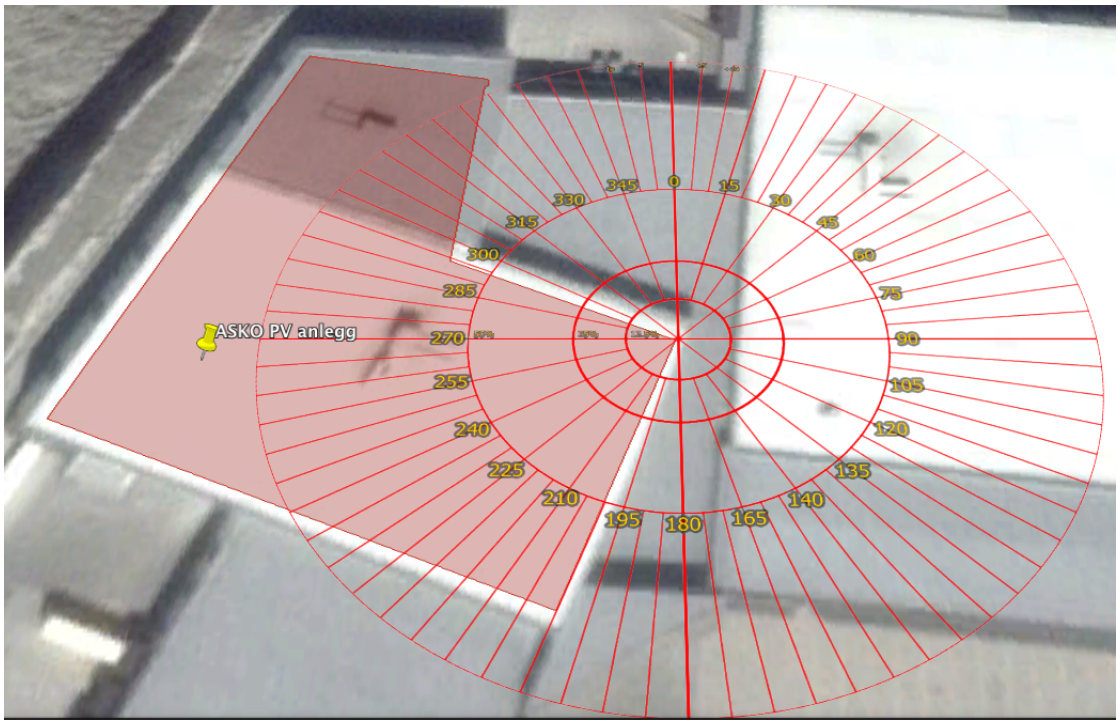

Figure 4.1: Excerpt from Google Earth shows the location, red marked area, of the PV system. Excerpt is taken February 10, 2016.

Remark: During the course of the thesis, Google Earth updated the satellite images over the ASKO ØST area. The result is a significantly higher resolution. More importantly, the PV system and installments related to the system at the roof was included in the images. Thus excerpts from Google Earth taken during the planning process in January and February does differ from the retaken excerpts in April and May. The updated images make planning and pre-evaluation of the site a lot easier. The lack of good images were the main reason for the necessity of a field trip to the site.

4.2 Matlab

Statistical analysis and evaluation of data used in the thesis have been executed with the Matlab programming software, version R2015b (mat (1998)). The codes written in Matlab analyze the different data used and applies statistical methods as Relative Error (RE) and Root Mean Square Deviation (RMSD). The software is used to create the numerous plots to visualize the statistical data.

4.3 PVsyst: An Introduction to the Software

PVsyst is a Swiss simulation software developed to accurately plan and design PV systems with the best technical and economical solution (PVsyst (2014)). PVsyst is a tool used by engineers and investors in the energy and solar industry to forecast and simulate production of energy. PVsyst is a comprehensive software that allows for a wide range of configurations in the design. It allows for preliminary design (quick studies), project design (full-featured studies), databases (sites, PV modules, inverters etc.) and tools. There are some parameters that are mandatory and some that are optional to execute a simulation. For a project as conducted in this thesis, the project design with the grid connection option in PVsyst is used. The project design menu is shown in figure 4.2. The menu shows options for site and meteo as well as albedo-settings. Then follows three mandatory input parameters: *Orientation*, *System* and *detailed losses*. The remaining input parameters are optional and consists of: *Horizon*, *Near shadings* and *module layout*.

This thesis divides parameters in PVsyst in two: Primary and secondary parameters. The primary parameters consists of the information entered into PVsyst when designing the system. Those are:

- Inverter type and characteristics, eg: maximum/minimum current and voltages.
- Module type and characteristics: maximum/minimum current and voltages, resistant for shunt and series, current temperature coefficients etc.
- The Meteorological file: Global horizontal irradiation, diffuse irradiation, temperature, wind speed, module temperature and more.

The secondary parameters are the parameters that can be adjusted by the user according experimental or measured data. These consist of albedo values and the losses included in the detailed losses option in PVsyst. These are listed and described in section 4.3.7.

Figure 4.2: PVsyst project design menu, displaying all parameters included in the design and configuration. The green color represents a completed stage that is accepted by PVsyst. The red color implies that the chosen configuration is not optimal and needs to be adjusted before being able to proceed.

4.3.1 Site and Meteo

The PV system at ASKO Øst is located in Vestby, Akershus county in Delitoppen 4. Location details about the system received from Tuv in FUSen was corresponded by the use of Google Earth to investigate the location. Location details are displayed in table 4.1.

Table 4.1: ASKO location details.

Variable	Value	Designation
Latitude	59,589571780313	Degrees
Longitude	10,742225646973	Degrees
Altitude	82	Meters
Timezone	Europe/oslo	hrs

Meteorological data is defined under the site and meteo settings. Meteonorm data is included in the PVsyst software as well as NASA data. Other data sets may be imported into PVsyst, as explained in section 4.3.2.

Simulation scenarios

The project is divided into several simulation scenarios (related to meteo parameters), to investigate the impact of the different parameters on the forecast result. This will also help to understand how PVsyst may improve simulation accuracy with more information.

- Scenario 1: Simulation with global irradiation and PVsyst default mandatory values.
- Scenario 2: 1 + diffuse irradiation, temperature and wind speed where accessible.

PVsyst temperature values

Ambient temperature is a mandatory input parameter in PVsyst and is obtained through Meteonorm´s database. The values from Meteonorm used in scenario 1 are shown in table 4.2 below. These values are thus the values used by Meteonorm in all scenarios and are also displayed in figure 5.3.

Table 4.2: PVsyst values for temperature used in scenario 1. Values are obtained form Meteonorm and is thus the values used by Meteonorm in scenario 2.

Date	**PVsyst Temperature (°C)**
Jan	-0,10
Feb	-0,60
Mar	1,60
Apr	6,30
May	11,10
June	14,40
Jul	16,90
Aug	16,50
Sept	12,50
Oct	7,60
Nov	3,90
Dec	0,50

4.3.2 Importing meteorological data

The meteorological (meteo) data provided by the different sources described in 3 was imported into PVsyst so the different scenarios could be analyzed. The import tool is found in PVsyst under the tab "Databases", and is named "import ASCII meteo file". The tool allows the user to define which parameters to include from the file. Hourly values for all sources were then imported and connected to the site. The imported data variables are presented in table 4.3.

Table 4.3: Variables in meteorological data.

Data variable	**PVsyst option**
Global irradiation	mandatory
Ambient temperature	mandatory
Diffuse irradiation	optional
Wind speed	Optional

Some of the meteo sources do not include all four variables. In the cases where only global irradiation is provided, PVsyst will supply Meteonorm temperature values as it is a mandatory input parameter. Irradiation incident on the plane, used to predict output energy, is calculated by PVsyst utilizing the global horizontal irradiation and a transposition model named the Perez model (PVsyst (2014)). After importing data, PVsyst advised to quality control the data with the "Graphs and tables"-tool to check a potential time shift of the data. The time shift is estimated by PVsyst with reference to the time record on the imported file and PVsyst estimated time assessed by the clear sky model. Recorded time on the meteo file should correspond to the PVsyst estimated time, which is used for evaluation of the solar geometry (PVsyst (2014). A detected time shift may be corrected by several measures. The most convenient is to apply a time shift correction, as shown in figure 4.3.

For the ASKO meteo file, PVsyst detected an average of negative 9 minutes that were corrected by applying a positive 9 minutes time shift correction. The Ås meteo file had a time shift of positive 12 minutes that was corrected. The Meteonorm and Meteocontrol meteo file had a negative and positive time shift of 3 minutes respectively, that were not corrected due to the small gap.

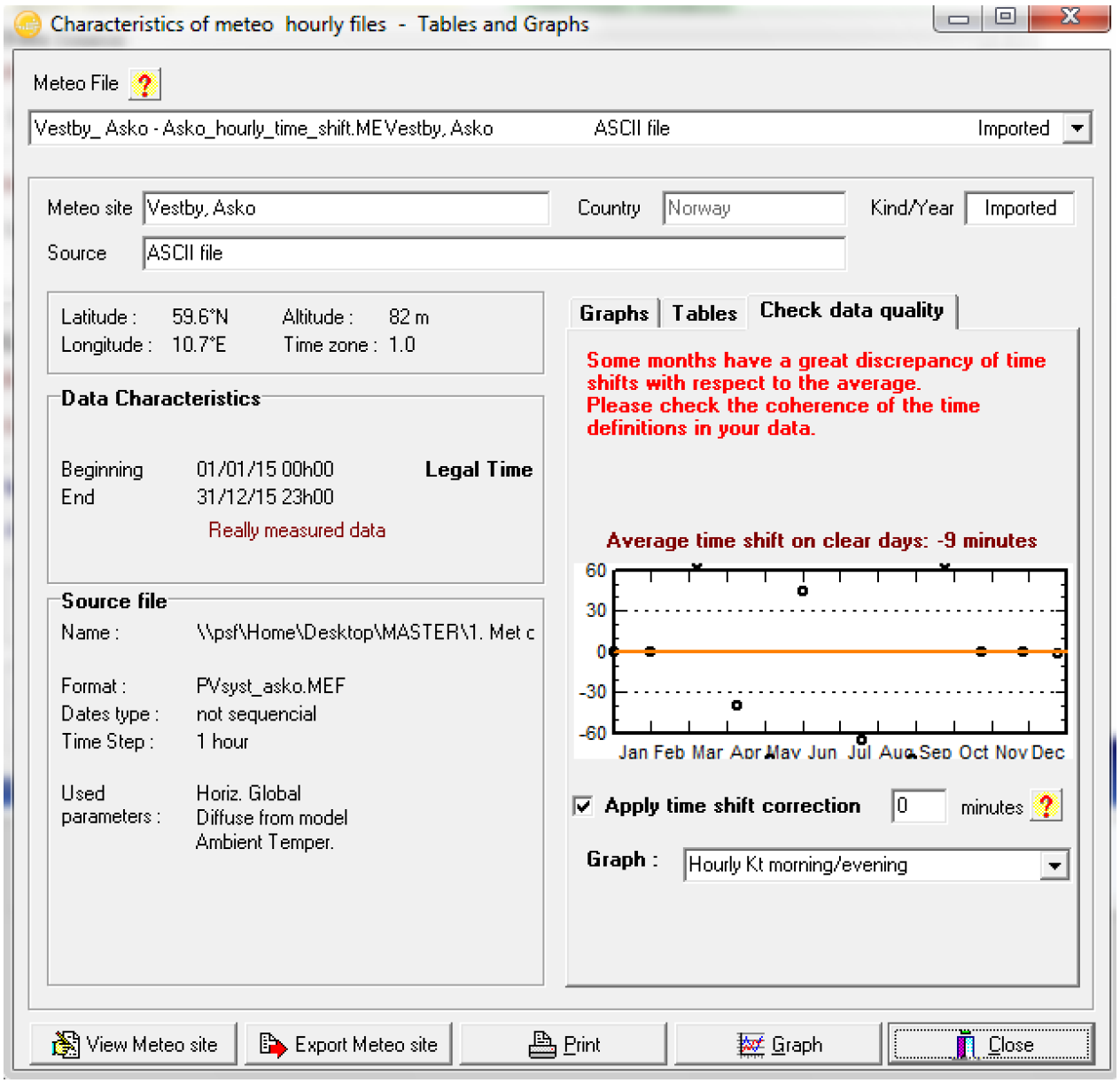

Figure 4.3: Excerpt from PVsyst showing the "Tables and graphs"-tool and the data quality check for the ASKO meteo file.

4.3.3 Albedo – settings:

This parameter adjusts for albedo values, the fraction of solar irradiation reflected from Earth. This value depends on the reflectivity of the surface. Dark materials absorb more light, than light colored materials. Albedo values are thus very dependent on the specific location. In PVsyst there are options for a yearly value or monthly values. In this thesis the standard values for monthly values will be used for the two main scenarios before values for albedo are adjusted based on albedo values for different surfaces. In PVsyst standard albedo values from some surface are included, as shown in table 4.4. In PVsyst, albedo value is set to 0,2 by default, but monthly values may be defined by the user.

Table 4.4: PVsyst standard albedo values.

Surface type	**Albedo value**
Urban situation	0,14-0,22
Grass	0,15-0,25
Fresh grass	0,26
Fresh snow	0,82
Wet snow	0,55-0,75
Dry asphalt	0,09-0,15
Wet asphalt	0,18
Concrete	0,25-0,35
Red tiles	0,33
Aluminmum	0,85
New galvanized steel	0,35
Very dirty galvanized steel	0,08

4.3.4 Orientation

Orientation consists of tilt and azimuth angles of the modules. The tilt of the modules at ASKO is 10 degrees. Because it is a two faced system, it has two azimuth angles. An excerpt pf the Orientation section in PVsyst is shown in appendix B.5. The first angle being is 110 degrees and the second is negative 70 degrees. As the system at ASKO is already operating, experimenting with tilt and azimuth for optimal performance is interesting and valuable, however not constructive for the study, as it can not be changed. The only reason for experimenting with alternative orientations is for further installment of PV systems at ASKO.

4.3.5 System

The system parameter consists of designing the sub-arrays of modules and inverters. This is done based on the schematics and configuration of the system received from FUSen, shown in figure 4.4 and table 4.5. The table shows the configuration and design of the five sub-arrays of the system. Further data about the inverters and modules are found in appendix A.

Figure 4.4: Schematic layout of the system at ASKO. The sub arrays termed SA described in table 4.5 are shown above each sub array of modules. The two red dots signalizes the locations where the cables from the different strings go beneath the roof and to the inverters that are stored inside the building. SA: 1, 2 and 3 are connected to inverters by the upper red dot, while SA 4 and 5 are connected to inverters by the lower red dot. With permission from FUSen

Table 4.5: Table including the system details about modules and inverters and how they are connected. The designation shows sub-array (SA) number, which is referenced in figure 4.4.

Designation:	**SA 1: 20kTL-6x15**	**Designation:**	**SA 2: 20kTL-6x17**
Power:	22,5 kWp	Power:	25,5 kWp
Area:	147,32 m²	Area:	166,96 m²
Tilt:	10 °	Tilt:	10 °
Orientation:	90 °/270 °	Orientation:	90 °/270 °
series-connected:	15/15	series-connected:	17/17
Parallel-connected:	3/3	Parallel-connected:	3/3
Inverter type:	Sungrow SG 20KTL	Inverter type:	Sungrow SG 20KTL
Number of inverters:	1	Number of inverters:	1
Module type:	IBC Solar PolySol 250 CS/	Module type:	IBC Solar PolySol 250 CS/
Number of modules:	90	Number of modules:	102
Designation:	**SA 3: 30kTL-6x19**	**Designation:**	**SA 4: 30kTL-6x24**
Power:	28,5 kWp	Power:	252 kWp
Area:	186,6 m²	Area:	1649,9 m²
Tilt:	10 °	Tilt:	10 °
Orientation:	90 °/270 °	Orientation:	90 °/270 °
series-connected:	19/19	series-connected:	24/24
Parallel-connected:	3/3	Parallel-connected:	3/3
Inverter type:	Sungrow SG 30kTL	Inverter type:	Sungrow SG 30kTL
Number of inverters:	1	Number of inverters:	7
Module type:	IBC Solar PolySol 250 CS/	Module type:	IBC Solar PolySol 250 CS/
Number of modules:	114	Number of modules:	1008
Designation:	**SA 5: 30kTL-7x24**		
Power:	42 kWp		
Area:	274,98 m²		
Tilt:	10 °		
Orientation:	90 °/270 °		
series-connected:	24/24		
Parallel-connected:	4/3		
Inverter type:	Sungrow SG 30kTL		
Number of inverters:	1		
Module type:	IBC Solar PolySol 250 CS		
Number of modules:	168		

4.3.6 Applying system information in PVsyst

There are some issues related to applying the system information in PVsyst. The PolySol 250 CS modules were not included in the PVsyst database. The result was that module characteristics were manually entered based upon information received from FUSen that are also available at the producers (IBC Solar) web page. The definition of the modules is presented in figure 4.5. This information is given appendix A.1 and A.2.

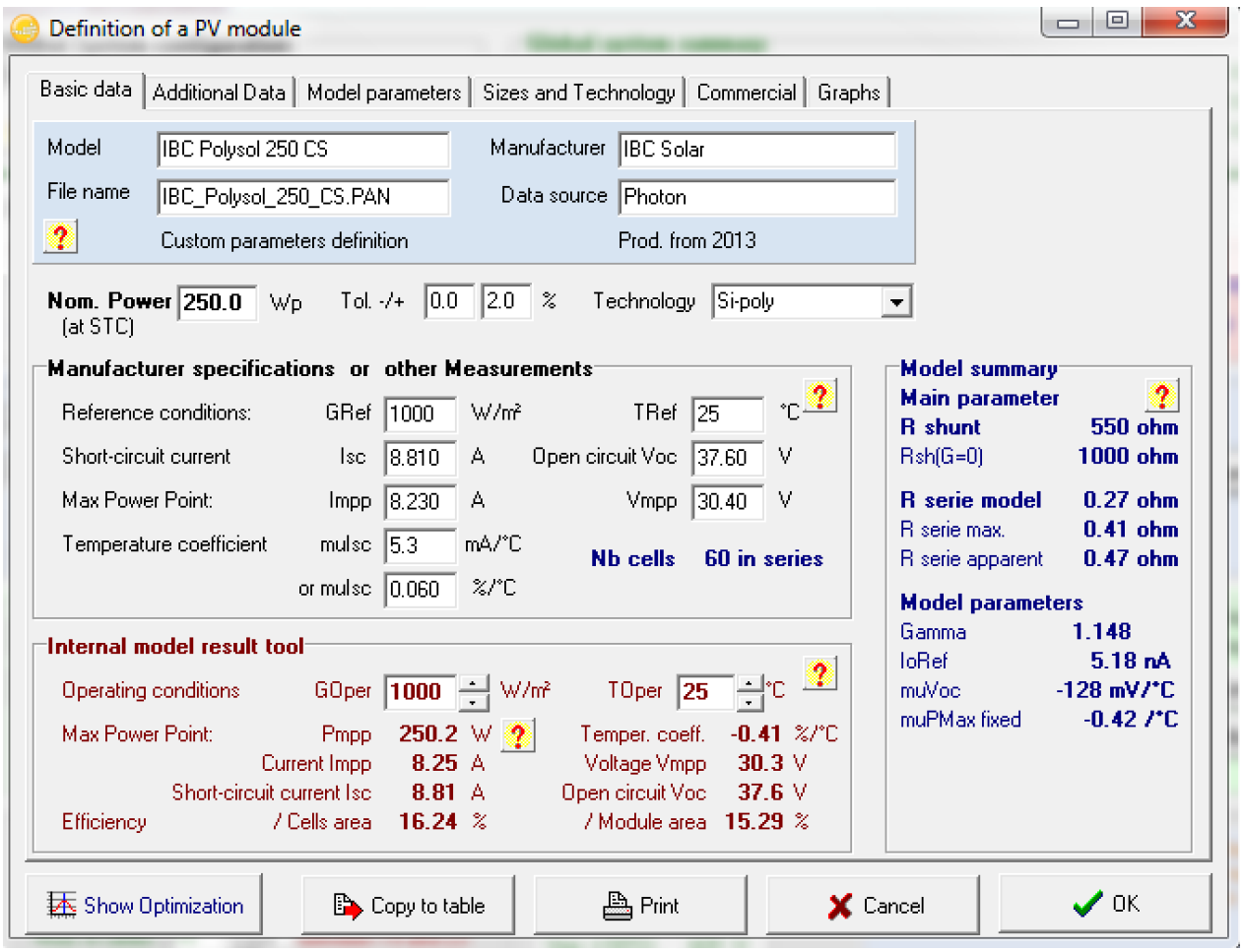

Figure 4.5: Defining the IBC PolySol 250 CS module characterstics in PVsyst according to the original data sheet.

After being in contact with IBC Solar regarding IAM loss and cable loss, new (alternative) information was received through e-mail with Bentley (l 21) (project manager in EPC International), April 21 2016, that changed some of the characteristics slightly. The alternative characteristic data sheet is given in appendix A.3. The shunt and series resistance (R_{sh} and R_s) of the cell were not specified in the original data sheet and were thus estimated by PVsyst based upon the given module characteristics. In the alternative, this information was given as $R_{sh} = 250\ \Omega$ and

$R_s = 0,13\ \Omega$. IBC solar includes a different temperature coefficient for the short circuit current in the second data sheet. The short circuit current is there specified to $I_{sc} = 2,2\ mA/°C$, compared to $I_{sc} = 5,3\ mA/°C$ in the original data sheet.

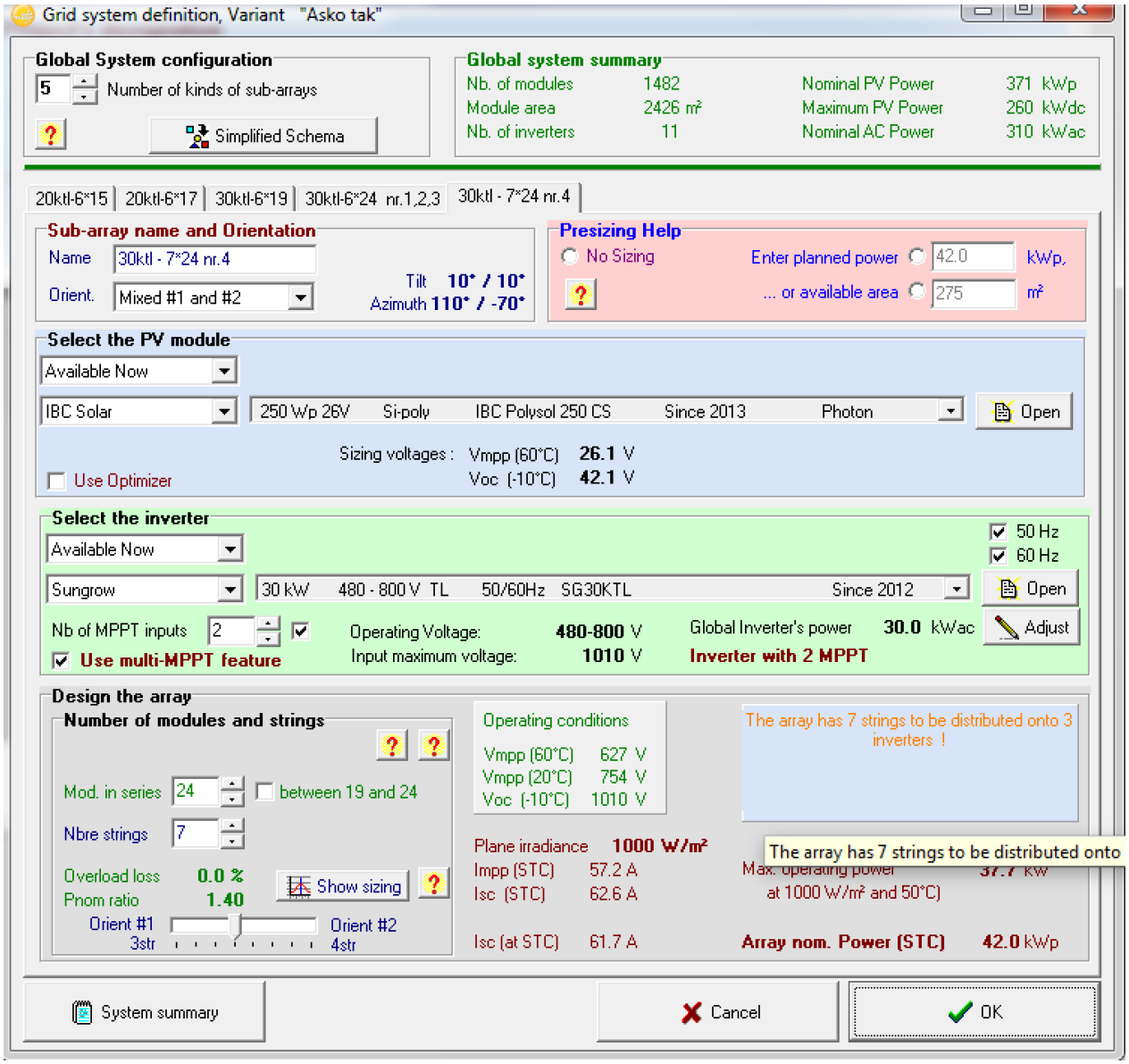

Figure 4.6: Excerpt from PVsyst presenting the system information section, where module and inverter configurations is described.

When designing the system with the sub-array as described in table 4.5, some of the arrays were not optimized for each other according to PVsyst. PVsyst corresponds inverter characteristics with string characteristics under certain operating conditions. For some of the sub-array´s (SA´s) the operating conditions of the string did not correlate with the rated specifications for

the inverter. The solution was to manually change the operating conditions of both the inverter and the module in order to be allowed to run a simulation by PVsyst. In figure 4.6 PVsyst presents some of the bugs experiences while designing the project.

The figure shows how PVsyst interprets 1 inverter with 2 multiple power point trackers (MPPT) as 3 inverters for SA 5. A bug that could not be located and fixed during this project. Also, the operating condition for V_{oc} of the modules at -10 $°C$ is estimate to 1010 Volts. According to characteristics about the inverter (appendix A.7), the input maximum voltage is rated at 1000 Volts. In order to continue the design of the system in PVsyst, save the project and run the simulation, the inverter characteristics had to be adjusted manually to 1010 Volts.

The new information was received after most of the scenarios were executed. As executing these simulations and analyzing the results is a time consuming process, the results will not be re-executed due to limited time. The results therefore operate mainly with the original data sheet. However, the impact of the new information on the simulation will be investigated, in order to analyze a potential uncertainty in the first simulation results.

4.3.7 Detailed Losses

Loss parameters in PVsyst are defined in detailed losses. PVsyst offer default values for parameters that are sufficiently established and proposed default values for parameters that are not proven to influence all systems. Most of these parameters can be adjusted according to the users own estimations, although some are quite comprehensive and depend on the type of modules used (IAM). Some parameters can be defined as yearly values and monthly values. Monthly values create more comprehensive and accurate estimations and simulations. An excerpt from the detailed loss section is included in appendix B.6, displaying the thermal loss option.

The default loss parameters included in PVsyst simulations, used in scenario 1 and 2 are shown in table 4.6. The thermal loss setting in PVsyst offer 3 default values according to the mounting of modules. Thermal loss in PVsyst depends on mounting as it determines the heat loss of the modules due to air flow around the modules as well as ambient temperature, as described by equation 2.7 and 2.8. The three mounting options and their heat loss values are listed below:

- 1. free mounted modules with air circulation

- 2. semi integrated with air duct behind
- 3. Integration with fully insulated back

At ASKO, the modules are mounted at the rooftop with a ten degree tilt. The best option for a default value in thermal losses is therefore "semi integrated with air duct behind". Other loss parameters that can be defined by the user, or specified included by the user (to PVsyst proposed default values) are LID loss and mismatch loss. The detailed losses are defined later in the thesis (4.5) according to estimations and calculations for the ASKO system.

Table 4.6: List of default loss parameters and their values included in PVsyst. The listed default values may be adjusted by the user. Other loss parameters can be included by user defined values or PVsyst proposed values.

Parameter	**Type**	**Value**	**Unit**
Thermal loss: "Semi-integrated with air duct behind	Constant loss factor, U_c	20	(W/m^2K)
	Wind loss factor,U_v	0	$(W/m^2K/(m/s))$
Ohmic Loss	Global loss fraction at STC	1,5	%
Module quality	Module efficiency loss	-0,5	%
	Mismatch loss, fixed voltage	2,5	%
Soiling loss	Yearly	3	%
IAM	ASHRAE model, defining b_o	0,05	Unitless

4.3.8 Horizon

The horizon is an important parameter in PVsyst as it defines objects that may shade for larger parts of the system, especially at low sun angles. In PVsyst the horizon profile consist of objects that are at a distance of about ten times the size of the system. The horizon profile can be defined manually by measuring distance and height of such objects and insert them into a PVsyst table. For this thesis, the horizon was calculated by the use of Meteonorm´s horizon calculation software, built into the Meteonorm software. The software uses a 180-degree panorama picture uploaded to Meteonorm´s software that creates the horizon profile through image analysis. The panorama picture is shown in figure 4.7 and the resulting horizon profile in figure 4.8. Meteonorm exports the horizon profile as a PVsyst friendly file that may be imported directly into PVsyst.

Figure 4.7: Panorama picture taken from the rooftop at ASKO. This was taken at module height level with the center of the picture facing south.

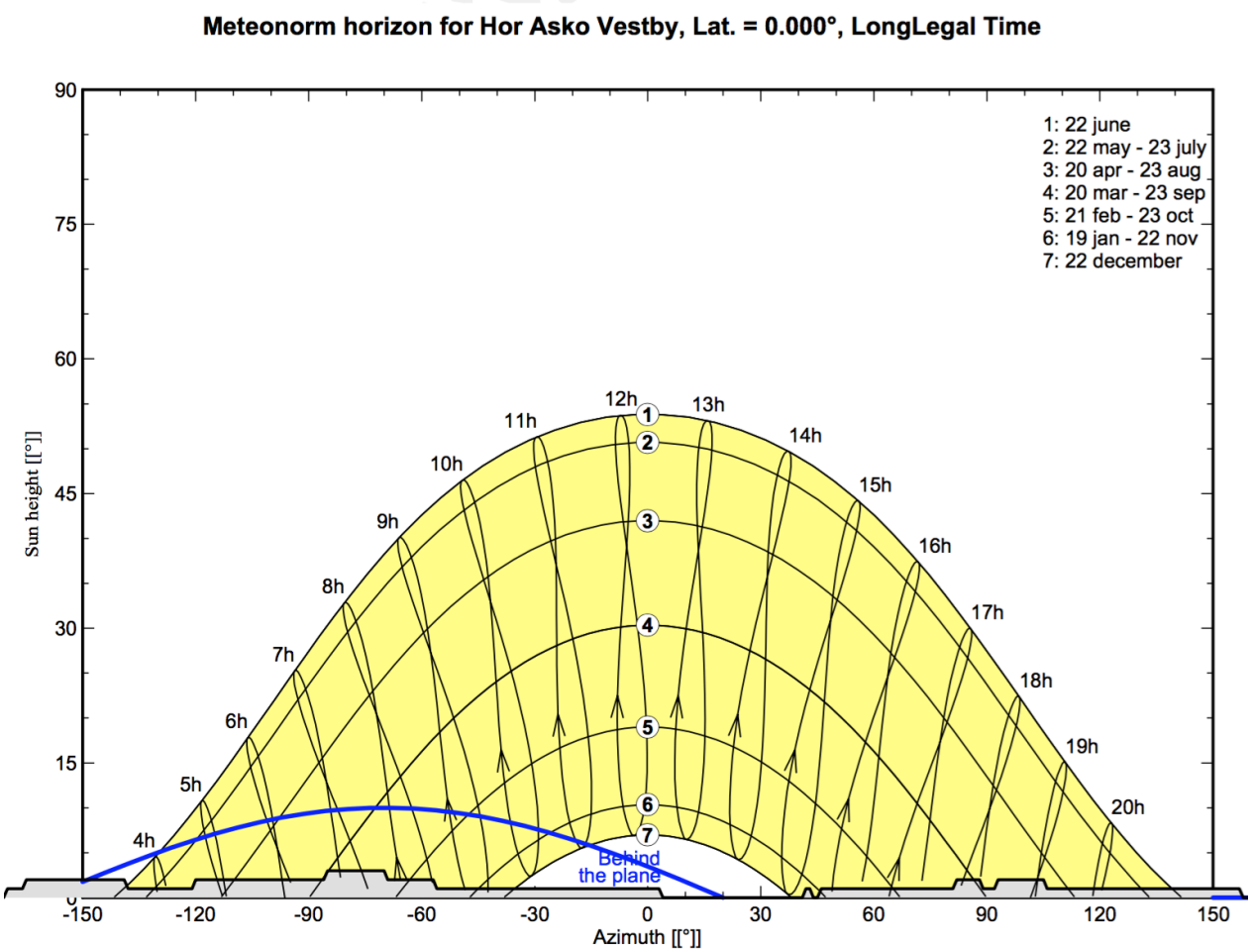

Figure 4.8: Excerpt of the horizon profile shown in PVsyst. The gray area is the resulting horizon profile created in Meteonorm´s software.

4.3.9 Near shadings

The near shadings section is a quite important process of the simulation with PVsyst and an impressive feature. In this section the PV system is carefully constructed in a 3D scene that allows shading calculations to be conducted. The construction includes relative placement of buildings and their sizes in a reference system. The modules in the project are then placed with correct tilt and azimuth on the proper location in the scene, as shown in figure 4.9. Information about the modules and the layout of the system are used to place the modules correctly on the roof, according the walls and with respect to each other. Near shadings also includes placement of objects in the scene that may cause shade for some parts of the system. Google Earth and a field trip to the site was necessary to gather data and measurements of the possible shading objects. Except for determining the horizon profile the two most important objects to measure was the small walls around the roof and the small storage house, shown in figure 4.9b.

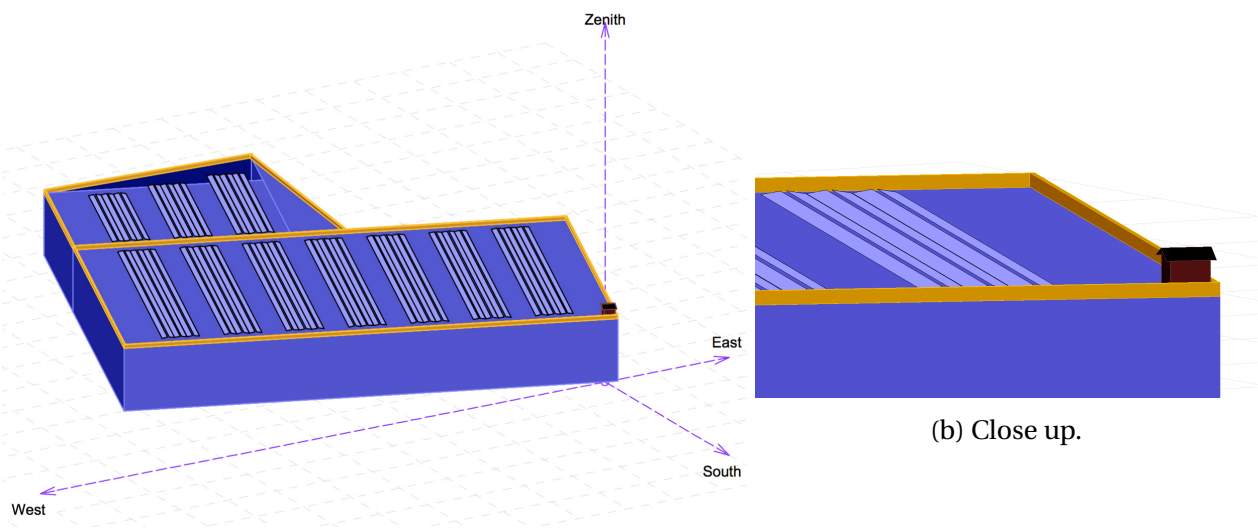

(a) Complete 3D shading scene.

(b) Close up.

Figure 4.9: Excerpt from PVsyst presenting the 3D shading scene. Figure 4.9a shows the complete shading scene with all the necessary buildings, walls and modules included. The ASKO building is represented with the blue/purple color, while the light blue color represent the strings of modules. The yellow color represents a small wall that surrounds the building. The small storage house (brown color) located at the roof is shown in a close up in figure 4.9b.

4.3.10 Module layout

The module layout is an optional design for a more accurate simulation. The near shadings influence on electrical losses are calculated by two methods in PVsyst. The simplest method is "according to strings" and is a rough estimate of the shading loss based upon system information. The most accurate method to calculate electrical loss is "according to module layout". This requires exact knowledge about the positioning of each module in the system. That is: where on the roof it is placed, which sub-array (SA) and on which string and inverter it is connected. Figure 4.10 shows an excerpt from PVsyst where modules are attributed to strings and sub-arrays according to the 3D-scene drawn in Near Shadings.

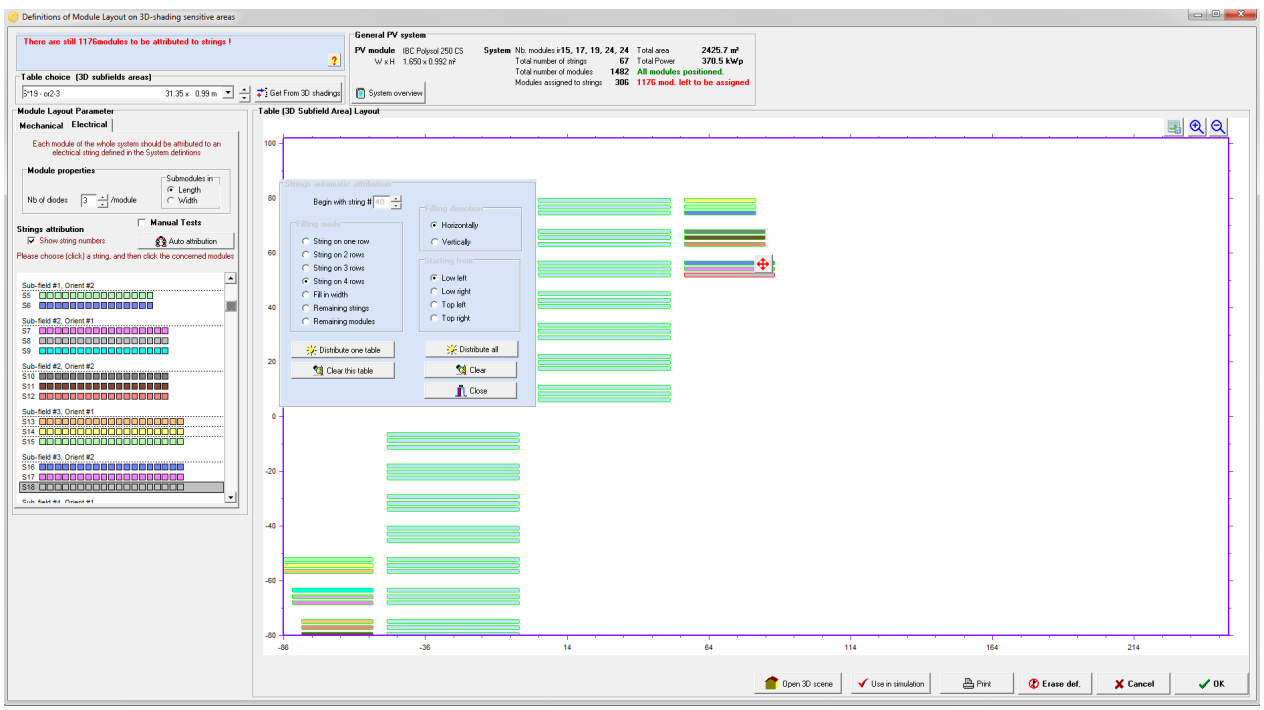

Figure 4.10: Excerpt from PVsyst presenting the definition of module layout.

After attributing modules to strings and inverters the module layout section allows to investigate the individual performance of each SA with respects to the impact of shading on the selected SA´s modules. Electrical loss can differ from SA to SA, dependent on solar movement, horizon and possible shading objects.

4.4 Further Procedure

4.4.1 Comparison

To evaluate the results, simulated energy is compared with produced energy from the PV system at ASKO for the year 2015. The energy values that are compared are the values fed to grid by the inverter. This may give an indication about the accuracy of the meteorological data and the simulation parameters. Then, parameters may be adjusted to investigate how the discrepancies between simulated and produced energy are influenced by the parameters. The simulation process in PVsyst results in a report evaluating the whole project, including energy fed to the grid and global horizontal irradiation estimations. The report also includes a loss diagram for the system, presenting parameters contributing to loss and their respective loss fractions.

4.5 Estimation of Loss Parameters

This is an important part of the methodology and for conducting the simulations in PVsyst. Estimation of loss parameters that may be adjusted in PVsyst are based on the theory explained in this thesis and by the use of the meteorological data presented in chapter 3. Loss parameters estimated in this section will be tested individually to analyze the impact on the simulation result and how they cause potential deviations and mismatches between simulated and produced energy. The aim is to investigate how each setting for a loss parameter influence the discrepancy between simulated and produced energy. It is important to note that all simulations based upon the individual parameters adjustments are based upon ASKO scenario 2.

4.5.1 Albedo

PVsyst standard albedo values was shown in table 4.4. The default setting in PVsyst for albedo is monthly values of 0.2. This is the values used in the two first scenarios as described in section 4.3.1. However, these values may not be very accurate for the surroundings at ASKO. NIBIO measured albedo values at Ås are shown in table 4.7.

This table indicates greater albedo values during winter, and a lower during summer. As the winter values may be affected by snow cover on the ground, the summer values depend on surface material. The rooftop at ASKO has a black and gray surface and may be assigned the values of the urban situation of 0,14-0,22 (4.4). PVsyst default values of 0,2 may therefore be

Table 4.7: NIBIO measured albedo values at Ås. Data is measured daily and presented as monthly averages.

Date	Measured albedo
Jan	0,58
Feb	0,55
Mar	0,32
Apr	0,23
May	0,23
June	0,24
Jul	0,23
Aug	0,23
Sept	0,24
Oct	0,24
Nov	0,27
Dec	0,30

good values for the months: April, May, June, July, August, September and October. November and December, may have slightly higher albedo values. The albedo values measured by NIBIO will be used in a run in PVsyst to analyze the effect on the simulation results.

4.5.2 Soiling

The estimation of soiling may divided into two categories. The first one in the normal manner as explained in section 2.4.4 and related to precipitation in the form of rain. The second as a method to adjust for snow covering the modules. It may therefore be seen as two separate evaluations, one for summer and one for winter. PVsyst enables the user to define monthly soiling values, generating a more accurate simulation.

There is to this date no integrated loss parameter to account for snow in PVsyst, except to use soiling as a method. To account for snow covering the modules and possibly diminish power production the values of monthly soiling has to be increased substantially from the default values mentioned in section 4.3.7. To estimate possible loss due to snow covering the modules, weather data from 2015 must be investigated. ASKO recorded snow weight at the location and NIBIO measured snow depth values for Ås, can be used as a possible reference.

Frequent snowfall in combination with low temperature in November and December makes it possible for the snow to cover the modules for a longer time. It will have to melt, due to ambient temperature and/or module-temperature rising or possibly hot spot heating. Then the snow

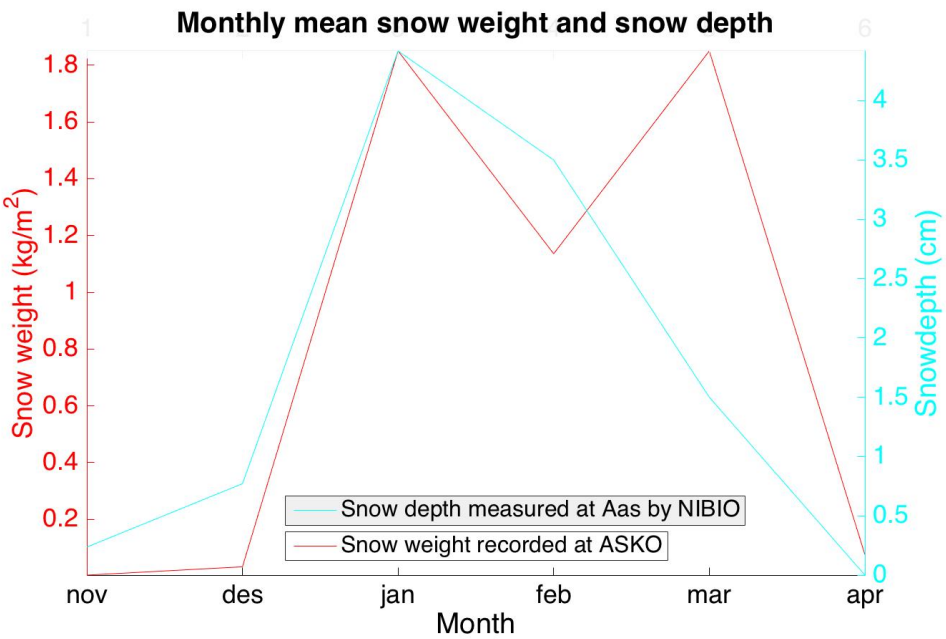

(a) Snow weight and snow depth.

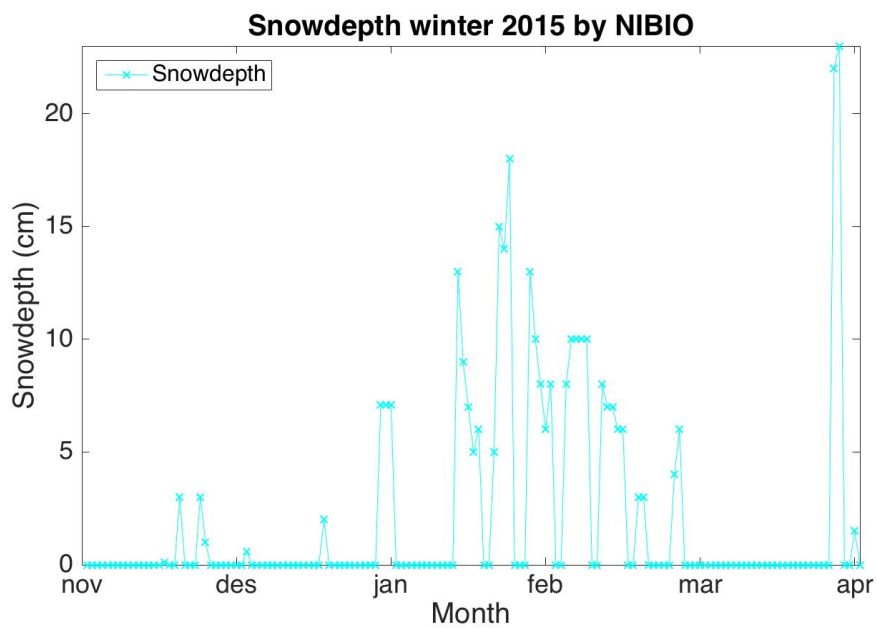

(b) Daily snow depth.

Figure 4.11: Figure 4.11a shows monthly measured and recorded snow depth and snow weight respectively. Snow depth is measured by NIBIO at Ås, while snow weight is recorded at ASKO. Figure 4.11b shows daily snow depth. Both figures show data from November to April.

will slide of the module and start receiving sunlight again. The low tilt of the system decreases the possibility of fresh snow sliding of the modules easily, whereas wet snow eventually will slide of. The problem of snow cover may be further increased due to the orientation of the system.

Since two strings of modules face each other, the snow sliding of from module with opposite tilt will collide and fill up the small gap in between and under the modules. This case will be more evident with heavier snowfall.

What may seem as an extreme value in figure 4.11a as the second peak in red, can be confirmed by the daily snow depth values in figure 4.11b. This graphs clearly show a major snowfall in the end of march that contributes to the red peak. The snow depth values are used to create the soiling scenario with respect to winter soiling levels. The soiling value equals the fraction of days during a month in the winter with more than 1 cm of snow relative to number of days in the month. This scenario is referred to as *snow frac*. Impact of frost, forming and covering the module is very hard to quantify. Reduction of produced power due to frost and partial snow cover is not accounted for in the deducted soiling scenario. That in combination with the snow depth and snow weight values in figure 4.11 may give reason to run a experimental soiling scenario for the winter month. Values derived for the soiling scenario are shown in table 4.8.

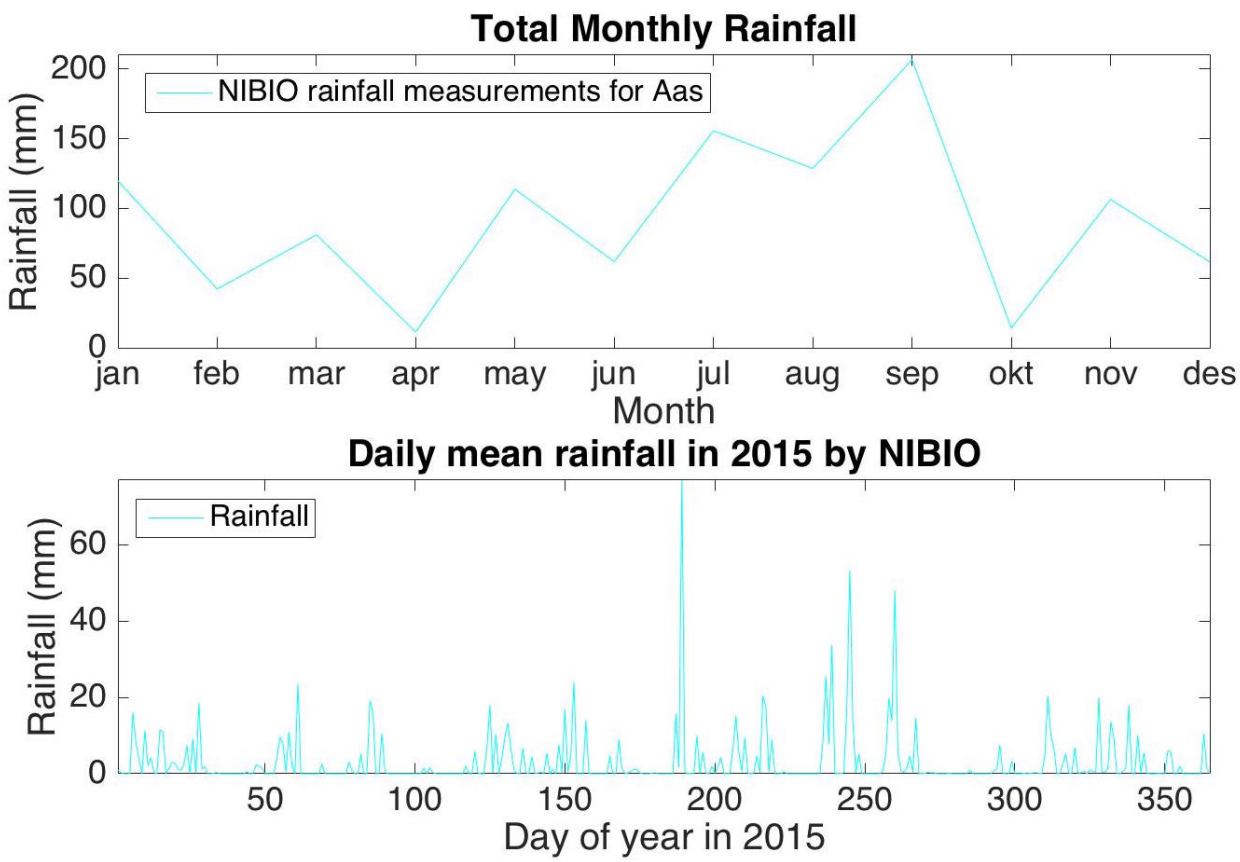

Figure 4.12: NIBIO measured monthly and daily rainfall at Ås.

The system at ASKO is an industrial system, including a substantial amount of modules over a great area. It can be exposed to soiling both from natural and industrial sources. ASKO may contribute to increased particle and dust contamination on the surface of the PV modules themselves, due to high traffic of trucks and other transport vehicles. This system is not regularly cleaned, thus the only source of cleaning is natural precipitation, both in the form of rain and snowfall.

ASKO Øst is located in area that experience frequent rainfall, of varying intensity as presented in figure 4.12. According to the theory explained in section 2.4.4 soiling levels in most of the summer months can be as low as 1 %. The summer soiling levels are used in both of the scenarios displayed in table 4.8 below.

Table 4.8: Soiling values derived from snow data. These values are represented in % and is used in detailed losses in PVsyst.

Date	Jan	Feb	Mar	Apr	May	Jun	Jul	Aug	Sep	Okt	Nov	Dec
Soiling: snow fraction (%)	45	50	10	3	1	1	1	1	1	1	7	13

Remark: The 2016 edition of PVsyst offer *unavailability days*. This option however, does only account for the total number of days the system may be unavailable during a year and not in which time periods of the years its unavailable. This option may be good to plan for the possibility of the system being shut down due to failures etc. (PVsyst (2014)), but not to conduct time accurate simulations.

4.5.3 Thermal loss - determining U-values

The default thermal loss for simulation 1 and 2 was explained in section 4.6. The semi-integrated option may underestimate the heat loss from the modules, partially due to lower heat loss behind the modules. Temperature values in table 4.9 are used with equation 2.7 and 2.8 to estimate how alternative settings impact the simulated energy production. The table shows the semi-integrated setting and compare the U-values with the alternative settings.

Table 4.9: Temperature settings used in PVsyst.

Thermal loss setting	$Uc \quad (W/m^2K)$	$Uv \quad ((W/m^2K/(m/s))$
Semi integrated (Base scenario)	20	0
Free mounted	29	0
PVsyst user def	25	1.4
According to module temp	Na	Na

The first alternative is the free mounted setting that has a higher loss due to more air circulation around the modules. The second is with custom U-values. These U-values are derived from previous studies done by the users and makers of PVsyst (2014). The factor U_v with a value of $1,4$ $(W/m^2K/(m/s))$ in combination with an average wind velocity recorded at ASKO of $2,27$ m/s results in an average U_v loss factor of $3,18$ (W/m^2K). That is a total U value of $28,18$ $(W/m^2)K$ and thus in effect (due to wind speed recorded at ASKO) about the same thermal loss factor as in the "free mounted" modules. The last thermal loss scenario is run according to module temperature recorded at ASKO. This may turn out to be the most accurate thermal loss setting as heat loss is estimated from the actual temperature of the modules instead of given constants.

4.5.4 Electrical loss

DC cable loss may be estimated by analyzing the layout presented in figure 4.4 and knowledge about the types of cables used. Information given with acceptance from FUSen includes an electrical sketch of the system that may be used to estimate the length and resistance of the DC cables. The reason PVsyst might miscalculate the resistance loss is because the inverter placement is not specified during construction of the 3D scene, and therefore the distance between any of the sub-arrays and the inverters are not exact.

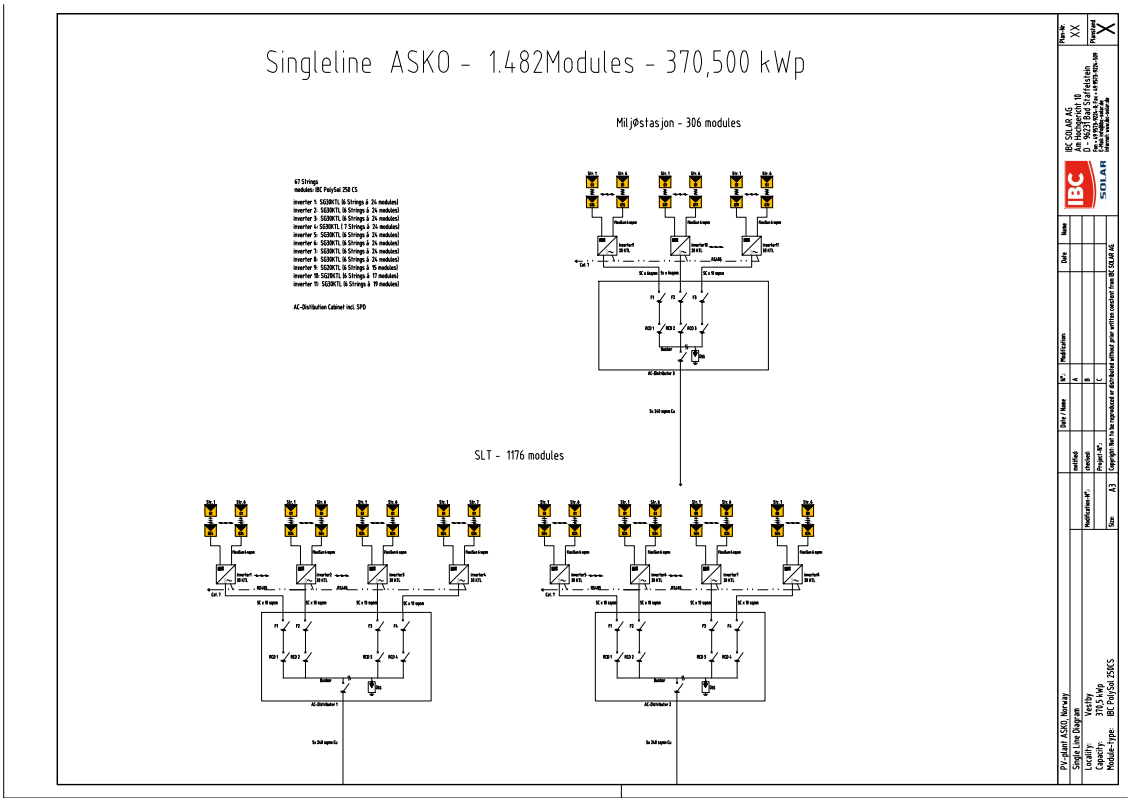

Figure 4.13: Electrical scheme of the components at ASKO with permission from FUSen

The layout in figure 4.13 shows that the cable assigned to each string runs directly to the inverter, making it a total of six cables from each sub-array to the inverters. The DC cables used are of the type FlexiSun and have a cross section of 6 sqmm (square millimeter). Further information about the cables is given in appendix A.8 and A.9.

According to information received from Bentley (l 21), (project manager in EPC International) the resistance per unit length of the FlexiSun 6sqmm cables is $3,3\ \Omega/kilometer$ at 20 $C°$. Using this value in combination with the length of the cables and equation 2.11, the resistance may be estimated. The estimated resistance per sub-array, shown in table 4.10, can then used be in PVsyst. The length of the cables were estimated by analyzing the layout shown in figure 4.4 and information given from T.C Tuv from FUSen. Due to the fact that the exact length of the cables is not recorded, this will be a rough estimate. The effective cable length for each string is taken to be half the length of the string, due to the resistance being divided between the plus and minus cable, that are connected to each side of a string. The length of the string on the fa side of each sub array will be used as a reference for length for that array. Thus, both length and resistance is slightly overestimated.

Table 4.10: Ohmc detailed computation in PVsyst

Sub array number	**1**	**2**	**3**	**4**	**5**
Estimated length (m)	80,655	70,905	61,155	71,725	54,625
Pvsyst calculated resistance (mOhm)	42	37	32	5,4	25
Loss fraction at STC (%)	0,5	0,4	0,3	0,3	0,2

In PVsyst default computation, type, length and cross-section of the cable is chosen. PVsyst calculates the ohmic loss as a power loss fraction at STC. The power loss is calculated with equation 2.10. Since the system will not experience irradiation at STC often, PVsyst´s the resulting power loss (presented in table 4.10) can be slightly overestimated. The global loss fraction of $0,3\%$ at STC is still considerably lower than the estimate of $1,5\%$ at STC in scenario 2. The detailed computation of ohmic loss makes it possible to estimate the wiring resistance for each array in the system.

4.5.5 IAM

IAM can be adjusted in detailed losses by two methods. Either by choosing the parameter b_0 or by defining a custom IAM profile. b_0 is a material dependent constant and should only be adjusted if the value is given by the producer of the modules PVsyst (2014). Some producers might even offer IAM profiles to be uploaded to PVsyst. Adjusting IAM loss accurately therefore depend on the producer. According to Bentley (l 21) IBC Solar do not have specific values for refraction or information regarding IAM for the modules in this case study. To validate a possible IAM loss, values refereed to in theory (2.4.5) will be used as a source for comparison.

4.5.6 Degradation

According to PVsyst (2014) LID loss is usually between 1 and 3 % depending on module type. LID is not a default loss, but an optional loss with a proposed default value of 2 %. Due to lack of knowledge, LID is more of an experimental parameter. The manufacturer has not specified explicitly any information regarding LID loss in their data sheet (appendix A.1 and A.2), therefore any losses due to LID can not be discarded. In terms of a possible aging loss this is neglected as the system at ASKO has not been operating long enough to experience significant aging loss. The aging loss is estimated by the producer as a linear decrease in power performance over the warranted life span. For the 250 CS modules the warranty is 80 % power performance after 25 years according to manufacturer (A.2).

Chapter 5

Results and Discussion

This chapter is divided into seven main sections. In the five first sections the associated results will be presented, analyzed and discussed, before proceeding to the next section.

- Section 5.1: Comparison of Meteorological data
- Section 5.2: Scenario 1 and 2 simulation results and errors
- Section 5.3: Results and errors of adjusting PVsyst parameters
- Section 5.4: A combination of parameters
- Section 5.5: Investigation of new module characteristics
- Section 5.6: General discussion of the study
- Section 5.7: Recommendations for similar simulation models

5.1 Meteorological Data

This section presents the meteorological (meteo) data from the four different sources used in this thesis. It aims to clarify similarities and differences of the meteo data utilized as the foundation in the simulation.

Figure 5.1a shows that the yearly measured and estimated irradiation received at ASKO do not differ significantly, independent of source. Monthly values are presented in figure 5.1b, which shows greater deviations between irradiation values. There are especially visible deviations in April, May and June. Measured irradiation at Ås is the closest to ASKO, both comparing yearly and monthly. The terrestrial measurements are thus more alike, compared to the interpolated satellite values derived by Meteonorm (MN) and Meteocontrol (MC). The satellite estimated

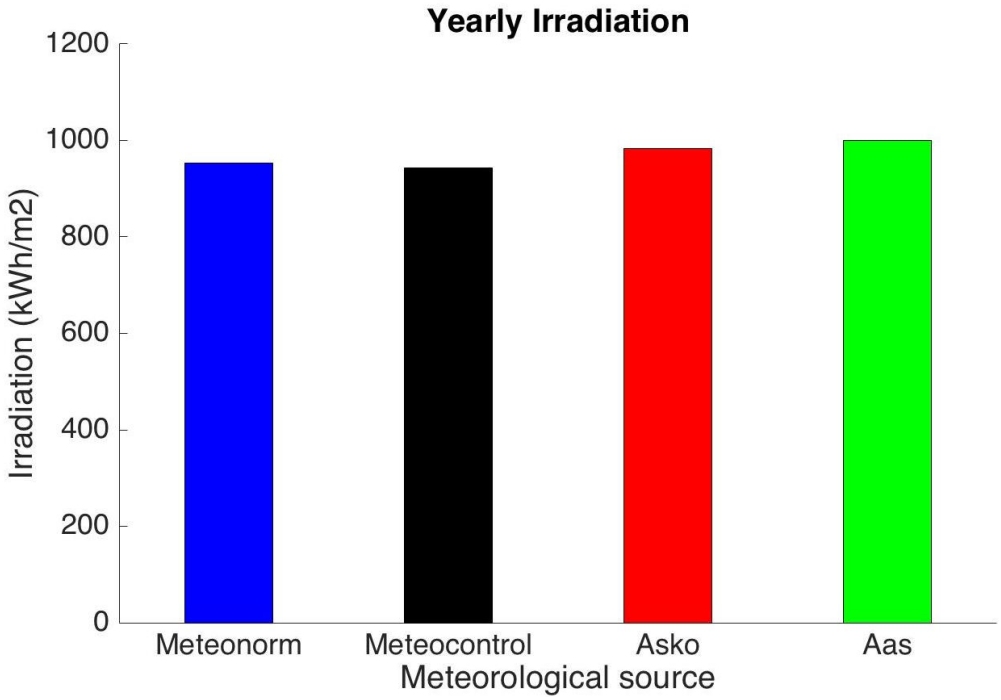

(a) Yearly irradiation values measured or estimated.

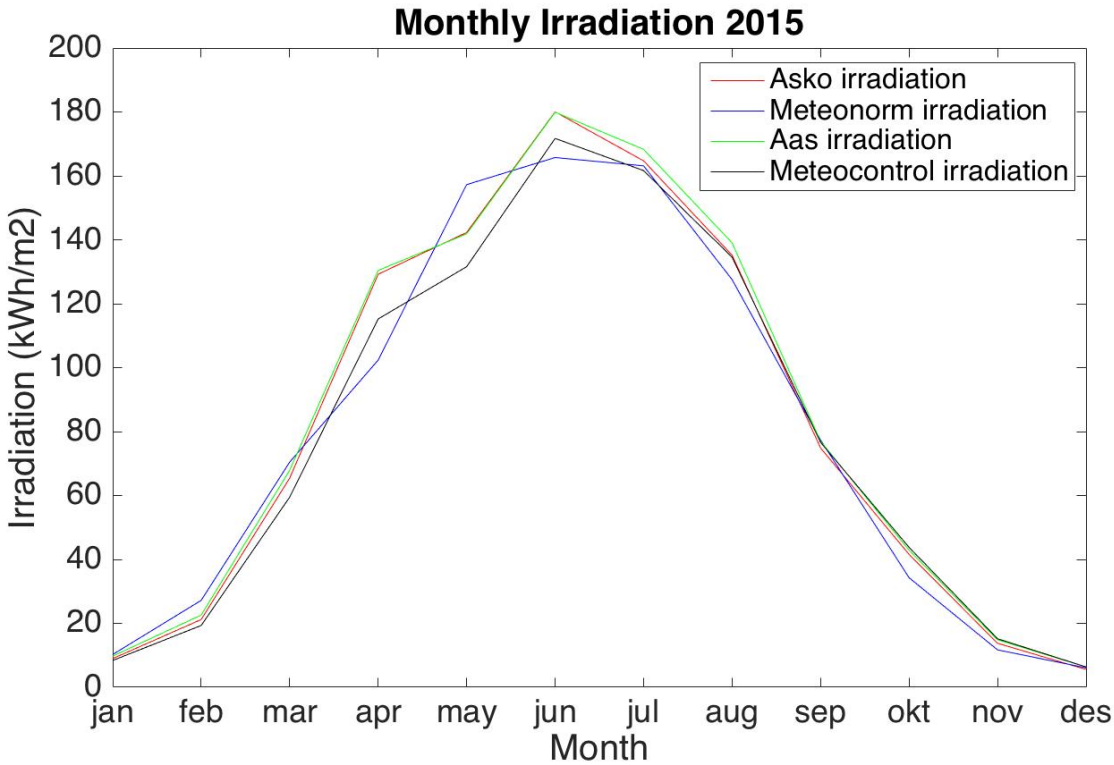

(b) Average monthly irradiation for all sources.

Figure 5.1: Yearly and monthly irradiation, both measured by weather stations and estimated by satellites

irradiation seem to fluctuate relative to each other almost every month. Since Ås is only 8 kilometers away from ASKO the pyranometer at Ås will experience different irradiation due to local differences as cloud cover and albedo. Yearly and monthly irradiation are so similar for ASKO and Ås that it provides a quality measure for ASKO because it implies that the meteo instruments at ASKO are located and mounted accurately. The instruments at ASKO are not maintained as frequently as the stations in Ås, as described in section 3.2.1. Yearly irradiation measured by Ås is very similar to the yearly irradiation interpolated by MN, although the monthly values differ considerably. This is attention worthy as Ås is the closest database in MN to ASKO by far, when interpolating meteo data (3.2.4).

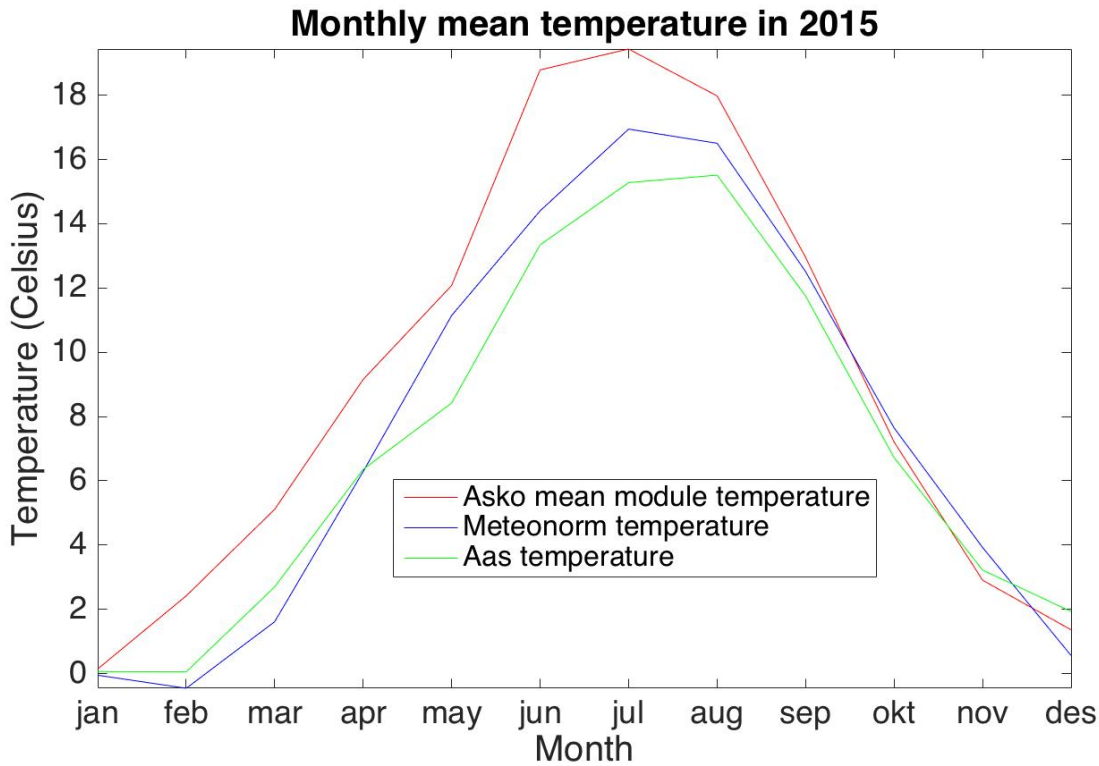

Figure 5.2: Monthly mean temperature values, estimated by weather stations and estimated by satellites. Meteocontrol values are not included. ASKO records module temperature and not ambient temperature, as opposed to other sources. The consistently higher temperature is thus expected.

Figure 5.2 presents the differences in measured monthly temperature. ASKO records module temperature and not ambient temperature as opposed the other meteo sources. The considerable higher temperature recorded throughout the year is therefore expected and can not be compared to the ambient temperature recorded by the other meteo sources. There is a notice-

able difference between Ås temperature and MN temperature. The deviation between these datasets are not as surprising as the irradiation. Although Ås is a source for irradiation in MN´s database, it is not for temperature. The temperature interpolation locations are all further away from ASKO compared to distance between Ås and ASKO (3.2.4).

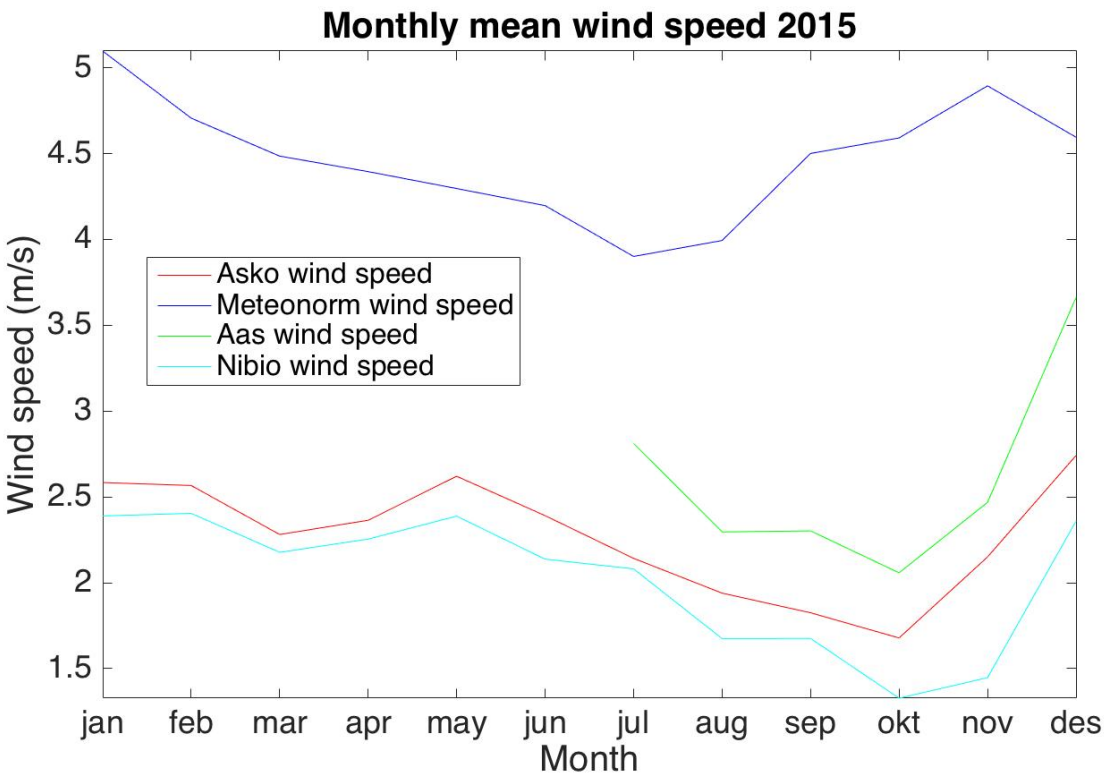

Figure 5.3: Monthly mean wind values, both measured by weather stations and estimated with satellites. Meteocontrol values are not included. ÅS records wind speed 10 meters above ground lever, whereas NIBIO record 2 meters above ground. Ås therefore are expected to have recorded slightly higher values.

Monthly wind data presented in figure 5.3 shows great deviation between some data sets. Meteonorm data shows consistently higher wind speed, while ASKO and NIBIO are very similar. Wind velocities recorded at 10 meter height at Ås are higher than at ASKO (for the recorded months), where the sensor is located about 2 meters above the roof (total of about 14 meters from ground).

5.2 Scenario 1 and 2 Simulation Results and Errors

This section presents the results from scenario 1 (S1) and scenario 2 (S2). The results are then analyzed in order to investigate deviations and discrepancies to determine which data sets are the most accurate. The monthly Root Mean Square Deviation (RMSD) will also be investigated in order to determine how the different parameters influence the results and by how much.

Yearly results

Table 5.1: Yearly result from scenario 1 and 2 with Relative Error (%) compared to measured value at ASKO. GHI is short for Global Horizontal Irradiation.

Yearly results	**Array - measured**	**MN**	**MC**	**Asko**	**Aas**
S1: Sim. energy (kWh)	299954	293416	289532	290030	306000
Relative Error (%)	0	-2,2	-3,6	-1,5	2
S2: Sim. energy (kWh)	299954	293463	Na	298770	307000
Relative Error (%)	0	-2,2	Na	-0,4	2,3
GHI (kWh/m^2)	982,8125	953,5	943,9	977,3	1000,8
Relative Error (%)	0	-3,1	-4,1	-0,6	1,8

Table 5.1 indicates that the average yearly simulated results by PVsyst are close to the real yearly value. The Relative Errors (RE) are on a yearly basis very low. The results based on yearly data does not show a clear trend between S1 and S2 (5.1). It is important to note the improvement from S1 to S2 for ASKO, whereas Ås slightly increases. However, more thorough investigation on a shorter time scale must be conducted to analyze potential differences within the year. In the introduction of this thesis, it was mentioned that previous studies reported an underestimation of global horizontal irradiation by up to 10 % for satellite estimated data (Øygarden Flæten). The underestimate is evident in the estimate of GHI in table 5.1, but not as significantly as in previous studies.

The yearly results corresponds to the yearly climate results presented in figure 5.1a. Evident patterns between meteo data are comparable to the patterns in the simulated results. Especially the yearly results show a strong correlation between simulated GHI and the predicted energy produced. Irradiation measured at Ås for 2015 was among the highest (yearly received kWh) of the sources, and Ås meteo results in the highest estimate of global horizontal irradiation (GHI) and the highest predicted energy. The same pattern is evident between the sources. MC meteo underestimates GHI more than MN. MC also underestimates predicted energy more than MN on a yearly basis. The sources with the most considerable deviations of GHI are the ones that result

in simulated energy with the most significant deviations, as presented in table 5.2. The 3,1 % underestimate of GHI for MN meteo constitutes enough energy (when converted) to compensate for the underestimate. The quality of the estimate or measurement of GHI can thus be argued to be the most important meteo parameter when simulating produced energy.

Table 5.2: Root mean square deviation between simulated and produced energy.

RMSD	**MN**	**MC**	**Asko**	**Aas**
S1: Sim. Energy (kWh)	3874,37	2546,35	1755,99	1685,84
S2: Sim. Energy (kWh)	3874,45	Na	1647,18	1478,89
GHI (kWh/m^2)	10,56	6,05	0,51	1,95

The monthly deviation presented in table 5.2 shows none, or small, improvements from S1 to S2. The RMSD for ASKO and Ås data decreases from S1 to S2. The MN RE does not change from S1 to S2, and the RMSD only insignificantly. As default temperature values in PVsyst originate from MN data, the only difference between S1 and S2 for MN is the addition of wind data. This addition may seem without effect on a yearly basis. Note that the RE for S2 Ås data increases from S1, while monthly deviation decreases.

S2 results did not improve notably from S1 with respect to RE and RMSD. On a yearly basis, the addition of recorded wind and temperature data did not seem to improve the simulation results significantly. As ambient temperature is a mandatory input parameter in PVsyst, the absence of serious deviations between S1 and S2 can be found in small difference between temperature data provided in S1 by MN and the other sources. The only exception is for ASKO where module temperature is added in the meteo file. Despite that thermal losses between S1 and S2 are equal, the module temperature impacts simulated energy at ASKO as it is the only source with a considerably decrease in RE from S1 to S2.

Monthly results

The monthly simulation results presented in figure 5.4 show greater deviation compared to the yearly values. The RMSD values in table 5.2 indicate that some sources deviate more than others. The cause is shown in figure 5.4a. The Relative Error (RE) is more significant during the winter half in Norway compared to the summer half, although the greatest energy gap is during summer as proven by figure 5.4a.

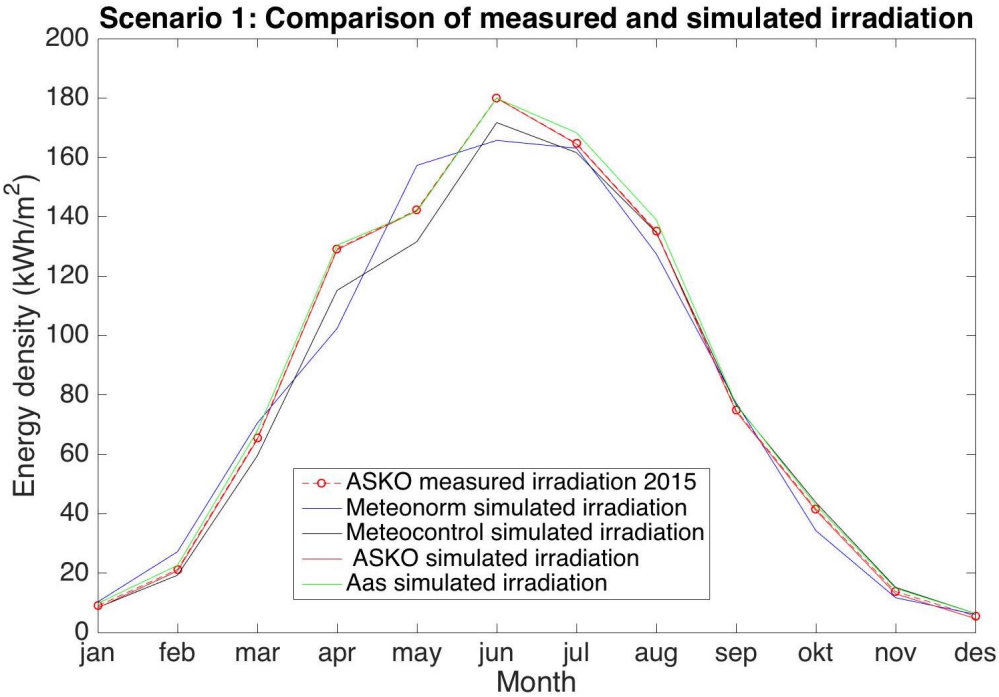

(a) Simulated and measured irradiation per month.

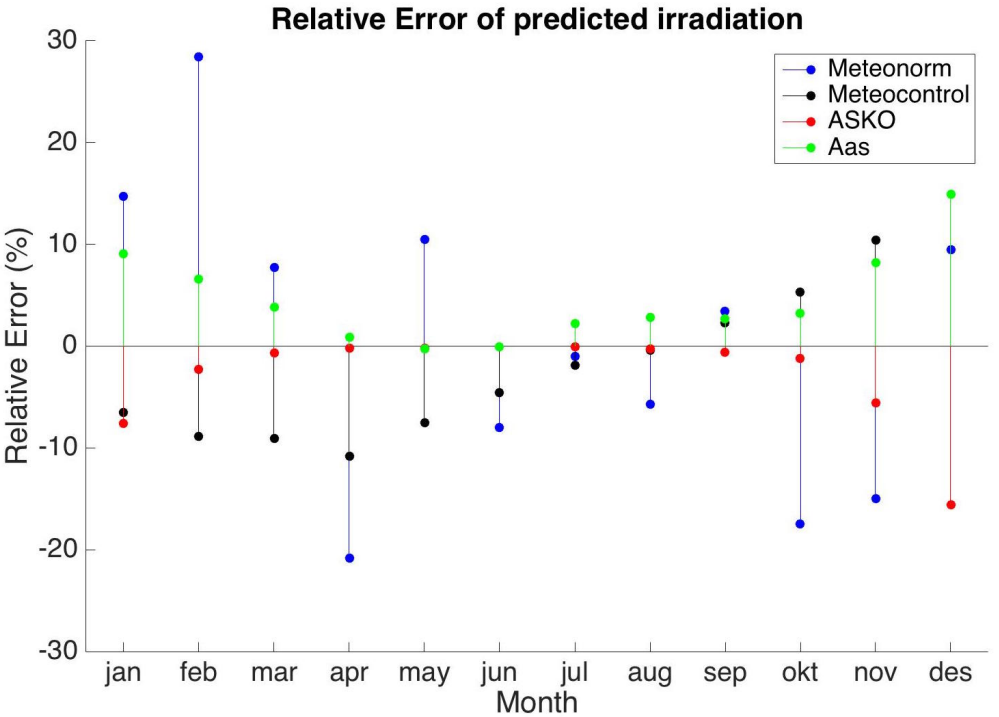

(b) RE for simulated (predicted) GHI.

Figure 5.4: The simulated irradiation values shown in figure 5.4a are the same for scenario 1 and 2 as irradiation values do not depend on temperature and wind velocity. Figure 5.4b displays substantial differences in estimated irradiation between the data sets.

ASKO remains the most accurate, which is not unexpected as it origins from the reference value. The two satellite data sets almost consistently underestimate during summer, while Ås data slight overestimates. Ås overestimates almost every month, while MN and MC estimations are more inconsistent.

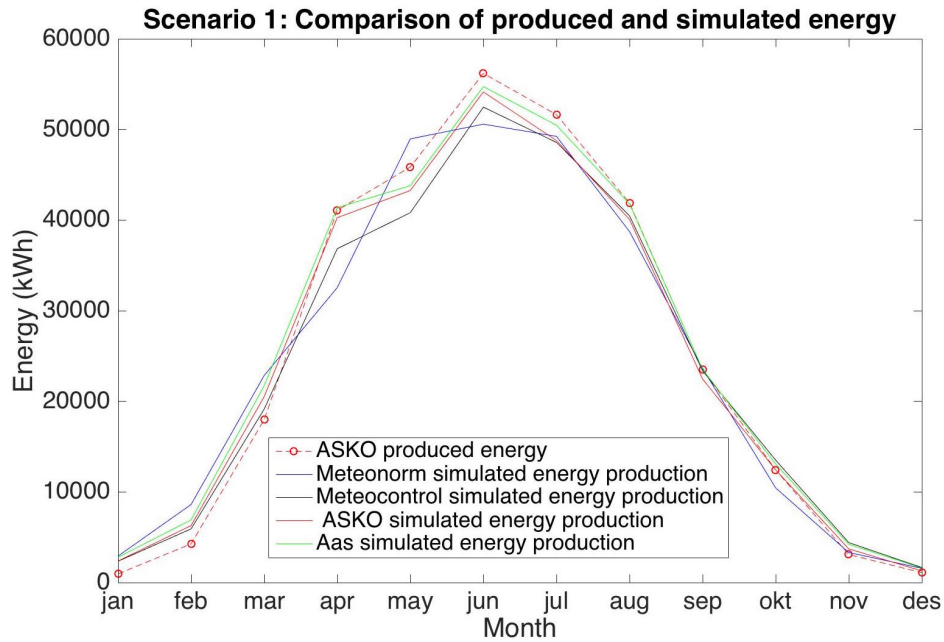

(a) Scenario 1.

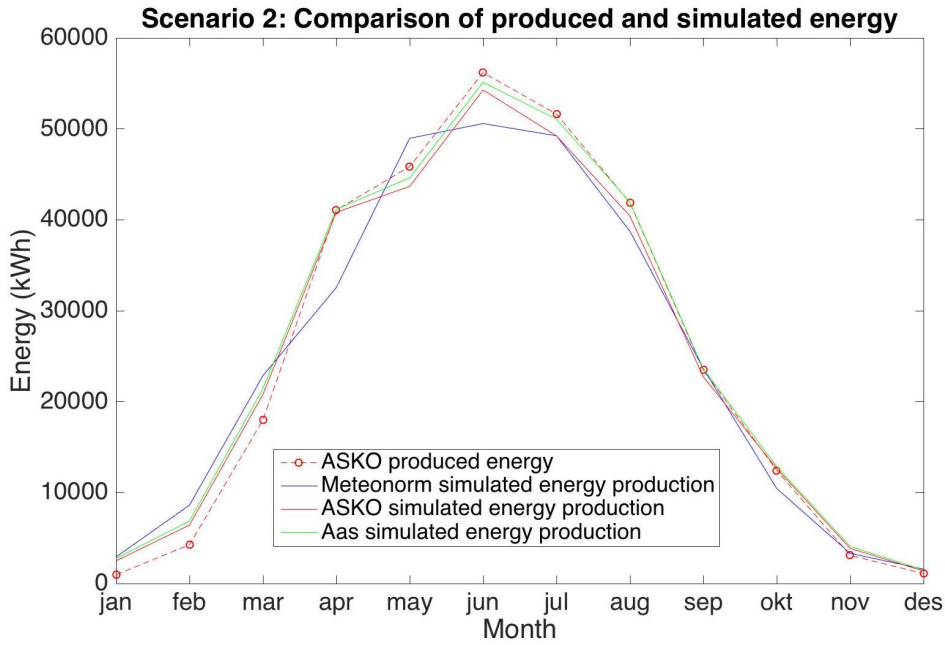

(b) Scenario 2.

Figure 5.5: Simulated and produced energy per month.

Figure 5.5 presents monthly simulated energy compared to the produced energy at ASKO. From monthly values it is clear that there are considerable deviations between simulated and produced energy. The trend is quite comparable to the one shown in simulated irradiation values in figure 5.4. Deviation and similarities of yearly and monthly S1 and S2 results corresponds strongly to the climate results presented in section 5.1. The RE in yearly data was very small, and by investigating monthly RE in figure 5.6 one may understand why.

There are two obvious trends in figure 5.6. The first one is an overestimation of energy during winter and the other, is an underestimation during summer. The RE is significantly greater during the winter half compared to the summer. Yet, the less significant error during summer accounts for a greater value, due to the higher value of energy (5.5). This is proven by the calculation of the RMSD values shown in table 5.2. In order to decrease the monthly RMSD one might have to increase energy estimation during summer half. The proven over and underestimation of predicted energy, neutralize each other as annual data is fairly similar.

Section summary

The results presented in this section shows a clear difference between the meteo data. Satellite collected data underestimates global horizontal irradiation (GHI) and predicted energy, and results in the highest monthly root mean square deviation (RMSD). Meteo data measured at weather stations are more accurate and results in lower RMSD. Higher GHI and predicted energy at Ås indicates regional differences due to geographical location and local climate.

Selection of meteo data set

In order to improve the accuracy of the simulation, monthly deviation must decrease considerably. Different parameters have to be adjusted, to account for errors. These may be general and/or specific to some parts of the year. The winter half stands out, due to snow covering the modules. The snow probably accounts for a major part of the underestimation shown in figure 5.6. Therefore, out of simplicity, the study is continued with ASKO as a meteorological source (Scenario 2) for the successive work presented. To adjust and compare for all meteo source is not time efficient. ASKO was proven to have the lowest RMSD and RE. Therefore, all the primary parameters in S2 are included in all successive scenarios. That implies that the adjusted detailed loss parameters are investigated individually, with the rest of the detailed loss parameters reaming default as in S2. After adjusting parameters and making some combined (optimized)

scenario models, it will be tested on the MN meteo file. The MN meteo files is chosen because the MN meteo causes the simulation results with the greatest monthly root mean square deviation in scenario 1 (S1) and S2. It is also the meteo database that is included in PVsyst.

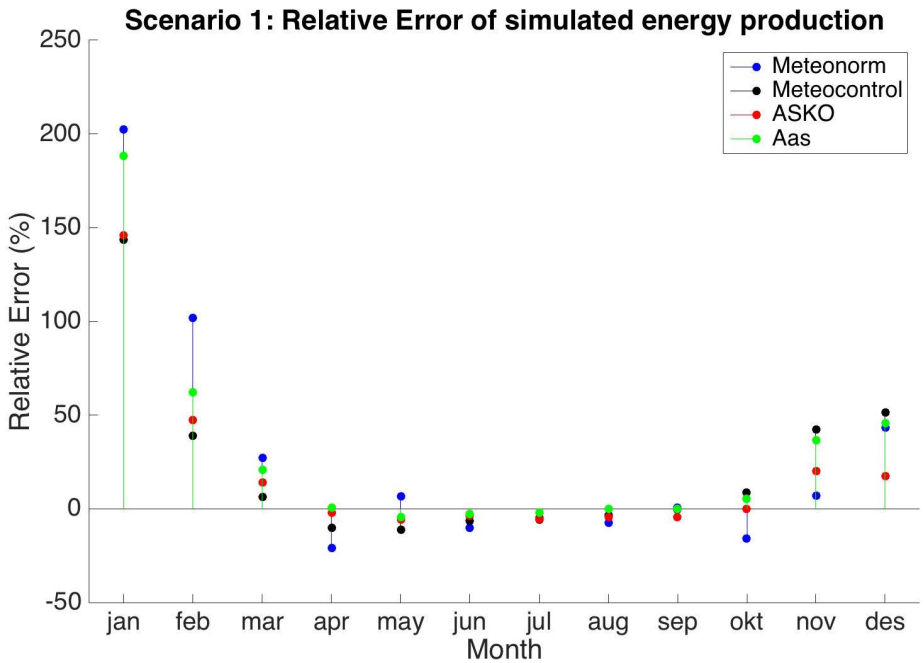

(a) Scenario 1

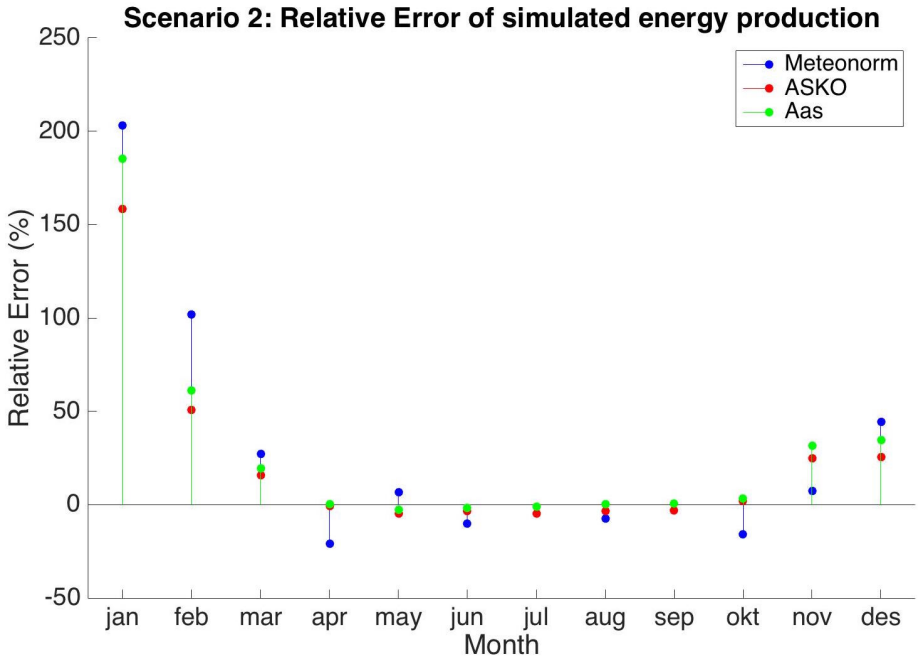

(b) Scenario 2

Figure 5.6: RE between simulated and produced energy at ASKO for S1 and S2, with default loss parameters.

5.3 Adjustment of PVsyst Parameters

Figure 5.7 presents the correlation between produced and simulated energy for S2. Some months are subject to considerable deviations, although there is a strong positive correlation. This is evident in the high root mean square deviation (RMSD) of $1647,18kWh$.

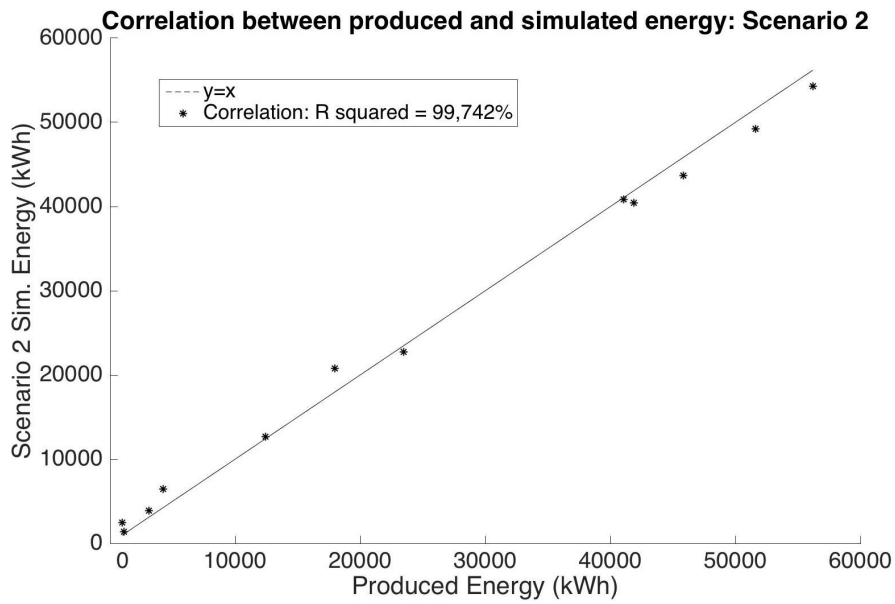

(a) Correlation plot between produced and simulated energy at ASKO for S2.

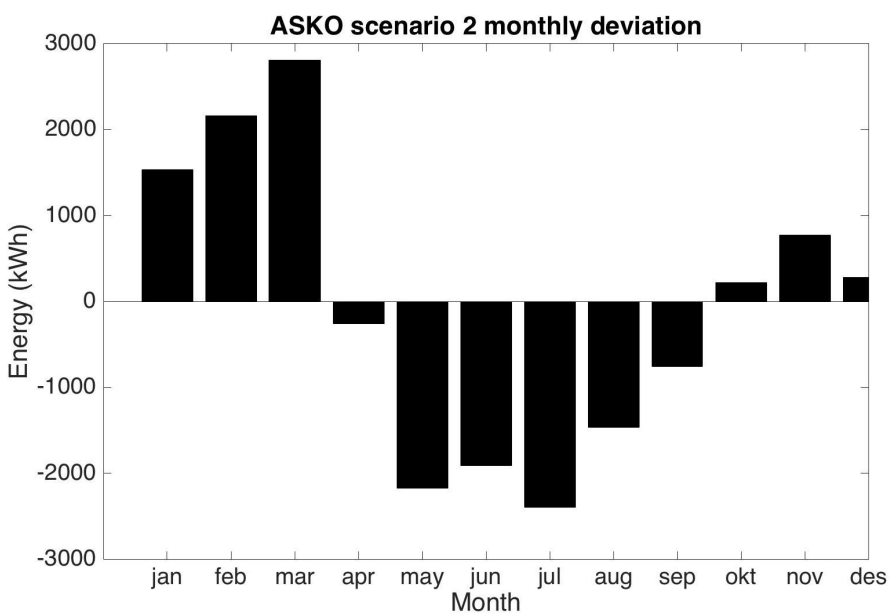

(b) Deviation plot.

Figure 5.7: Figure 5.7a shows a strong positive correlation, with R-squared of 99,742 %. Figure 5.7b presents the monthly deviation for S2.

In figure 5.8 the parameters that contribute to loss over the year are shown with their estimated impact on the system. The loss diagram clearly show the loss factors PVsyst uses and how much these losses contribute. The following section shows how default settings in PVsyst as well as other possible loss factors in PVsyst may be adjusted and included to decrease the discrepancies between simulated and produced energy per month.

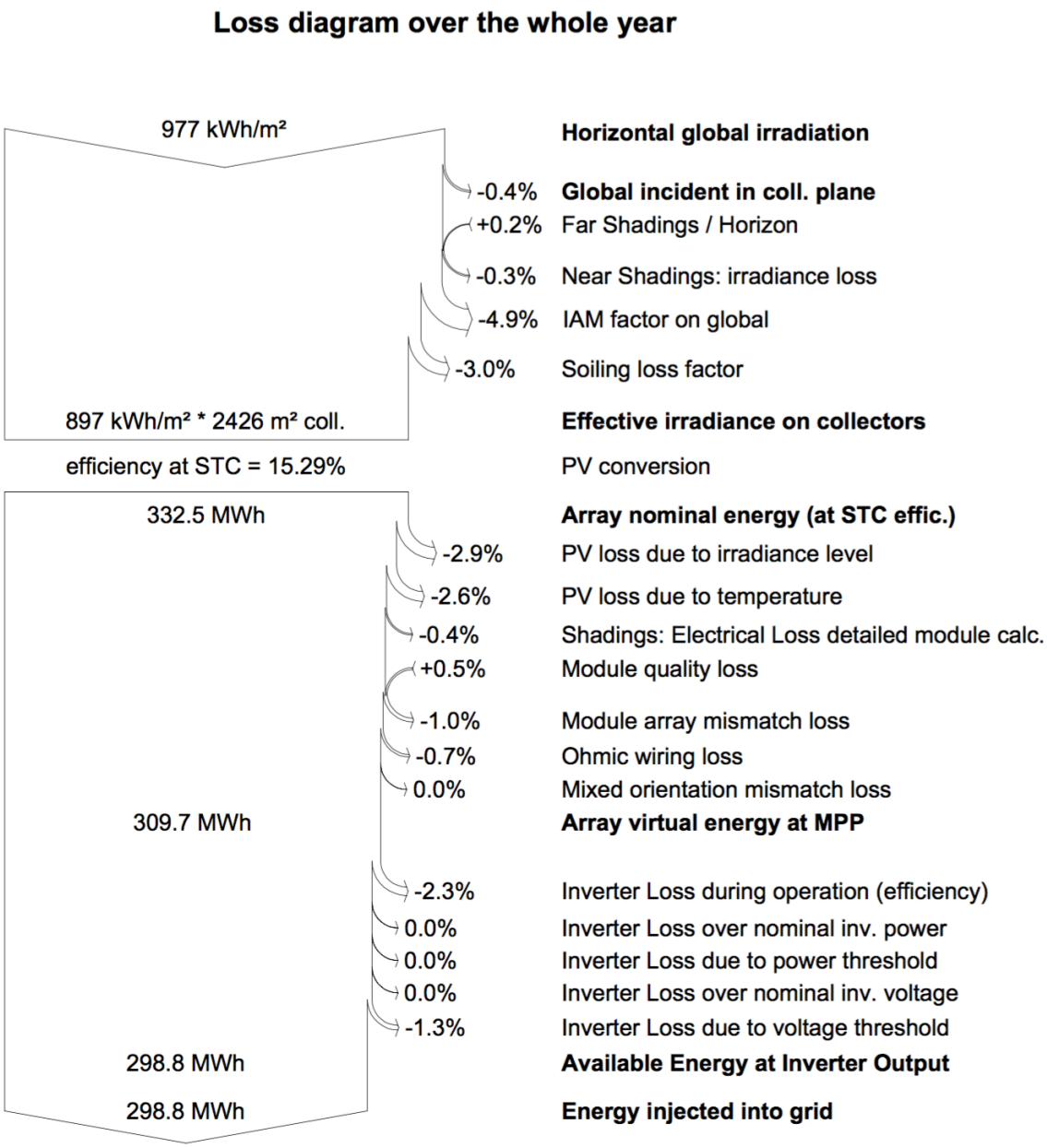

Figure 5.8: Excerpt from PVsyst showing a loss diagram for ASKO meteo for scenario 2.

Array incidence loss due to reflection (IAM) contributes to a major loss. The IAM loss parame-

ter will not be adjusted, as explained in section 4.5.5. The IAM loss estimated by PVsyst is very similar to the 5,31 % reflection loss derived in the study by Martín and Ruiz (2005), described in section 2.4.5. Loss due to shading is only 0,3 %. This loss is relatively insignificant when compared to the losses due to IAM, soiling and temperature. The construction of the shading scene in PVsyst is a time consuming process that can play an important part in estimating shading losses, if there is cause to believe there are objects that may cause considerable shading. At ASKO there is only the small house and the short walls surrounding the building displayed in figure 4.9 that can cause shading. Some of the shading loss might be due to the concept of self shading (strings shading nearby strings), at low solar height. Inaccurate construction of the 3D scene in PVsyst introduces error that can propagate to the final simulation result. Near shadings loss and electrical loss are both estimated based upon the 3D scene. If the placement of the modules is not corresponding to the layout (actual placement), both these losses can be miscalculated. The constructing of the 3D scene did not have a major impact on the simulation result for this study, thus the errors due to uncertainty in constructing the 3D scene are minimal.

The system loss due to voltage threshold was estimated to -1,3 % and inverter loss during operation (efficiency) was estimated to -2,3 %, as presented in figure 5.8. The inverter efficiency loss corresponds well with the max rated efficiency at 97,3 % for the SG-20ktl inverter (appendix A.5) and 98 % for the SG-30ktl inverter (appendix A.7). These losses may differ from each sub array (SA) due to different number of modules in a string. If any of the losses are influenced by the manual adjustment of component characteristics in PVsyst is uncertain. Voltage threshold can occur on clear days with very high irradiation and efficiency, especially right after removal of cloud cover. The adjustment in PVsyst was needed because the module power is over-sized compared to inverter power, as shown in table 4.5. The module power will therefore in some instances operate at the maximum inverter capacity, and thus possibly, increase power loss due to voltage threshold. The positive module quality loss is explained by the module power tolerance rated at -0 %/+2 %. The positive tolerance implies that the modules are more likely to produce more than the rated power at standard test conditions (STC).

Figure 5.8 presents a positive loss due to far shadings/horizon. This is noteworthy as the loss is estimated by shading acting globally on the system. How global shading can contribute to increased irradiation in the collector plane is uncertain. A possibility is through increased diffuse irradiation from the horizon at low sun angles. The far shadings/horizon loss is estimated to a negative value for the other sources, as for Meteonorm shown in the loss diagram in appendix

B.3. This raises a question about the the exactness of this estimate for ASKO meteo.

PV loss due to irradiation level (+2,9 %) is relative to the energy the system would be produce at STC, and is a fair estimated loss. The short circuit current from a module decreases with decreasing irradiation level as explained by equation 2.6. The result is lower power production and performance ratio (PR), as illustrated by figure 2.8. Considering Norway´s geographical location with solar irradiation received from low solar angles (winter), STC operating conditions are rare. The system is working at an average yearly PR of 82,8 %, which implies that it operates (from an irradiation perspective) at 800 W/m^2 and produces about 200 W per module (figure 2.8). The monthly performance ratio for ASKO S2 is included in appendix B.1.

5.3.1 The impact of albedo

Adjusting for albedo values in PVsyst by substituting default values with NIBIO measured values yielded a yearly result of 298880 kWh. This is a very similar result to that of ASKO in S2. The resulting RMSD value of $1647,39$ kWh, show a monthly discrepancy from measured production that only deviates from the discrepancy in S2 (5.2) by 0,01 %. Figure 5.9 presents the Relative Error (RE) of adjusting the monthly albedo values relative to S2. The figure shows that albedo adjustments impact the simulations result in a minor way, both on monthly and yearly values. It may be interpreted that albedo adjustment does not contribute to decrease the proven discrepancies in a considerable way. Furthermore, it may be argued that PVsyst does not emphasize the impact of albedo values in the simulation in a considerable manner. Therefore, conducting albedo measurements at the roof of ASKO (or other panned ares for PV systems) do not improve the accuracy of simulation.

The impact of adjusting albedo values during winter from the default value of 0,2 to about 0,3-0,6 only changes the result in the same period under 0,5 % (RE) from S2. The exception is for December when albedo decrease predicted energy almost 1,5 % from s2. The December value is interesting as the albedo value only changed from 0,2 to 0,3.

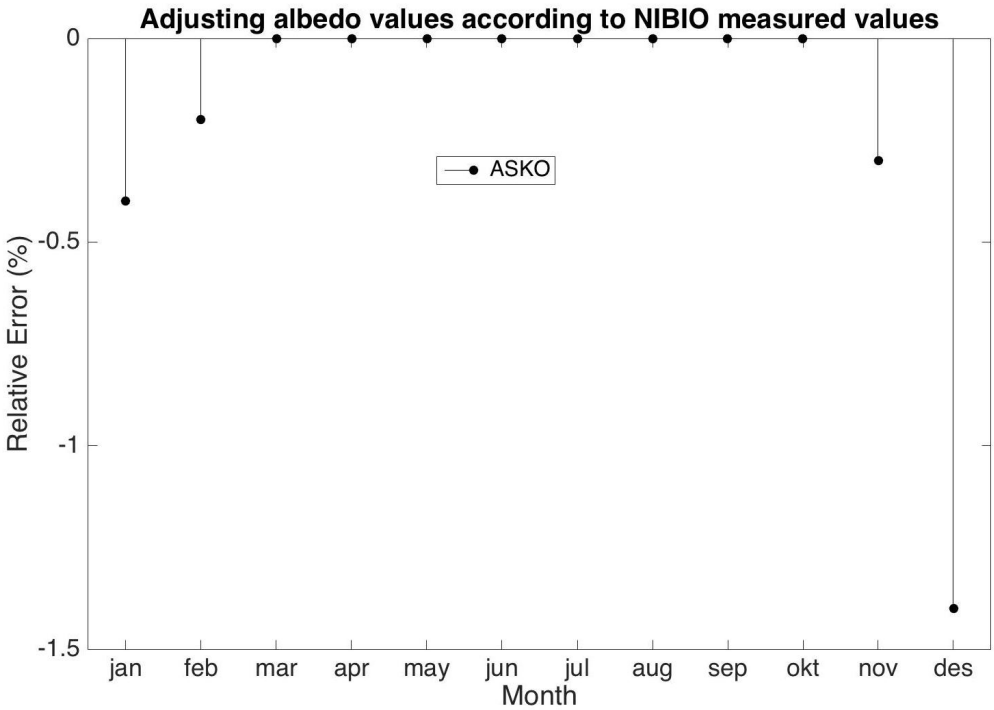

Figure 5.9: RE between simulated energy with NIBIO albedo values and simulated energy for ASKO in S2.

5.3.2 The impact of soiling

Simulation in PVsyst with monthly soiling values as shown in table 4.8 reduced the monthly mean deviation considerably. Yearly estimate of 298006 kWh is 0,65 % lower than the actual value. The soiling scenario according to calculated snow fractions resulted in a RMSD of 887,17 kWh . That is 46,14 % reduction in monthly RMSD compared to S2.

Figure 5.10 shows considerably less deviation between simulated and produced energy when monthly soiling values are adjusted. The results is increased production during the summer and decreased during the winter due to snow. There are however still significant deviations from produced energy during winter months. During summer, there is a small underestimate compared to produced energy. That is even with a soiling level at 1 %. This may indicate that soiling alone is not the only reason PVsyst underestimates simulated energy production during summer. The snow fractions were derived by counting number of days in a month with more than 1 cm of snow. Less than 1 cm can still completely cover the modules and therefore diminish power production. Another important impact on power production is shading due to snow or frost. Light frost, snowfall or non-uniform snow melt may result in a string containing modules that are completely shaded, partially shaded and completely clear. Shading of cells can, as

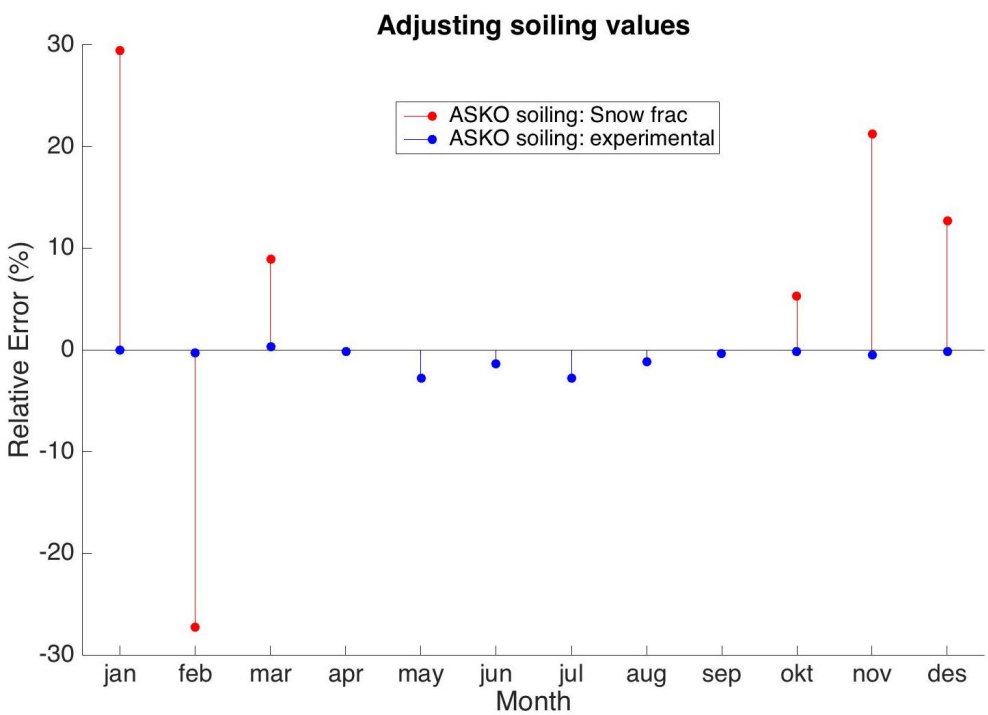

Figure 5.10: A comparison between produced and simulated energy with soiling adjustment. The blue values are according to experimental soiling values as described.

described in section 2.4.3, lower the current and diminish the power production in a string to a minimum. The loss due to shading (figure 5.8) was very low compared to the loss due to soiling. However, the shading scene in PVsyst does not account for partial shading due to snow or frost. The system at ASKO consists of string inverters, thus partial shading of one module can significantly decrease the production for a string with up to 24 modules.

To account for the considerable deviations in the winter months, a new, experimental soiling scenario was derived with the intention to reduce deviation during the winter months. Such a scenario is possible due to the problem of quantifying snow and frost losses, as described above. The experimental soiling values are presented in table 5.3 and the results of the simulation is presented in the first figure.

Table 5.3: Experimental soiling values derived from snow data and the results presented.

Date	Jan	Feb	Mar	Apr	May	Jun	Jul	Aug	Sep	Okt	Nov	Dec
Soiling: snow fraction (%)	45	50	10	3	1	1	1	1	1	1	7	13
Experimental soiling scenario (%)	55	34	17	3	1	1	1	1	1	6	22	21

The experimental soiling scenario resulted in a RMSD of $615,6\ kWh$, almost 16,5 percentage

points further reduction in mean monthly deviation compared to the first soiling scenario. That is a 62,63 % reduction in mean deviation per month compared to that of S2. The experimental scenario is a better estimation with an obvious decrease in RE for the winter months compared to the snow fraction scenario. Yearly energy estimate is however further reduced to 295824 kWh, which is about a 1,34 % underestimate.

The soiling values used in the experimental soiling scenario simulate produced energy in the winter months more accurately than in the snow fraction scenario. Total losses due to snow and frost may therefore be greater than the losses estimated by the snow fraction scenario. Shading due to snow can be prevented by the use of micro-inverters instead of string inverters. The overestimation in S2 for some of the winter months prone to snowfall and frost (January, February, March, November and December) is 7557 kWh in total, which is 2,5 % of the produced energy at ASKO. If micro inverters are better suited for systems as ASKO is an economic decision.

Adjusting for soiling with the aim to improve the accuracy of the simulation in the winter can give an indication of how much energy is lost due to snow covering the modules. For small systems and even for an industrial system as this, the lost energy does not constitute a significant part of the total production. Estimation of energy loss can be important to deduct if measures have to be made in order to reduce loss. To pay for cleaning snow of the modules is both expensive and time consuming, and most likely not worth the cost in terms of the extra energy received. However, other design options that reduce snow covering may be explored, such as adjusting the tilt and orientation of the system. Frame-less modules for systems with low tilt can decrease the effect of soiling accumulation and increase the cleaning effect of rainfall . Soiling values will change from year to year, depending on the weather conditions.

During simulations in PVsyst, soiling loss is accounted for as an irradiation loss. Although the impact of soiling on system performance is uncertain, some questions are evident from the results. Increasing the soiling levels, results in an increased soiling loss, from the default 3 % to 4 % in the experimental soiling scenario, presented in appendix B.2. At the same time, irradiation loss and electrical loss according to detailed module calculation due to near shadings decreased. The decrease in irradiation loss is very small, however the electrical loss decreases from 0,4 % to 0 %. Based upon theory about shading, increased soiling (especially snow) should results in higher shading losses, and then in particular electrical loss. However, this aspect is not included in the estimation of soiling impact in the PVsyst software. A result of this may be that PVsyst

underestimate predicted energy more during winter than assumed, or based upon snow depths. The underestimate must therefore be corrected by even higher soiling levels for winter months. PV loss due to temperature increased slightly. The only adjustments made were soiling levels. Assuming that is the cause, it can seem as increased soiling on modules contains more of the heat inside the modules. That is not far from the the case of snow, which is a good insulator.

5.3.3 The impact of thermal loss adjustment

Thermal loss adjustments resulted in deviations decreasing for all summer months. Simulated energy in S2 in the winter month deviates significantly from produced energy, and adjusting thermal losses is thus predicted to increase simulated energy for all months and therefore also the deviations. PVsyst overestimated during winter, but underestimated during summer. Adjusting for thermal loss thus decreases the deviations in the summer months, as proven by figure 2.4.2, but increases deviation during winter months.

Table 5.4: RMSD values for different thermal loss scenarios. The table includes deviations based on all months in a year and the months from April throughout October. Notice that the RMSD values in the latter are considerably lower for all thermal loss scenarios.

Rmsd monthly deviation	**All months**	**April through October**
Thermal loss - free mounted (kWh)	1290,22	541,75
Thermal loss - custom U_c and U_v (kWh)	1284,85	539,84
Thermal loss - according to module temperature (kWh)	1263,56	511,15

Table 5.4 show RMSD values for the different thermal loss scenarios. Monthly deviations do not differ much between the different scenarios. Thermal loss according to module temperature is shown to have the lowest deviations, and may therefore be argued to be the better thermal loss scenario of the three. RMSD values based on the whole year are significantly higher for the thermal losses compared to that of soiling losses. Table 5.4 shows RMSD values obtained from the months April through October and how they deviate less compared to the soiling scenarios. All 3 thermal loss scenarios are thus better simulation options compared to the default "semi integrated" option used in S2, especially comparing with summer simulated energy. Yearly estimates are as a result increased notably. The two first thermal loss scenarios are nearly identical, as proved both by the RMSD and the RE values presented in figure 5.11, and result in a yearly energy estimate of about 307000 kWh. Thermal loss according to module temperature results in an even higher estimate of 310816 kWh, which is a 3,62 % overestimate.

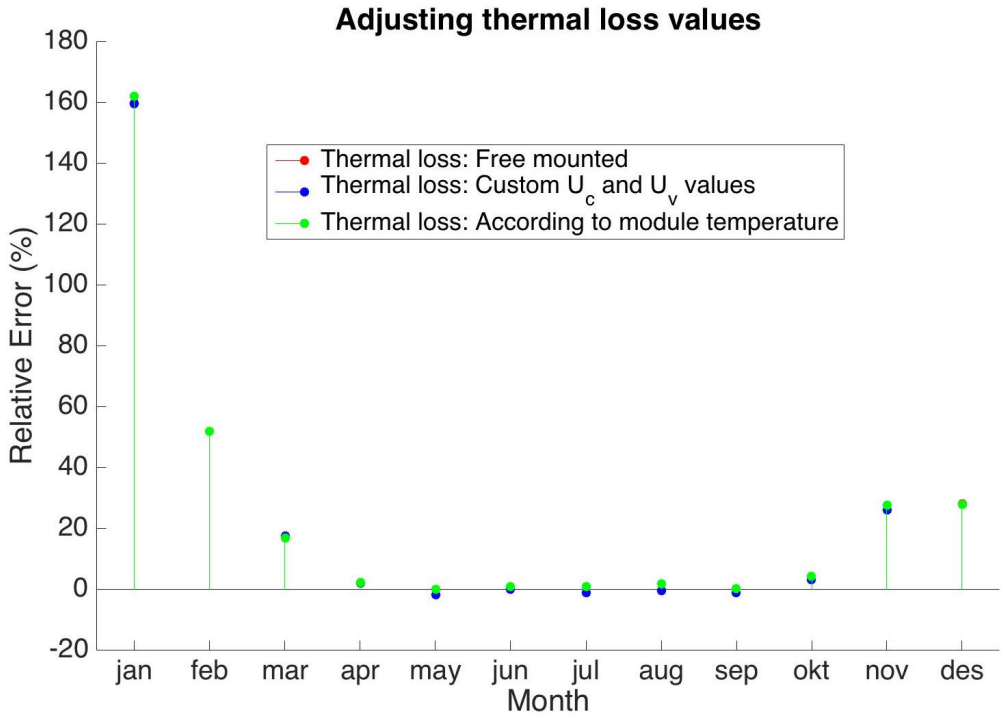

(a) Months affected by snow.

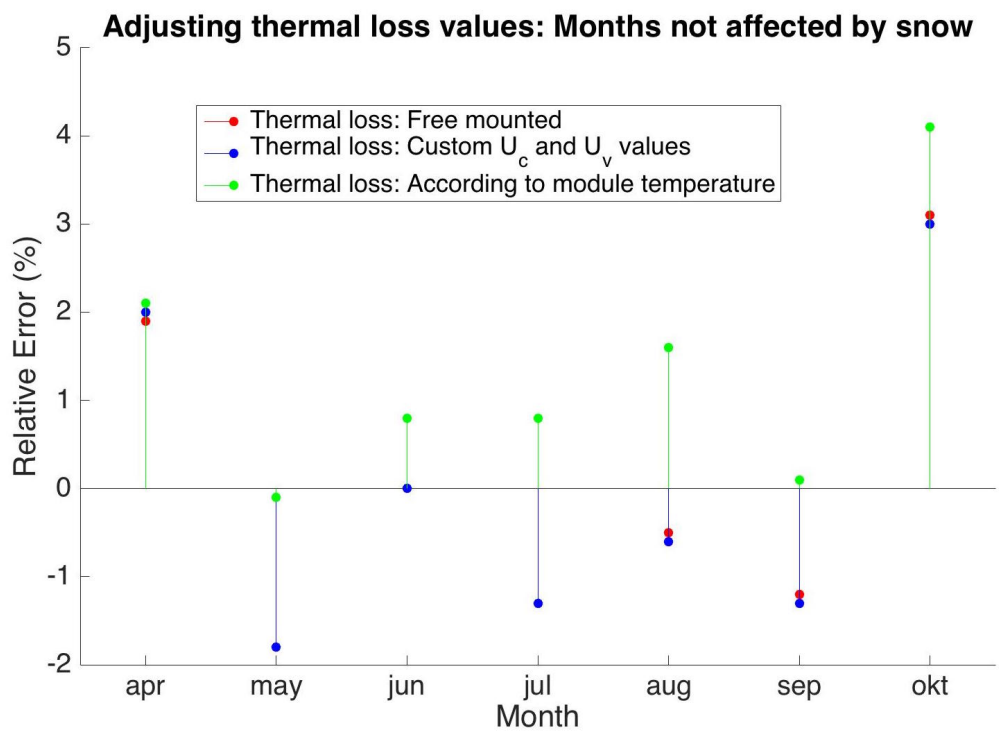

(b) Months not affected by snow.

Figure 5.11: Relative Error for the 3 different thermal loss scenarios. Note: thermal loss according to free mounted modules results in almost identical Relative Errors (RE) to the custom heat loss constants, and is therefore not visible in figure 5.11a.

Figure 5.11 shows that the RE for the thermal loss: free mounted is almost identical to that of the custom U_c and U_v values. The lower U_c value 25 (W/m^2K) used in the custom scenario compared to the higher U_c value 29 (W/m^2K) in the free mounted scenario is apparently neutralized by the addition of the U_v 1,4 ($W/m^2K/(m/s)$) value. Including U_v may seem to have a major impact on the total thermal loss estimated in PVsyst in combination with wind speeds recorded at ASKO. The recorded velocities at ASKO include some uncertainty as explained in section 3.2.1. Wind data influenced simulated energy more significantly though thermal losses than in the basic scenarios between S1 and S2.

The two latter thermal loss scenarios do seem to offer some advantages over the first and especially over that in scenario 2 with semi integrated modules. Using recorded wind values the heat loss depends on the the wind speed, which again depend on the season. Since wind speeds constantly change throughout the year, the modules will not experience a constant heath loss. Thermal heat loss according to module temperature can also be argued to be a more accurate method as recorded module temperature at ASKO creates a better foundation for estimating thermal loss from the modules compared to that in equation 2.8. The module temperature depends on ambient temperature as well as wind speed and the direction of the wind. Therefore, this method most likely creates the most accurate method of estimating thermal loss.

Another factor for the alternative thermal loss scenarios being more accurate compared to the semi-integrated option is the fact that the meteo file used for ASKO does not contain ambient temperature. The ambient temperature is thus supplied from Meteonorm and is used (equation 2.7) to estimate the heat loss from the modules. The monthly mean temperature estimated by Meteonorm is higher for most of the year (especially during summer) compared to Ås, as shown in figure 5.2. Ås data was proven to be more similar to ASKO than Meteonorm. Higher ambient temperature results in lower estimated heat loss. The heat loss estimate in scenario 1 and 2, may therefore be lower than it would have been if recorded ambient temperature would have been used.

It can be concluded that thermal loss according to module temperature is the most accurate thermal loss option in order to improve simulation accuracy. It also suggests that heat loss constants for the free mounted option and the custom U_c and U_v option are too conservative. Thermal loss according to "free mounted" modules is more accurate than the chosen default "semi integrated" option, even though the semi integrated option is what best describes the config-

uration of the system at ASKO. The results signifies that wind speeds impact the thermal loss estimation and thus the predicted energy result considerably. Ambient temperature is the normal measurement for temperature and the only temperature parameter that can be used to plan and design a system in advance. Heat loss constants for a PV system of similar construction and configuration as at ASKO should therefore at least be that of the custom scenario.

5.3.4 The impact of ohmic resistance adjustment

Adjusting the ohmic loss by the use of detailed computation resulted in reduced global ohmic loss by more than 1 %, and thus an overall increase of simulated energy. Yearly estimate of 301896 kWh is an overestimate of 0,65 %. The simulation resulted in a RMSD of $1570,72\ kWh$. Compared to S2 it is a monthly RMSD reduction of of 4,6 %. That makes the simulation more accurate than S2 on monthly basis, but does not reduce the deviations as much as adjusting for soiling and thermal losses. Figure 5.12 presents the relative deviation from scenario 2. Adjusting for ohmic loss increases simulated energy production in all months.

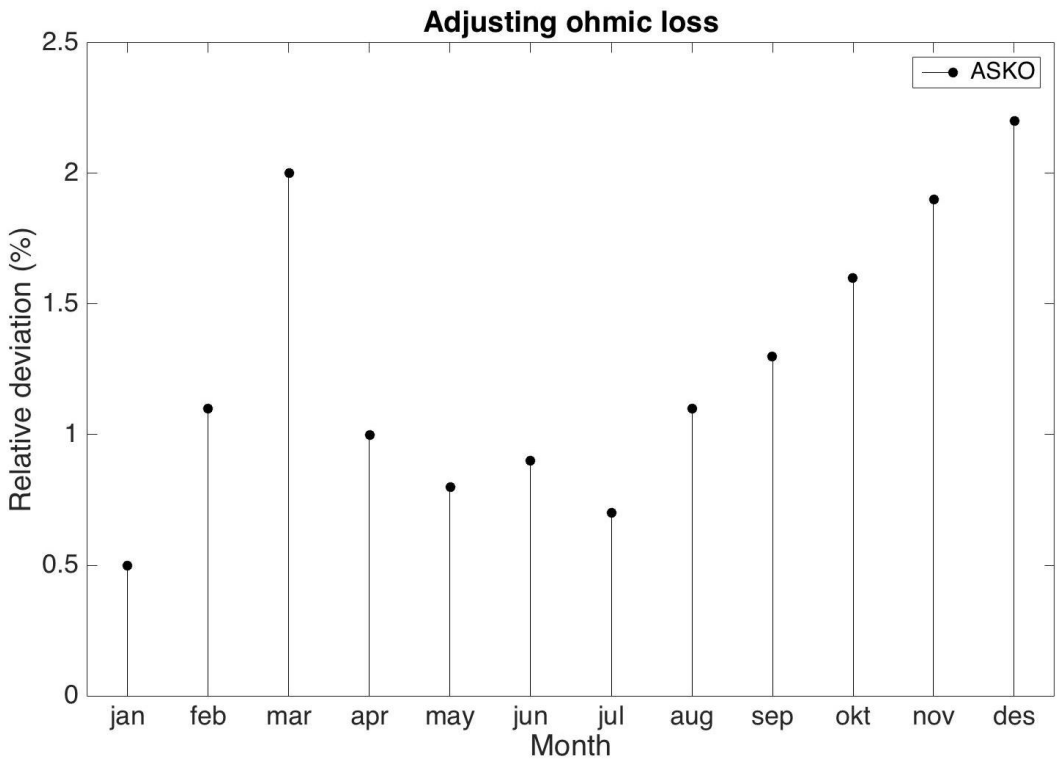

Figure 5.12: Relative Error compared to the simulation results in scenario 2.

Calculated ohmic resistance based upon the information received from Bentley (l 21) and detailed computation is more accurate compared to the default estimate done by PVsyst. That is mostly due to a wrong estimate about length and lack of knowledge about cross-section of the copper cable. All resistance power loss estimated by PVsyst is calculated with reference at STC. The system at ASKO does not experience STC conditions at most of its operating time and the detailed computation in PVsyst may still be slightly to high compared to the actual power loss due to cable resistance.

Section summary

ASKO meteo scenario 2 results originally show acceptable coherence between simulated and produced energy. The results of this section shows that adjusting thermal loss and monthly soiling influence simulation results significantly for the PV system at ASKO, by improving the simulation accuracy on a monthly basis. Thermal loss according to module temperature increased predicted energy in all months and reduced monthly root mean square deviation (RMSD). Increasing soiling levels for winter and decreasing soiling levels for summer reduced RMSD considerably. Increased soiling levels does not increase losses due to shading. Adjusting albedo and ohmic resistance is not as influential and does not improve the simulation model notably.

5.4 Combination of Parameters

5.4.1 Combination scenarios with ASKO meteo

A combination of the parameters with the lowest RMSD values may be a good fit in order to reduce monthly deviation in a combined parameter scenario. Deriving a combination from the previous results based upon thermal loss according to module temperature and experimental soiling may be a good start. Albedo did not affect the simulation result noticeably and is not included. The reduced ohmic resistance loss is more accurate than the PVsyst estimation and is included in the combined scenario, named Comb-1. Other discrepancies can then be investigated and evaluated.

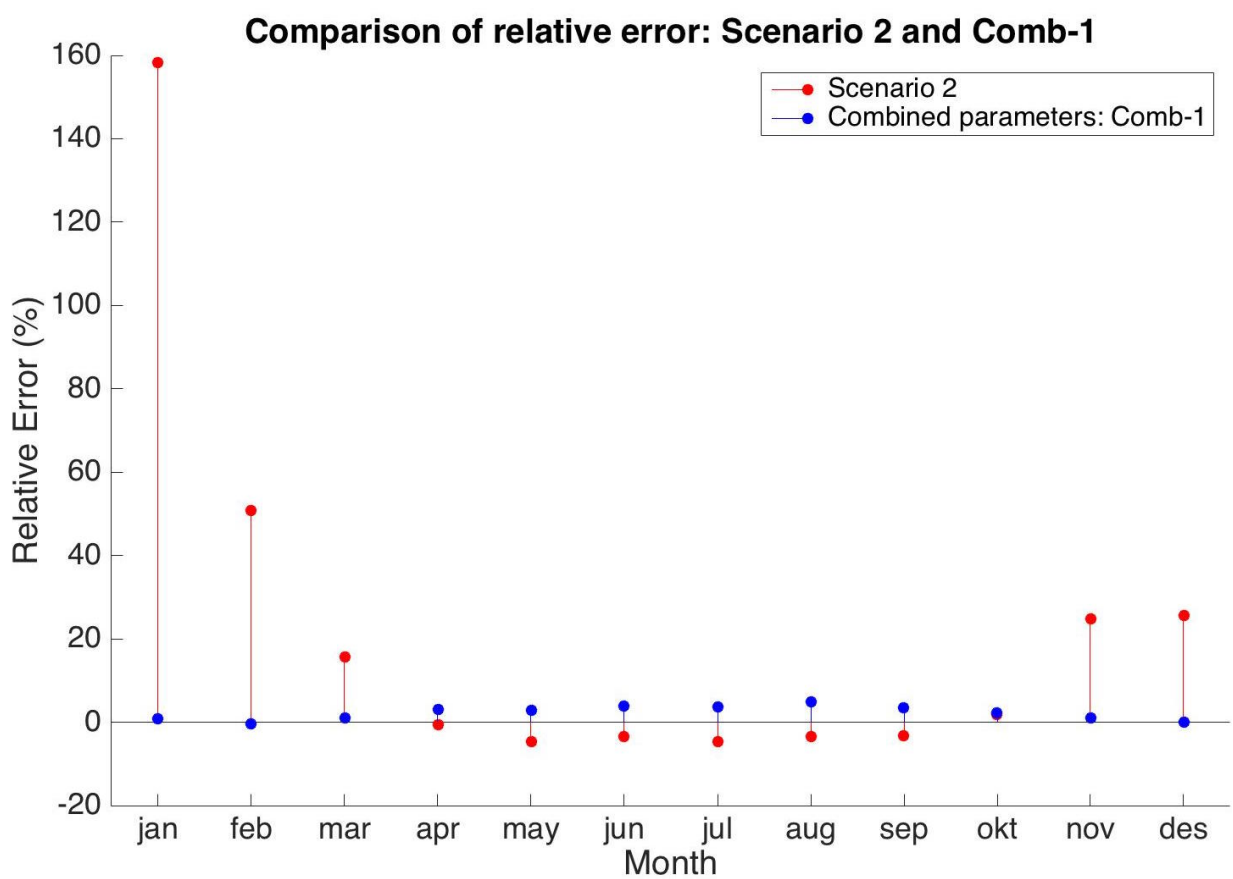

Figure 5.13: Monthly Relative Error (RE) for S2 and Comb-1. The Comb-1 RE shows consistent lower estimations.

Comb-1 presents a notable overestimation for all summer months as presented in figure 5.13. The result is a yearly energy estimate of 309858 kWh, an overestimation from produced energy of 3,3 % compared to the underestimation of 0,4 % in S2. The combination of these parameters resulted in a RMSD of $1165,23\ kWh$. That is a 29,26 % reduction from the deviation in S2. The figure shows how combining the parameters create a more consistent error compared to S2. The increase of yearly simulated energy corresponds with an increased performance ratio (PR) of 85,9 %. The Comb-1 scenario results in more accurate estimations on a monthly basis. The RMSD is reduced, resulting in a stronger positive correlation compared to S2. The correlation is presented in figure 5.14. In S2, the over and under estimations neutralized each other, creating a false impression of yearly accuracy. Monthly error in S2 was more significant and as figure 5.14 shows, the R-squared value for Comb-1 is stronger, indicating a better fit than the values estimated in S2.

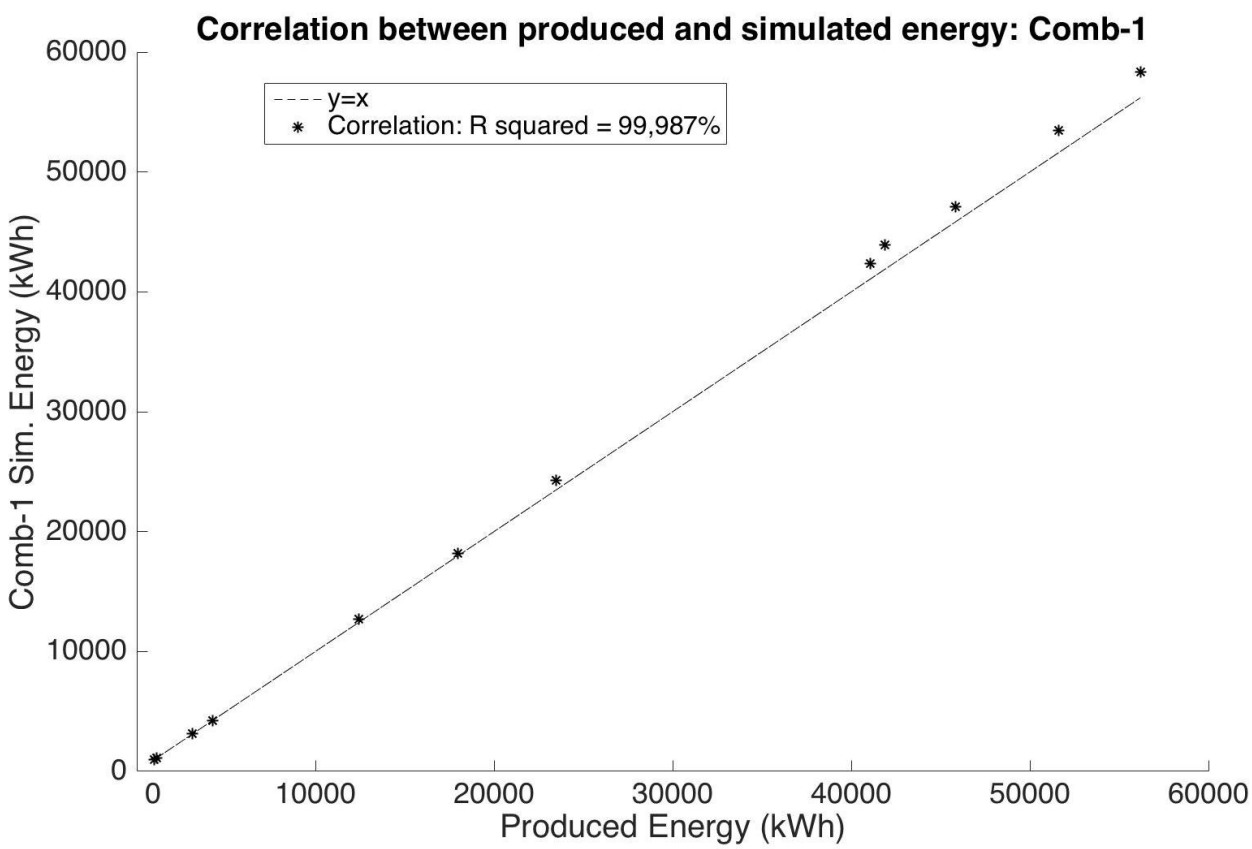

Figure 5.14: Correlation plot for the Comb-1 scenario. The plot shows a strong positive correlation. The R-squared value is 99,987 %.

The results so far prove considerable monthly deviations in S2. Adjusting some of the parameters individually reduced deviation significantly. When combining all the parameters however, the simulation result is not as accurate as the individual results indicate that a combined scenario could become. It is hard to argue to what extent each parameter contribute to loss for the real system. Also, the influence of experimental parameters as LID and IAM must be discussed. As figure 5.13 show, the combined simulation results in an overestimate. This may be because adjusting ohmic and thermal loss both contributed to increased simulated energy production. Experimental soiling increased simulated energy during summer months although it resulted in a yearly underestimate.

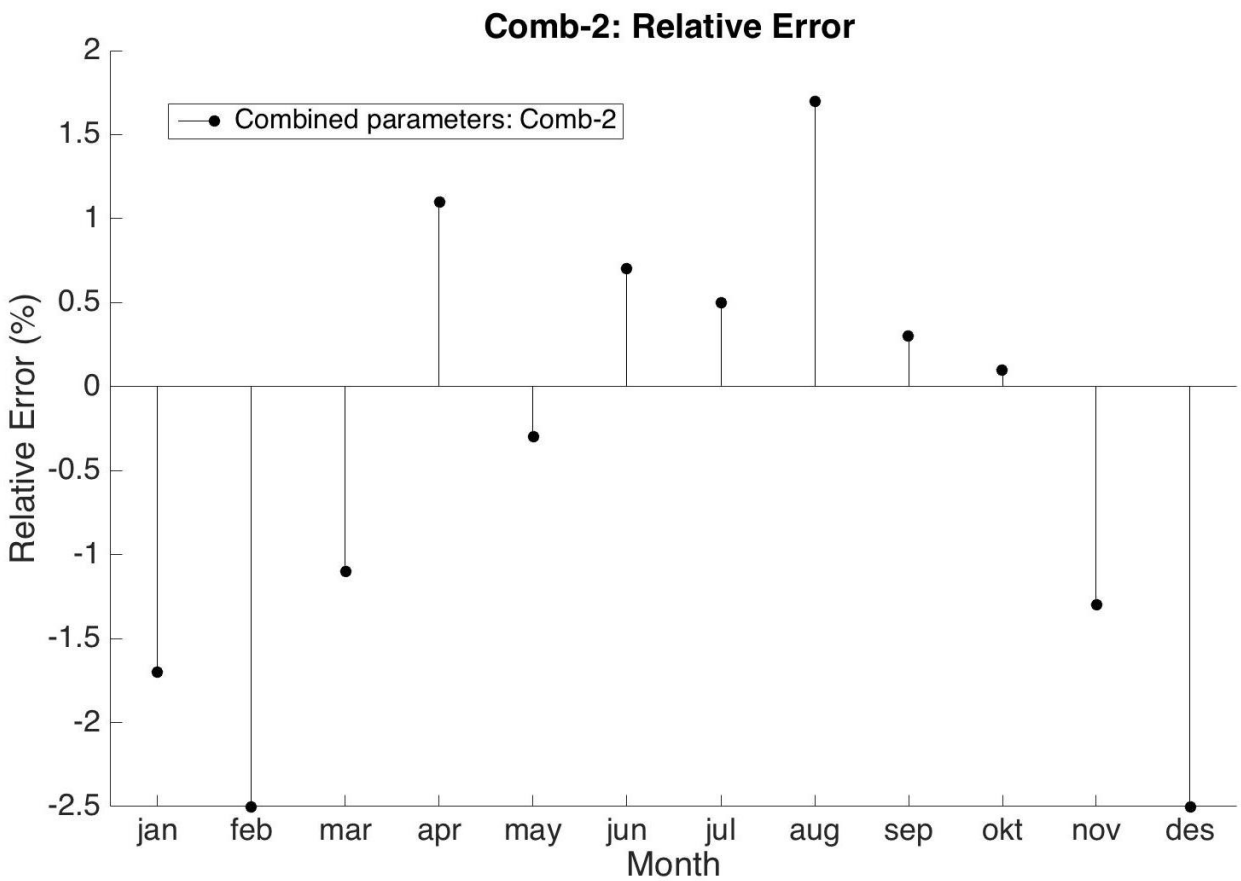

Figure 5.15: Comb-2 scenario: Relative Error.

In the combined scenario (Comb-1), the most significant deviations are during summer. Analyzing the combined result, the soiling values used for summer may have been too low. Perhaps the system at ASKO is prone to more dust and contaminant particles accumulating on the surface of the modules than first assumed, despite frequent rainfall. For the combined scenario, one may

also consider losses due to LID. As the Comb-1 result estimate too much, a proposed default LID loss of 2 % does not seem so far-fetched and will reduce simulated energy on a monthly basis. A Comb-2 scenario, combing LID loss with an increased summer soiling loss of 2 % (all 1% values replaced by 2 % values) results in a yearly simulated energy of 301329 kWh. That is a 0,46 % overestimation of produced energy. The RE decreases significantly from the previous scenario, as presented in figure 5.15.

The Comb-2 RE is not as consistent for every month, as Comb-1. The RE is lower and results in a RMSD of 287 kWh, which is a 82,58 % reduction from S2. That decrease in deviation from both S2 and Comb-1 is considerable. The PR decreased slightly to 83,6 % due to increased losses. The result is a stronger correlation between simulated and produced energy, as presented in figure 5.16. The corresponding R-squared of 99,990% indicates a very strong correlation.

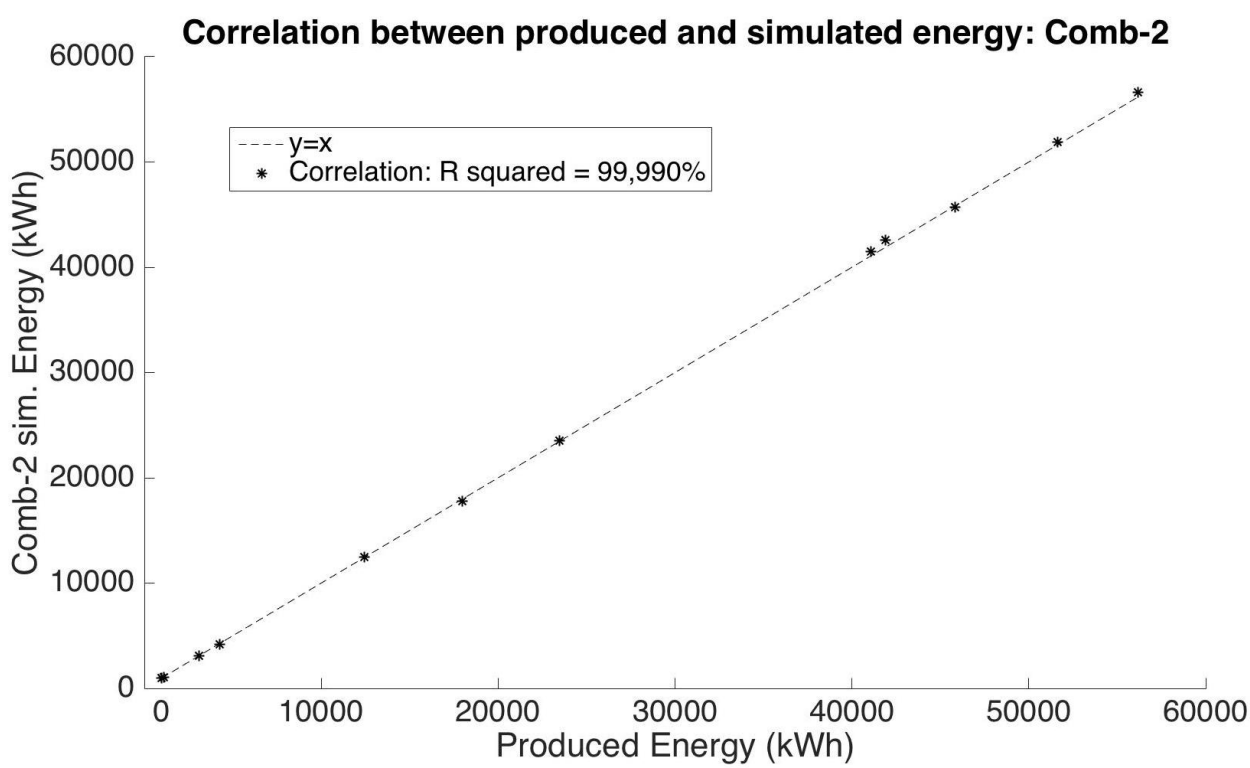

Figure 5.16: Correlation plot for the Comb-2 scenario. The plot shows a strong positive correlation. The R-squared value is 99,990 %.

The comb-2 scenario includes LID. More parameters included in the simulation, results in further introduced error. Although the correlation of the data is strong, values of the parameters can be discussed. The soiling values of 2 % are lower than the default of 3 % in PVsyst. These val-

ues are experimental and include a lot of uncertainty. These values are based upon meteo data from 2015 and will most likely differ from other years. However, the soiling values used are an indication of how the issue of soiling should be treated in PVsyst. The RE for Comb-2 indicates that the experimental soiling values for months affected by snow are too high, as the 2 %LID loss is introduced. The LID loss is a researched and discussed loss that may be completely wrong for this system. To determine if this system is exposed to LID, a study of the actual module at ASKO should be conducted.

Section summary

A combination of parameters for ASKO meteo data results in an over estimate of yearly simulated energy. Performance ratios are increased from ASKO scenario 2. The root mean square deviation is decreased compared to scenario 2, and presents a stronger correlation between simulated and produced energy. The overestimate suggests possible losses due to LID and increased soiling levels for summer months, which (when included) results in better coherence between simulated and produced energy.

5.5 Investigating Impact of New Information

As mentioned in section 4.3.6, new information regarding the characteristics of the modules were discovered. The change in module characteristics consists of changing the shunt resistance of $R_{sh} = 250\ \Omega$ and series resistance $R_s = 0,13\ \Omega$ and the short circuit current temperature coefficient to $I_{sc_tc} = 2,2\ mA/°C$. Simulating energy production with default loss settings as described in scenario 2 (S2) resulted in a yearly energy estimate of 286036 kWh. That is a underestimate of 4,64 % compared to produced energy and more than a 4 percentage points lower estimate compared to scenario 2. The resulting monthly deviation is $2606,1\ kWh$, which is about a 58 % increase of monthly deviation from S2. There are two aspects that have to be analyzed from this result. The first is the reason for the increased underestimate from S2 (greater deviations) and the second is how it may impact the other results.

Performance ratio drops from 82,8 % in S2 to 79,3 %, indicating increased losses. The loss diagram for the combined scenario is presented in appendix B.4. The loss that emerge from the diagram is the notable increase in PV loss due to irradiation level. The loss increased 3,9 percentage points from S2, which constitutes most of the total underestimate of 4,64 %. PV loss due to irradiation level is a result of the intrinsic behavior of the solar cell, described by the one diode model (2.7), and is thus mostly determined by the module resistances. Most of the reaming loss is due to increased PV loss due to temperature, a result of the decrease of I_{sc_tc}. According to PVsyst (2014) modules with low R_{sh} and high R_s have the best performances under low light conditions. Due to the increased loss, it appears that the decrease of R_s influence the results more than the decrease of R_{sh}. The decrease of R_{sh} should ideally contribute to better low light performance, as R_{sh} increases exponentially when irradiation is decreased. As illustrated in figure A.10b, the increased R_{sh} contributes to a higher gap in saved efficiency, however, mostly at irradiation levels below 400 W/m. Figure A.10a shows how a higher R_s maintains high efficiency for lower irradiation levels compared to R_s of lower values. Adjustment of module resistances can occur with upgrades of PVsyst and as a result change loss due to irradiation level, as reported by PVsyst users at the PVsyst forum Mermoud. That is mainly due to the manner in which the resistance are estimated by PVsyst is changed (PVsyst (2014)). As some estimation models in PVsyst changes with an update, PVsyst should not be updated during a project. These changes can be hard to track.

Analyzing the impact of adjusting the module resistances in PVsyst proved the above theories. Decreasing R_{sh} slightly increased yearly estimated energy, while decreasing R_s resulted in a sig-

nificant decrease. The significant decrease in simulated energy with decreased R_s explains why the original module resistances performs better than the alternative characteristics. This is interesting in two manners. Firstly, it implies that the impact of reducing R_s in Norway reduces produced energy. At STC conditions, low R_s resistance performs better than high. High irradiation levels results in high currents, which again results in high power losses (eq. 2.6 and eq. 2.10). That indicates that most of the received irradiation at ASKO must be much lower than the 1000 W/m^2 (STC). Low-light performance measurements of the module included in PVsyst can thus improve accuracy of the simulation, as PVsyst will be more able to adjust the series resistance accordingly. The second, is the impact of the shunt resistance. Studies done by Bunea et al. (2006) and Reich et al. (2009) argue that a higher shunt resistance will retain more of its efficiency at lower irradiation levels, while low shunt resistances will decrease linearly with irradiation.

For the previous results this implies an uncertainty, and that the results may be reduced with the proven underestimate to account for the additional losses presented in this section. The additional underestimate applies to scenario 1 (S1) and S2, as well as the adjustment of each parameter based on S2. That is because the factors causing the changes lie within the modules, which are used in all simulations. The increased underestimate corresponds better compared to previous studies, as described in the introduction (1). Yet, the coherence between simulated and produced energy is more accurate than the results of previous studies. The patterns described when adjusting individual parameters still apply, although deviation is now more significant. The optimized scenario (Comb-1) shows a considerable overestimation. This overestimation is compensated for, when the new information is applied. With the new information PVsyst underestimates simulated energy more compared to S2. That implies that all meteo sources in S1 and S2 will underestimate even more than what is shown in the result. The overestimation of the Comb-1 scenario is to some extent neutralized with further underestimation of the original S2 result. A new combined scenario (Comb-3) can be simulated based upon the exact same detailed loss parameter as in Comb-1, except that the new R_{sh}, R_s and $I_{sc-Temperature-Coefficient}$ is updated for the module characteristics.

The Comb-3 scenario resulted in a yearly energy estimate of 297713 kWh, only a 0,75 % underestimate of actual energy. The performance ratio increases to 83,1 %, indicating that the losses are reduced for the combined scenario. The Relative Error (RE) for the new combined scenario (Comb-3) is presented in figure 5.17. The RE for the Comb-3 scenario shows a significant un-

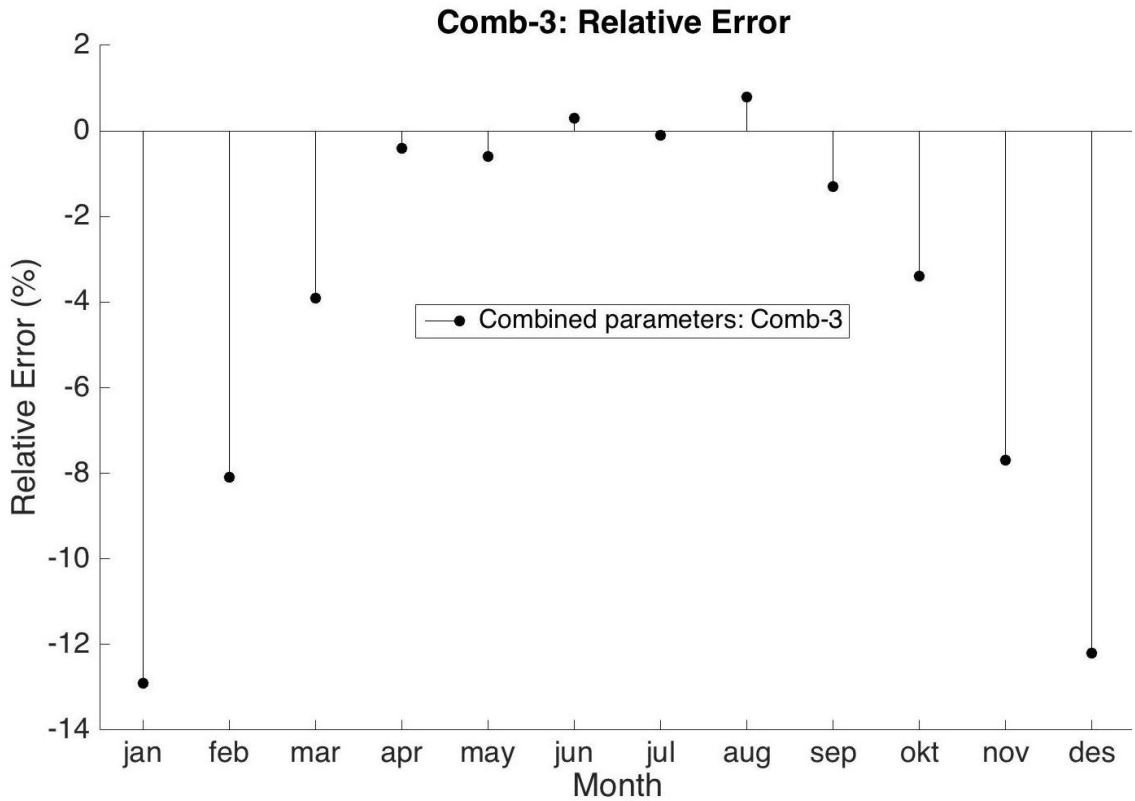

Figure 5.17: Relative Error for the Comb-3 scenario. This scenario is based upon the Comb-1 scenario with the only difference being the adjustment of R_{sh}, R_s and $I_{sc-Temperature-Coefficient}$.

derestimate during winter months. The summer RE values are all below 1 %. The experimental soiling values used in the combined scenarios aimed to reduce the considerable overestimate during winter moths. Further reduction caused by the new module characteristics, as proved for S2 above, results in the negative RE values. Due to the nature of the one diode model, the result is more evident during winter (higher RE) due to lower light conditions. The Root Mean Square Deviation (RMSD) for the Comb-3 scenario is $317,28\ kWh$, which is a 80,74 % reduction of monthly deviation from S2. Although it is not lower than the RMSD in Comb-2, it does not include the LID factor and increased summer soiling levels. The Comb-3 scenario presents a strong positive correlation with a R-squared value of 99,988 %, as shown in figure 5.18.

Further adjusting the experimental soiling levels to reduce the underestimation in Comb-3 for winter months improves the accuracy of the simulation drastically. Decreasing the winter soiling levels, as described in appendix B.3, results in monthly RMSD of $167,29\ kWh$. That is half the monthly deviation of the Comb-2 RMSD, and a corresponding R-squared value of 99,993 %, presenting a very strong correlation between the simulated and produced energy. Thus, half the

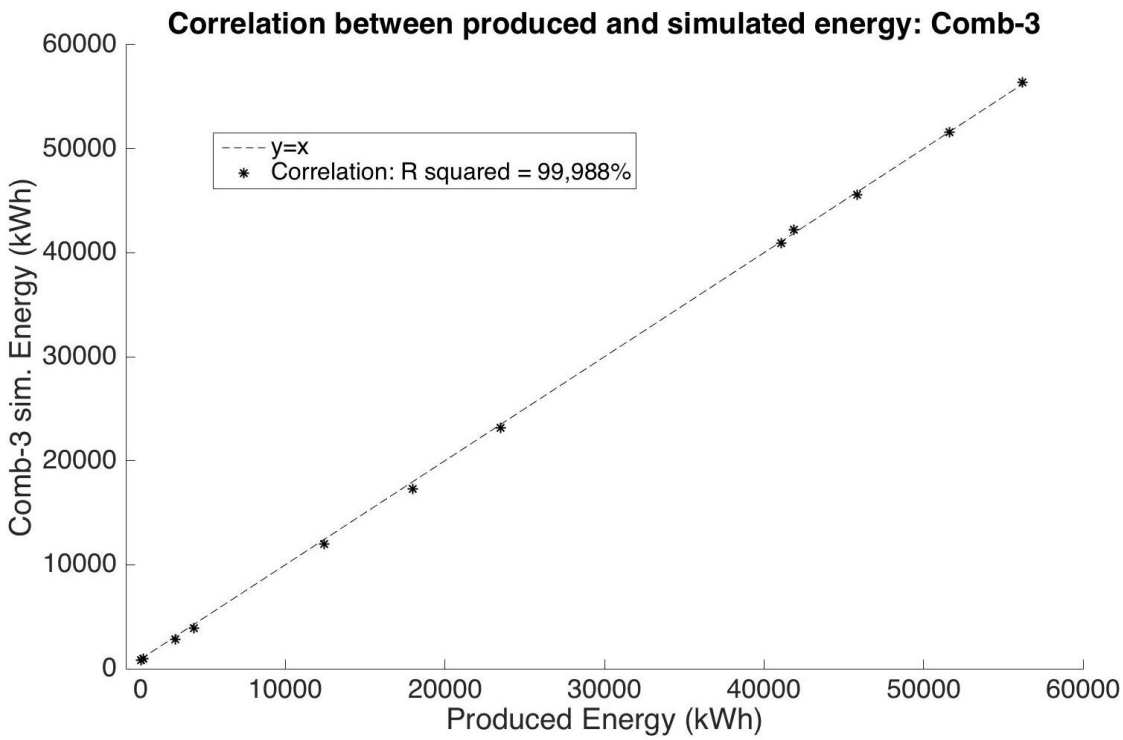

Figure 5.18: Correlation plot for the Comb-3 scenario. The plot shows a strong positive correlation. The R-squared value is 99,988 %.

deviation in Comb-3 was due to underestimation of predicted energy during winter, which was a result of the experimental soiling values.

The results of this section is also rather interesting. Input parameters and characteristics of modules are as important for the simulation estimate as simulations parameters (detailed losses). A change in module resistance to $R_{sh} = 250\ \Omega$ and $R_s = 0,13\ \Omega$ reduced yearly simulated energy over 4 %. The results presented in this chapter shows that albedo and ohmic adjustment influence simulated energy relatively small compared to aggressive soiling values or thermal losses according to module temperature. That implies that quality of data used when simulating is just as important as which detailed losses are included and how much the impact. For example is the yearly impact of changing the R_{sh} and R_s more significant than adjusting soiling values.

5.5.1 The combined scenarios on the Meteonorm data

The Comb-1 and Comb-3 scenarios are applied with the Meteonorm (MN) meteo file to investigate how adjustments of the detailed loss parameters work on the other meteo files. These scenarios are named MN-Comb-1 and MN-Comb-3. Since MN does not included module temperature, thermal loss according to own defined heat loss constants are used, $U_c = 25$ (W/m^2K) and $U_v = 1,4$ $((W/m^2K/(m/s))$. The detailed loss parameters in Comb-1 and Comb-3 are exactly the same. The only difference is the update on module characteristics.

The MN-Comb-1 resulted in a yearly simulation estimate of 293328 kWh , which is a 2,2 % underestimate of actual energy production. Although the underestimate is about the same for MN-Comb-1 and MN meteo in scenario 2 (S2), the monthly RMSD decreased to 3118,6 kWh (about a 20 % reduction). Compared to the RMSD for Comb-1 with ASKO meteo, this is almost 3 times the deviation. Yearly performance ratio was estimated to 83,4 %, which is not that much lower than combined parameters for ASKO meteo data. That suggests that expected energy production at STC is lower for MN meteo than for ASKO meteo. The monthly Relative Error (RE) is presented in figure 5.19. The figure presents high RE´s, with both under- and overestimations. The results from the MN-Comb-1 is distinct from the Comb-1 result in the way adjusting the parameters impacted the simulation results. The comb-1 scenario resulted in a significant increase in predicted yearly energy from S2 for ASKO meteo. However, for MN meteo, the yearly result is about the same.

It is uncertain why the adjustment of detailed loss parameters does not impact the simulation result in a similar manner for MN meteo as for ASKO meteo. By analyzing the loss diagram for MN-Comb-1 it is clear that some of the loss factors are increased compared to Comb-1 for ASKO meteo. This may be due to how the meteo data impact the individual loss parameters. MN recorded higher wind values, which should contribute to a higher thermal heat loss (increased predicted energy), compared to ASKO meteo. The estimated ambient temperature by MN is higher than ÅS meteo contributing to a decrease in thermal heat loss. Although yearly irradiation is about the same for ASKO and MN meteo, monthly irradiation by MN is less in June and July, a pattern seen in figure 5.19.

The alternative module characteristics in the MN-Comb-3 scenario resulted in a yearly simulation of 282277 kWh, which is a underestimate of 5,9 % of actual energy production. Considering the accuracy of the Comb-3 for ASKO meteo, this scenario resulted in a significant underesti-

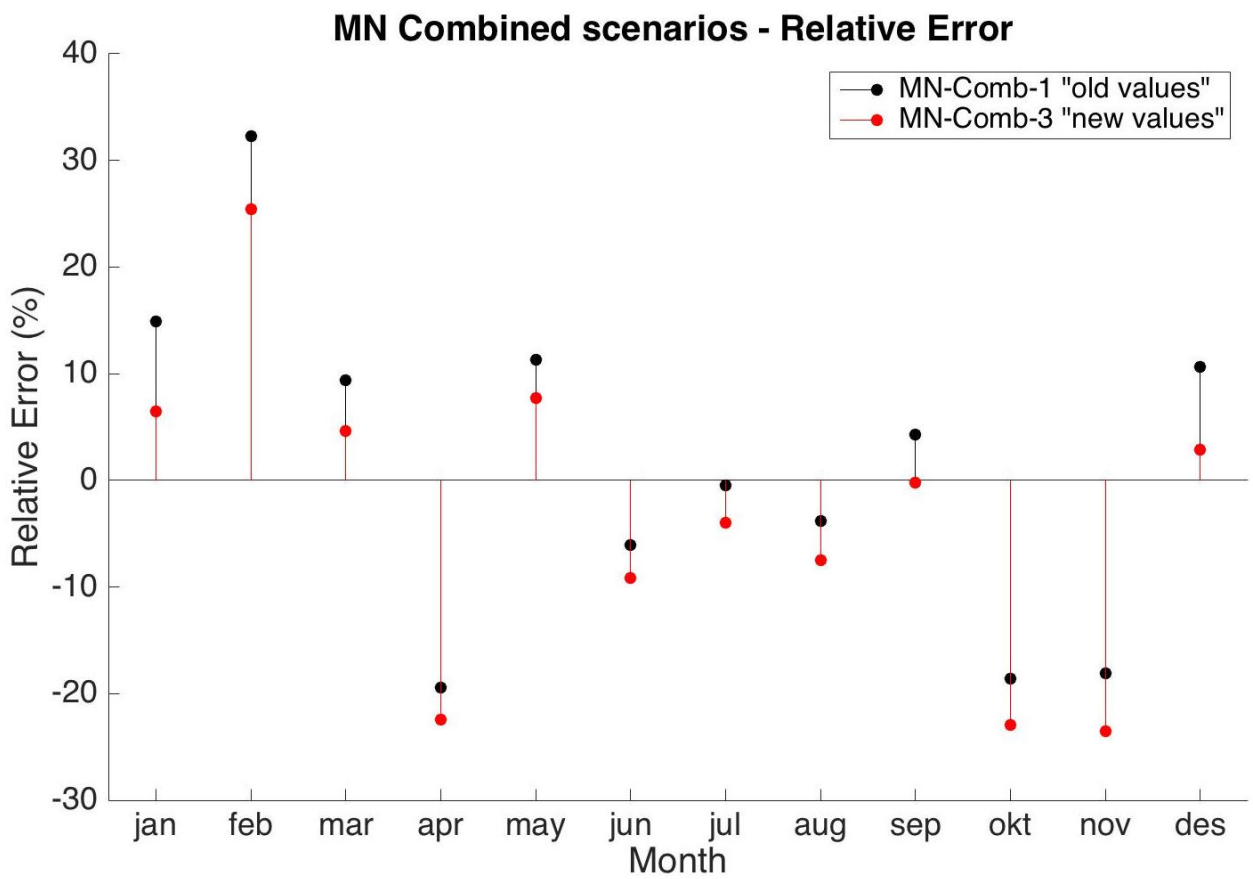

Figure 5.19: Relative Error for MN-Comb-1 and MN-Comb-3 scenarios compared to produced energy at ASKO.

mate. Monthly RMSD was 3524,9 kWh, which is an increase from the MN-Comb-1 scenario. Figure 5.19 presents the decrease in predicted energy. The performance ratio drops from the MN-Comb-1 to 80,3 %, indicating increased losses. It is clear that with the alternative module characteristics, MN meteo underestimate considerably. The underestimate seen with the alternative module characteristics correlated better with previous studies, as described in section 1.

The results presented for the combined scenarios with MN meteo data implies that satellite collected data underestimate significantly more than meteo data collected from weather stations, as ASKO. MN underestimated the most for S2, and combining the parameters did not improve the simulation result notably. The validity of introducing a possible LID loss and increasing summer soiling levels in the Comb-2 scenario with ASKO meteo data, can be discussed considering the underestimate with alternative module characteristics. Comb-3 with ASKO meteo and MN-Comb3 both resulted in a a underestimate. The underestimate in MN-Comb-1, implies that there is no reason to introduce these losses in a Comb-2 scenario with MN meteo data.

Section summary

New module characteristics reduced yearly simulated energy and performance ratio significantly, mostly due to a increase in PV loss due to irradiation level. The impact will be evident in all presented results with ASKO meteo. The alternative module characteristics are not confirmed by the manufacturer after it was discovered a difference within their two data sheets. Satellite collected data by MN underestimates considerably more compared to measured meteo data at ASKO. Adjustment of detailed loss parameters influence ASKO simulation results more than MN simulations result. Decreasing series resistance significantly decreases yearly simulated energy. The combined scenarios question the introduction of a LID loss, and supports low summer soiling levels (1 %). Furthermore, it implies lower experimental soiling levels during winter.

5.6 General Discussion

This section provides a general discussion of the study, analyzing the meteo data, methodology and results of the study.

Discrepancies between simulated and produced energy is proven. The problem is to determine which parameters causes the deviations. As shown in the results, most parameters may be adjusted to reduce the RMSD. In the methods it was argued how several parameters may be adjusted based upon meteo data or system characteristics. Therefore, it is most likely a combination of several parameters that must be adjusted to yield more accurate simulation results. To what extent each parameter should be adjusted in a combined scenario to contribute to a more accurate simulation result is a difficult question. This is mainly due to the levels of research and knowledge about how the parameters influence a particular system. As described in section 4.5.2, quantifying soiling levels of measuring heat loss from modules are complicated. Both these values are therefore experimental values, although based upon research.

Reliable information and characteristics about modules and inverters is essential for the accuracy of the simulation results, as is evident from the results of this study. Inaccurate information, or uncertainty in the producers own tests and measurements presented in their data sheets may result in deviations between simulated and produced energy. If these errors and uncertainties are not known or detected, resulting deviations may by accident be corrected by

experimental adjusting of secondary parameters (soiling, thermal loss etc.). The impact of using the wrong information in the simulation implies that system information in PVsyst should be carefully checked before proceeding with the simulations. For inverters and modules that exists in PVsysts´s database, the information and time of modification of the file should be controlled. The best option would be to contact the producer in advance of designing the system, for quality assurance of characteristics, or ask for updated or extra information. Some producers may have reflection constants for IAM and IAM profiles for their modules that are not accessible on their web page.

The foundation for simulating energy production with a simulation tool as PVsyst is meteorological (meteo) data. There are many stages where errors and uncertainty may be introduced in the meteo file. Hourly meteo data used in PVsyst contains a lot of information, that may be hard to quality assure. The uncertainty related to the estimates or measurements of these data is explained in chapter 3. The logging and storage of data and how it is applied in PVsyst do also introduce uncertainty. Missing data points in a meteo file have to be detected before being imported, so values for the missing points can be interpolated. If it is not detected or the information is simply logged wrong, a time shift issue may appear when importing meteo data into PVsyst. The time shift will be detected by the "tables and graphs" tool, as explained in section 4.3.2, that will suggest to apply a time shift. Possible deviations in time can be caused by the meteo file not including a time shift due to a difference in summer and winter time. Time difference due to summer and winter time can be corrected in PVsyst if the user knows whether the file is adjusted for the time shift or not. Other causes for deviations can be due to different time labeling when logging data. Irradiation values for the different sources are logged at different frequencies and then stored as hourly values. The time stamp these values are stored to may differ. That is, a 12.00 hourly irradiation value may for example be logged between 11.00-12.00 or from 11.30-12.30. How this works in detail and influence the simulation is not investigated thoroughly in this thesis.

The meteo file from ASKO contained irradiation values that for time stamps during the day that were not exposed to sunlight (mostly night) showed negative values. These values are very small on an hourly scale. However, when summarized for a whole month, the difference was between 0,1 % and 7% depending on the month. In Matlab, these values were detected and replaced by zero-values. Error in the PVsyst treated meteo files can thus occur due to human error. During the study, Matlab was used to organize and group data into monthly values for analysis and

calculations. All statistical values of simulated and produced energy, as well as the analysis of meteo data is conducted with Matlab. Error in the Matlab code will propagate and result in possible errors in the simulation results. Although the codes are controlled, error may occur and is very hard to detect.

PVsyst calculates irradiation incident on collector plane based upon supplied global horizontal irradiation and the Perez transposition model. This model is a sophisticated model that requires good horizontal data according to PVsyst (2014). The simulations in this thesis are based upon the Perez model. The alternative model included in PVsyst is Hay´s model, which requires some knowledge about the diffuse irradiation. The Perez model is default in PVsyst as it offer lower RMSD. A more accurate simulation of energy can occur if diffuse irradiation is measured explicitly instead of estimated in PVsyst. The ASKO meteo file does not include diffuse irradiation and is therefore (as with irradiation incident on collector plane) estimated with the Perez model. Yearly estimate of global incident in collectors plane is about -0,4 % lower than global horizontal. It is important to remember that the global horizontal irradiation includes both direct and diffuse irradiation, as described by equation 2.1. Therefore, the purpose of importing diffuse irradiation into PVsyst is to improve the accuracy of calculating the irradiation incident on the plane, opposed to utilizing the transposition model.

The conducted study analyzed yearly and monthly simulated energy and compared the results with produced energy at ASKO. Comparison of data at a hourly basis would result in a more thorough study of the accuracy of PVsyst simulations. A study based upon hourly data rely on good data from PVsyst and from the PV system. PVsyst allows output of hourly simulation values for certain parameters as global horizontal irradiation and energy injected to the grid. The problem for this study was access to good hourly production data. The stored PV system data was logged as average values every fifth minute, and to be able to compare this data with PVsyst data it had to be transposed to hourly values. The issue of data quality was prominent in this case. Several absent log stamps were detected each day within the production data for the PV system at ASKO for the year 2015. The production file should have contained about 105120 recorded values, not 104397. To be able to compare, the missing data must be detected and replaced by interpolated values. Interpolated values introduces new uncertainty in the file. Furthermore, a mistake in replacing one missing value can result in a time shift of the data, increasing the possibility of deviations between simulated and produced energy.

Energy estimations by PVsyst are not far from any of the sources considering the rated uncertainties for each source, as described in section 3. Any error in the hourly measured or estimated irradiation will propagate when used as a source for energy estimation. A deviation in the irradiation data alone creates a significant impact on the deviations, as described in the results. A -5 % error (underestimate) measuring irradiation in May month with a 15,29 % efficiency of the modules, constitutes 1 kWh increased energy for the case of scenario 2 with ASKO data. That accounts for almost half the underestimate presented in figure 5.7b, by one parameter. The uncertainty in the instrument can also cause increased deviations, if the instrument overestimate.

5.7 Recommendations for similar simulation models in PVsyst

The conducted study shows that quality and precision of irradiation data is critical for the accuracy of simulated energy. Drawn conclusions can strongly depend on what type of meteo data set and module characteristics that are used in the study. The results of this study indicate some methods to be accounted for when simulating similar systems in the south-eastern part of Norway. Conducting measurements of JV curves at STC and low-light conditions and at different temperatures can greatly improve simulation accuracy, especially if it is not included by the manufacturer. The results can be imported to PVsyst and help improve estimation models.

Measured irradiation data from a pyranometer at a weather station in the vicinity of the planned PV system is more accurate than the estimates by satellites. The closer the weather station is to the planned PV system, the more accurate will the measurements be. Satellite data underestimate global horizontal irradiation more than irradiation measured by a pyranometer. If satellite data is used in the planning process of a PV system an underestimation of irradiation of a about 3 -4 % should be expected.

Albedo adjustments did not improve the simulation accuracy as implementing measured values did not change the simulation result much. Estimating ohmic loss increased predicted energy on a monthly basis, as default ohmic loss estimated by PVsyst is calculated at STC and is slightly overestimated. The estimated loss by the detailed computation is more than 1 % lower than the default global loss fraction at STC. Therefore, rough estimations of cable length combined with knowledge about the cross-section and type of cable will improve the accuracy of the result. A ohmic loss fraction between 0,3 and 0,6 % for PV systems of similar size as ASKO is ideal.

Measured ambient temperature and especially wind data results in more accurate simulations results, when applied in the thermal loss estimation. For modules mounted just above the roof with a small tilt, the thermal loss constants should be about $U_c = 25$ (W/m^2K) and $U_v = 1,4$ $((W/m^2K/(m/s))$ or according to the free mounted option with $U_c = 29$ (W/m^2K). The results show that these heat loss constants are still a bit conservative compared to thermal loss according to module temperature. For PV systems mounted with greater distance from the roof and with a higher tilt angle, the thermal loss option should be" free mounted", and perhaps even with the addition of $U_v = 1,4$ $((W/m^2K/(m/s))$. Including a wind loss factor is important if the PV system is located in areas with high wind velocities.

To quantify exact soiling values to be used in a simulation model is difficult as it is very dependent on geographical location. Different snow patterns from year to year influence soiling values during winter. A recommendation for plausible monthly soiling intervals have been defined in table 5.5.

Table 5.5: Recommended interval for soiling values derived from the results of the study. Note that the size of the intervals during winter are large due to unpredictable amounts of snow. The underestimate during winter months for the combined scenario with ASKO meteo data, and alternative module characteristics are also accounted for.

Date	Jan	Feb	Mar	Apr	May	Jun	Jul	Aug	Sep	Okt	Nov	Dec
Recommended soiling interval (%)	47-57	29-39	12-18	1-3	1-2	1-2	1-2	1-2	1-2	3-6	15-25	15-25

Chapter 6

Conclusion

One of the main problems predicting energy production with a simulation tool as PVsyst is determining which parameters to include, both meteorological (meteo) and loss related. Most problematic is deriving explicit values for loss parameters. Conclusions depends on which meteorological data set is utilized. The results of the conducted study are related to the PV system at ASKO, although applicable for PV systems of similar configuration and geographical location.

The impact of meteo data quality and adjustment of loss parameters on simulation accuracy with PVsyst have been investigated and analyzed. The results presents a clear difference between the choice of meteo data set. Satellite collected data underestimate yearly global horizontal irradiation about 3 - 4 % and predicted energy about 2-4 % for the default scenario models (scenario 1 and scenario 2). Monthly Root Mean Square Deviation (RMSD) was 3874kWh for Meteonorm (satellite data). Measured meteo data at weather stations are more accurate than satellite meteo data and results in 40 - 50 % lower monthly RMSD. The weather station at Ås overestimated predicted energy 2,3 % and ASKO underestimated 0,4 % for the default scenario 2 model. Higher irradiation values at Ås compared to ASKO indicates that accounting for local climate differences (due to different geographical locations) is important for the accuracy of the simulation.

The underestimation observed seems to be less severe than what previous studies have reported for similar simulations. A reason might be an improvement of meteo data, and then especially satellite data. The weather station at Ås has been included in Meteonorm´s database, increasing the accuracy of the weather interpolations significantly for areas in the vicinity of Ås. The impact of alternative module characteristics, mostly shunt and series resistances, contribute to increased PV losses due to irradiation level. The result is a more serious underestimate of yearly

predicted energy, about 4,6 % and 6,4 % for Meteonorm (MN) and ASKO respectively. That result corresponds better with previous studies.

Adjusting albedo according to measured values impacted the accuracy of the simulation in a minor way. Mostly, because the treatment of albedo in PVsyst regarding the influence on predicted energy is negligible. A rough estimate of ohmic loss resulted in a 1 % decrease from the default at 1,5 %, and thus increased predicted yearly energy. Accuracy was improved by reducing RMSD 5 % from S2 with ASKO meteo.

The impact of thermal loss and monthly soiling were the most influential detailed loss parameters, increasing simulation accuracy. Simulating thermal loss according to module temperature resulted in a yearly overestimate of 3,6 % and RMSD of 1263 kWh. Thermal loss in PVsyst is underestimated as it is based upon ambient temperature and conservative heat loss constants. Wind velocities impact the simulation result significantly when a constant for thermal wind value is included. Monthly soiling values resulted in a decrease of overestimation during winter and underestimation during summer. Adjusting for soiling was the parameter that individually improved simulation accuracy the most, by reducing monthly RMSD to $615,6$ kWh.

Combining monthly soiling loss, thermal loss according to module temperature and ohmic loss in combined models resulted in better coherence between predicted and actual energy production. ASKO meteo resulted in consistent monthly overestimation, suggesting a possible Light Induced Degradation (LID) loss of 2 % and/or soiling values of 2 % during summer. MN meteo in the combined model resulted in a more severe underestimate compared to ASKO meteo, a pattern evident from lower estimated irradiation. Introducing new shunt and series resistants of lower ohmic values, decreased module low-light performance. The result was a decrease in predicted energy on a monthly basis.

Chapter 7

Further Studies

The conducted study includes simulations with many parameters, analyzing several aspects. There are, as described in the discussion, room for more in depth study of certain parameters. Thorough analysis of individual parts presented in the results can improve simulation accuracy.

The first measure to improve the study is related to the choice of a case study system. The PV system at ASKO is a commercial system that is not optimal for research, as frequent field trips are complicated. Measures to experiment on parameters as soiling or thermal losses are problematic, and cable lengths can be estimated more accurately. Research systems with easy access are better opted for thorough studies. Attempts to measure soiling levels for different orientations and tilts can be conducted. More important, quantifying soiling levels for different types of materials, as the accumulation of dust and contamination particles, and to measure how snow and frost behave on the modules. The formation of frost and the accumulation and melting behavior of snow can be filmed. Thermal loss estimations may be improved by studying the impact of air ducts behind strings of modules. Interesting topics is how different areas (cross-sections) and wind speeds impact heat loss from modules. For example, three different air duct areas can be used and wind speed in the air ducts can be measured in order to more accurately determine the thermal heat loss constants. Improving knowledge about soiling levels and thermal heat loss of modules will improve the accuracy of monthly energy simulations.

More control of the PV system includes more control and reliability of data from the system. Meteorological (meteo) data can be collected in manners that reduce the uncertainty of the data, through optimal placement and maintenance of instruments. Desired meteo data instruments can be installed in order to increase the number of simulation parameters. In the conducted study, ASKO meteo included module temperature, while ÅS meteo included wind direction and

diffuse irradiation. Thus, one meteo source did not contain all the desired parameters needed for in-depth study of the influence of different parameters on the simulation result. An option is to include meteo data from several sources to create a more comprehensive meteo file. For example, the impact of diffuse irradiation on estimated irradiation incident on the collector plane can be conducted.

Access to good, reliable and continuous production data is vital for in-depth comparison between simulated and produced energy. To verify good production data before the study is conducted, should be done if the aim of the study is to compare accuracy of a model at hourly basis. An alternative is to continue on an existing project to conduct a more thorough and in-dept study of the coherence between simulated and produced energy at an hourly basis. Analyzing the discrepancies between hourly simulation results and actual energy production can improve the accuracy of the simulation model. It can be important for some systems to verify that a system can produce enough energy during morning and evening, and not only during mid-day. That implies spending less time comparing and analyzing climate data from different meteo sources. The focus does not need to be on more than two sources, so they may be compared more thoroughly.

Hourly data creates opportunities to analyze low light conditions, especially during morning and evening. Solar height influences received irradiation and air mass (distance irradiation has to travel in the atmosphere increases). Since the solar height in Norway changes on a daily and on a seasonal basis, the relation (if any) between the solar height and accuracy of energy prediction should be explored. The impact of shading can be analyzed on an hourly basis, by comparing the shading estimations in the shadings construction with produced energy. For example, if PVsyst predicts a high shading loss in the morning this should be compared to actual energy production. The shading loss in this study was very low, and thus a thorough analysis of shading was not the most concerning loss to investigate. For more analysis of shading losses (yearly, monthly and hourly) a similar type of study should be conducted on an industrial PV system, with potential for higher loss due to shading.

Energy and power output data from the system, and each inverter could be accessed for individual analyze of sub arrays (SA) in the system. That introduces interesting comparisons of the configuration of the system, between inverters and number of modules in a string. The system at ASKO consist of several SA´s with different configurations in terms of number of modules and inverter ratings. This study did not investigate the individual performance of each SA and its cor-

respondence to PVsyst analysis in the module layout section. As presented in figure 5.8 some of the system loss estimated for the global system may differ from SA to SA. An investigation could be conducted to analyze how each SA operated in order to determine which configuration performs more efficiently, and if the losses are influenced by manually adjusting the component characteristics.

PVsyst allows the user to apply characteristics about modules and inverters to a project. In this study, the module characteristics were applied due to the absence of information about the modules in the database. This section in PVsyst also allows the user to supply measured data about the modules that improve the accuracy of actual module characteristics. The section includes options for importing measured JV-curves, low-light performance data (e.g. at 800 W/m) and a customized IAM profile. Creating an IAM profile is difficult to conduct and is thus dependent on the producer of the modules. However, the first two options can be measured and estimated in a study. The JV-curve and low-light performance should of course be measured for several modules in order to make an accurate estimate that is applicable for all the modules in the system. Low-light performance can be used by PVsyst to more exactly determine the series resistance and its impact on predicted energy. As the importance of accurate module characteristics is investigated and discussed in this thesis, it would be interesting to investigate plausible improvements in simulation accuracy with better and more accurate module characteristics. Low-light performance may be interesting for Norwegian conditions as PV systems in this region rarely operate at STC, but rather at lower irradiation values.

Bibliography

(1998). The mathworks. *Inc., Natick, MA*, 5:333.

Alet, P.-J., Cuony, P., Dutoit, J., Scharrenberger, L., Currat, B., Perret-Aebi, L.-E., and Ballif, C. (2014). Soiling and value of cleaning for low-tilt pv systems in temperate climates: a swiss case study. In *Renewable Power Generation Conference (RPG 2014), 3rd*, pages 1–5. IET.

Amin, N., Lung, C. W., and Sopian, K. (2009). A practical field study of various solar cells on their performance in malaysia. *Renewable Energy*, 34(8):1939–1946.

Andersen, M. (2014). Analysis of actual and forecasted power production for a solar energy system in norway.

Bentley, S. (2016, April 21). Aw: Stellenanfrage über die englische homepage.

Bernhard, P., Thorud, B., Nordahl, S., Bugge, L., and Authen, M. (09-11-2012). Solstrøm i norge. Technical report, Multiconsult and Asplan Viak.

Brenden, M. and Ruud-Hansen, O. Itas – scanmatic instrument technology as. `www.it-as.no`.

Bunea, G. E., Wilson, K. E., Meydbray, Y., Campbell, M. P., and De Ceuster, D. M. (2006). Low light performance of mono-crystalline silicon solar cells. 2:1312–1314.

Caron, J. R. and Littmann, B. (2013). Direct monitoring of energy lost due to soiling on first solar modules in california. *Photovoltaics, IEEE Journal of*, 3(1):336–340.

Chen, C. J. (2011). *Physics of solar energy*. John Wiley & Sons.

Egger, E. Meteocontrol - energy and weather services. *University of Oldenburg*.

Goossens, D. and Van Kerschaever, E. (1999). Aeolian dust deposition on photovoltaic solar cells: the effects of wind velocity and airborne dust concentration on cell performance. *Solar Energy*, 66(4):277–289.

Honsberg, C. and Bowden, S. (2014). Pv education. *ORG.(access Jan-Apr 2016) http://www.pveducation.org/pvcdrom/properties-of-sunlight/measurement-of-solar-radiation*.

Iqbal, M. (2012). *An introduction to solar radiation*. Elsevier.

Lee, D. M. and Raichle, B. W. (2012). A side-by-side comparison of micro and central inverters in shaded and unshaded conditions. In *World Renewable Energy Forum, Denver, USA*.

Lmt.nibio.no. Landbruksmeteorologisk tjeneste - Ås.

Martín, N. and Ruiz, J. (2005). Annual angular reflection losses in pv modules. *Progress in Photovoltaics: Research and Applications*, 13(1):75–84.

Mermoud, A. Pv loss due to irradiance level on pvsyst 6.3. `http://forum.pvsyst.com/viewtopic.php?f=25&t=1836`.

Multiconsult. Vekst i solkraftmarkedet 2015.

Nofuentes, G., Muñoz, J., Talavera, D., Aguilera, J., and Terrados, J. (2011). Technical handbook. the installation of ground photovoltaic plants over marginal areas. Technical report, Technical report, PVs in BLOOM Project—a new challenge for land valorisation within a strategic eco-sustainable approach to local development.

Paraskevadaki, E. V. and Papathanassiou, S. A. (2011). Evaluation of mpp voltage and power of mc-si pv modules in partial shading conditions. *Energy Conversion, IEEE Transactions on*, 26(3):923–932.

PELLANDS, R. et al. (2013). Photovoltaicand solarforecasting: stateoftheart. Technical report, IEAPVPSTask.

Perers, B., Furbo, S., Han, J., Kong, W., and Stergiakis, S. (2015). Long term testing and evaluation of pv modules with and without sunarc antireflective coating of the cover glass. *Energy Procedia*, 70:311–317.

PVsyst (1994-2014). *Pvsyst Help*. PVsyst.

Reich, N., Van Sark, W., Alsema, E., Lof, R., Schropp, R., Sinke, W., and Turkenburg, W. (2009). Crystalline silicon cell performance at low light intensities. *Solar Energy Materials and Solar Cells*, 93(9):1471–1481.

Reich, N. H., Mueller, B., Armbruster, A., Sark, W. G., Kiefer, K., and Reise, C. (2012). Performance ratio revisited: is pr> 90% realistic? *Progress in Photovoltaics: Research and Applications*, 20(6):717–726.

Remund, J. and Kunz, S. (1997). *METEONORM: Global meteorological database for solar energy and applied climatology*. Meteotest.

Smets, A., Jager, K., Rene Van Swaaij, O. I., and Zeman, M. (2016). *solar energy:The physics and engineering of photovoltaic conversion technologies and systems*. UIT Cambridge Ltd.

Tuv, T. Fusen. `http://www.fusen.no`.

UNION, P. (2009). Directive 2009/28/ec of the european parliament and of the council of 23âapril 2009 on the promotion of the use of energy from renewable sources and amending and subsequently repealing directives 2001/77/ec andâ2003/30/ec.

Younes, S., Claywell, R., and Muneer, T. (2005). Quality control of solar radiation data: Present status and proposed new approaches. *Energy*, 30(9):1533–1549.

Øygarden Flæten, S. Norsk solinnstråling er opptil 10 prosent høyere enn tidligere antatt.

Appendix A

Module and Inverter Information

This appendix adds further information about the components used in the PV system at ASKO. This information is available from the producers.

A.1 Modules

A.2 inverters

A.3 Cables

A.4 Module Behavior

Smart Systems
for Solar Power

IBC SOLAR

IBC EcoLine - For particulary stable output

IBC PolySol 240 CS, 245 CS, 250 CS

Solar modules made by polycrystalline silicon

Whether for single family homes, industrial roofs or open spaces - the trusted solar modules, IBC PolySol, are perfectly suited for anyone placing high demands on quality and cost efficiency. IBC SOLAR defines the most stringent specifications for components, ensuring you the best results. Thanks to the modules´ positive power tolerance and linear performance guarantee, you´ll benefit from high output and returns.

Highlights

- 10-year product warranty*
- 25 years linear power warranty*
- Positive power tolerance: -0 /+5 Wp
- Low-iron solar glass (thickness 3,2 mm) and sturdy hollow-chamber frame
- Tested according IEC 61215 for snow loads up to 5400 Pa (ca. 550 kg/m²)
- IEC 61730, application class A for system voltages up to 1000 V, protection class II
- Produced in ISO 9001 and ISO 14001 certified factories
- 100% end control with individual registration of the electrical characteristics
- Quality tested by IBC SOLAR in own laboratory with climate chambers and flasher with integrated electroluminescence measurement

CE

Figure A.1: IBC PolySol 250 CS data sheet, page 1

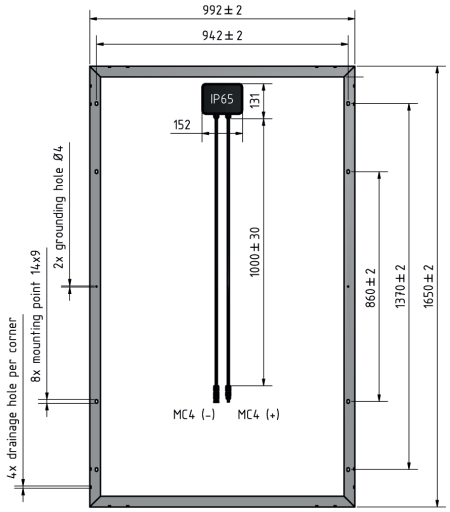

Progression of the power warranty

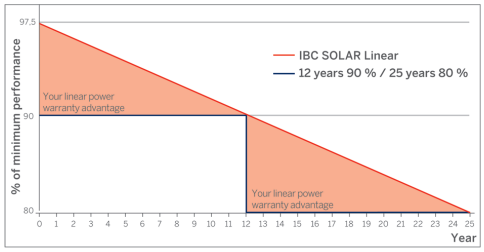

TECHNICAL DATA

IBC PolySol	240 CS	245 CS	250 CS
STC Power Pmax (Wp)	240	245	250
STC Nominal Voltage Umpp (V)	30.0	30.2	30.4
STC Nominal Current Impp (A)	8.01	8.12	8.23
STC Open circuit voltage Uoc (V)	37.2	37.4	37.6
STC Short circuit current Isc (A)	8.56	8.69	8.81
800 W/m² NOCT AM1.5 Power Pmax (Wp)	175.63	179.23	183.01
800 W/m² NOCT AM1.5 Nominal Voltage Umpp (V)	27.4	27.58	27.78
800 W/m² NOCT AM1.5 Open Circuit Voltage Uoc (V)	34.06	34.58	35.05
800 W/m² NOCT AM1.5 Short Circuit Current Isc (A)	6.84	6.88	6.92
Rel. efficiency reduction @ 200W/m² (%)	3.9	3.9	3.9
Tempcoeff Isc (%/°C)	+0.06	+0.06	+0.06
Tempcoeff Uoc (mV/°C)	-119	-119	-120
Tempcoeff Pmpp (%/°C)	-0.43	-0.43	-0.43
Module Efficiency (%)	14.7	15.0	15.3
NOCT (°C)	48	48	48
Max. System Voltage (V)	1000	1000	1000
Max. Reverse Current Ir (A)	20	20	20
Current value String fuse (A)	15	15	15
Fuse protection from parallel strings	4	4	4
Height (mm)	45	45	45
Weight (kg)	20.5	20.5	20.5
Article number	2203800001	2203800002	2203800003

2014-01-31

Presented by:

* The linear power warranty is only valid for installations within Europe and Japan. For further information, please refer to the corresponding product and power warranty in accordance with the version of the full warranty conditions received from your specialized IBC SOLAR partner at the time of installation. This warranty is valid only when the product is installed in accordance with the applicable installation instructions. Electrical values under standard test conditions: 1000W/m²; 25°C, AM1.5. 800 W/m², NOCT. Specifications according EN 60904-3 (STC). All datas according DIN EN 50380. Subject to modifications that represent progress.

IBC SOLAR AG | Am Hochgericht 10, 96231 Bad Staffelstein, Germany | Phone +49 (0) 9573 9224 0 | Fax +49 (0) 9573 - 92 24 111 | info@ibc-solar.com | www.ibc-solar.com

Figure A.2: IBC PolySol 250 CS data seet, page 2

PVSYST V6.41	IBC SOLAR AG (Germany)	21/04/16 13h54
IBC SOLAR AG does not give any warranty for the completeness and accuracy		

Characteristics of a PV module

Manufacturer, model : **IBC Solar, IBC PolySol 250 CS**

Data source : Manufacturer

File : IBC_Polysol_250_CS.PAN of 10/10/14 11h06

STC power (manufacturer)	**Pnom**	**250**	**Wp**	**Technology**		**Si-poly**	
Module size (W x L)		0.992 x 1.650	m²	Rough module area	Amodule	1.64	m²
Number of cells		1 x 60		Sensitive area (cells)	Acells	1.54	m²
Specifications for the model (manufacturer or measurement data)							
Reference temperature	TRef	25	°C	Reference irradiance	GRef	1000	W/m²
Open circuit voltage	Voc	37.6	V	Short-circuit current	Isc	8.81	A
Max. power point voltage	Vmpp	30.4	V	Max. power point current	Impp	8.23	A
=> maximum power	Pmpp	250.2	W	Isc temperature coefficient	muIsc	2.2	mA/°C
One-diode model parameters							
Shunt resistance	Rshunt	250	ohm	Diode saturation current	IoRef	122.71	nA
Serie resistance	Rserie	0.13	ohm	Voc temp. coefficient	MuVoc	-120	mV/°C
				Diode quality factor	Gamma	1.35	
Reverse Bias Parameters, for use in behaviour of PV arrays under partial shadings or mismatch							
Reverse characteristics (dark)	BRev	3.20	mA/V²	(quadratic factor (per cell))			
Number of by-pass diodes per module		3		Direct voltage of by-pass diodes		-0.7	V
Model results for standard conditions (STC: T=25°C, G=1000 W/m², AM=1.5)							
Max. power point voltage	Vmpp	30.8	V	Max. power point current	Impp	8.14	A
Maximum power	Pmpp	250.5	Wc	Power temper. coefficient	muPmpp	-0.42	%/°C
Efficiency(/ Module area)	Eff_mod	15.3	%	Fill factor	FF	0.756	
Efficiency(/ Cells area)	Eff_cells	16.3	%				

PV module: IBC Solar, IBC PolySol 250 CS

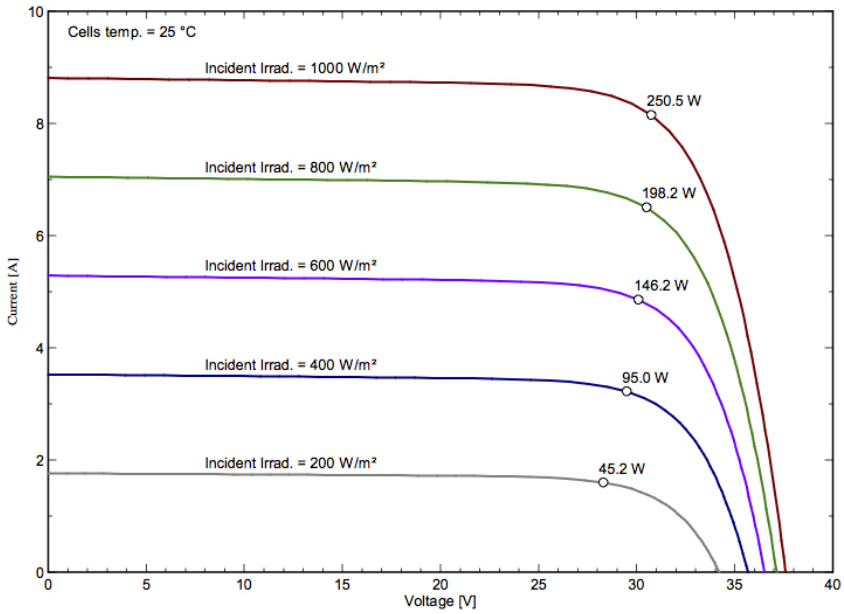

PVsyst Licensed to IBC SOLAR AG (Germany)

Figure A.3: The alternative module information received by e-mail from Bentley (l.21)

SG 15 / 20KTL

SUNGROW

Grid-friendly

- Active power continuously adjustable (0~100%)
- Reactive power control with power factor adjustment from 0.8 overexcited to 0.8 underexcited

Efficient

- Max. efficiency at 98.0%
- Film capacitor, increase system reliability
- Wide DC input voltage range, max. 1000V

Flexible

- Handy and light, easy to handle without lift machinery assistance, lower the cost of installation and maintenance
- DC switch, safe and convenient for maintenance
- Dual MPPT

Qualified

- TÜV, CE, DK5940, G59/2, AS4777, BDEW, VDE AR N 4105, CGC certified, compliance with Italian medium voltage grid requirement

Efficiency Curve

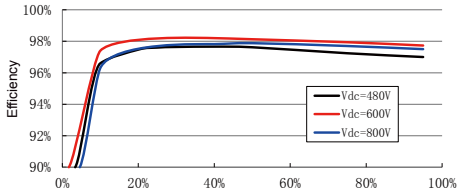

Figure A.4: The Sungrow 20KTL inverter - page 1

SUNGROW www.sungrowpower.com

Input Side Data	SG 15KTL	SG 20KTL
Max. PV input power	15800W (7900W/7900W)	21000W (10500W/10500W)
Max. PV input voltage	1000V	
Startup voltage	270V	300V
Nominal input voltage	650V	
MPP voltage range	250~950V	280~950V
MPP voltage range for nominal power	380~800V	480~800V
No. of MPPTs	2	
Max. number of PV strings per MPPT	3	
Max. PV input current	40A(20A/20A)	42A(21A/21A)
Max. current for input connector	10A	
Output Side Data		
Nominal AC output power	15000W	20000W
Max AC output power (PF=1)	16700W	22200W
Max. AC output apparent power	16700VA	22200VA
Max. AC output current	25A	33A
Nominal AC voltage	3/N/PE, 230/400Vac	
AC voltage range	310~480Vac	
Nominal grid frequency	50Hz	
Grid frequency range	47~53Hz	
THD	< 3 % (nominal power)	
DC current injection	<0.5 %In	
Power factor	>0.99@default value at nominal power, adj. 0.8 overexcited~0.8 underexcited	
Protection		
Anti-islanding protection	Yes	
LVRT	Yes	
DC reverse connection protection	Yes	
AC short circuit protection	Yes	
Leakage current protection	Yes	
DC switch	Yes	
DC fuse	No	
Overvoltage protection	Varistors	
System Data		
Max. efficiency	98.00%	
Max. European efficiency	97.30%	
Isolation method	Transformerless	
Ingress protection rating	IP65(Fan IP55)	
Night power consumption	<1W	
Operating ambient temperature range	-25~60℃(>45℃ derating)	
Allowable relative humidity range	0~100%, no condensing	
Cooling method	Smart forced air cooling	
Max. operating altitude	4000m (>2000m derating)	
Display	Graphic LCD	
Communication	RS485 (RJ45 connector)	
DC connection type	MC4	
AC connection type	Plug and play connector	
Certification	EN62109-1, EN62109-2, EN61000-6-2, EN61000-6-3, VDE0126-1-1, CEI-021, C10/C11, EN50160, RD1669, IEC61727, UTE C 15-712-1, EN50438, AS/NZS3100, AS4777.2, AS4777.3, G59/2, VDE-AR-N-4105, BDEW, CGC	EN62109-1, EN62109-2, EN61000-6-2, EN61000-6-3, VDE0126-1-1, CEI-021, AS/NZS3100, AS4777.2, AS4777.3, VDE-AR-N-4105, BDEW, CGC
Mechanical Data		
Dimensions (W*H*D)	648*686*246mm	
Mounting method	Wall bracket	
Weight	50kg	55kg

Circuit Diagram

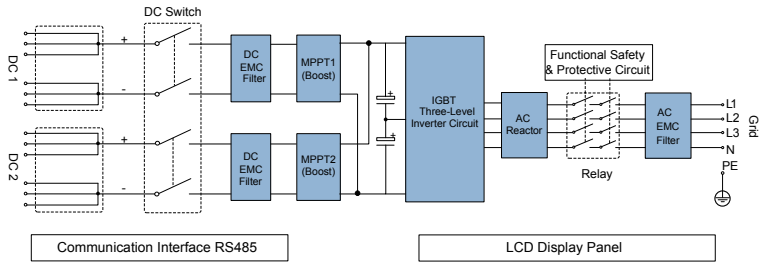

Figure A.5: The Sungrow 20KTL inverter - page 2

SG 30KTL-M/SG40KTL

SUNGROW

Flexible

- Handy and light, easy to handle without lift machinery assistance, lower the cost of installation and maintenance
- Integrated DC combine and surge protection function, lower the system cost
- DC switch, safe and convenient for maintenance
- Dual MPPT

Efficient

- Max. efficiency at 98.3%
- Wide DC input voltage range, max. 1000V

Qualified

- TÜV, CE, DK5940, G59/2, AS4777, BDEW, VDE AR N 4105, CGC certified, compliance with Italian medium voltage grid requirement

Grid-friendly

- Active power continuously adjustable (0~100%)
- Reactive power control with power factor adjustment from 0.8 overexcited to 0.8 underexcited

Photon International A www.photon.info

Photon International A www.photon.info

Efficiency Curve

SG 30KTL-M

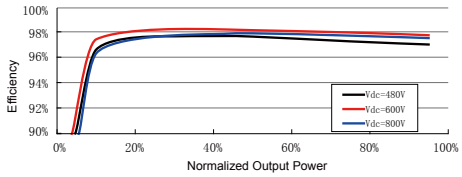

SG 40KTL

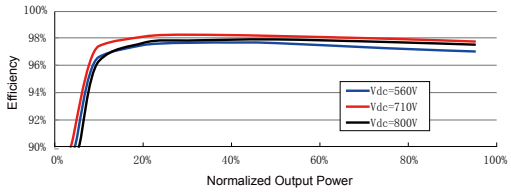

Figure A.6: The Sungrow 30KTL inverter - page 1

SUNGROW www.sungrowpower.com

Input Side Data	SG 30KTL-M	SG 40KTL
Max. PV input power	32000W (16000W/16000W)	40500W (20250W/20250W)
Max. PV input voltage	1000V	
Startup voltage	300V	
Nominal input voltage	620V	710V
MPP voltage range	280~950V	
MPP voltage range for nominal power	480~800V	560~800V
No. of MPPTs	2	
Max. number of PV strings per MPPT	5	4
Max. PV input current	66A (33A/33A)	
Max. current for input connector	12A	
Output Side Data		
Nominal AC output power	30000W	36000W
Max AC output power (PF=1)	30000W	39800W
Max. AC output apparent power	33120VA	39800VA
Max. AC output current	48A	
Nominal AC voltage	3/N/PE, 230/400Vac	3/N/PE, 277/480Vac
AC voltage range	310~480Vac	422~528Vac
Nominal grid frequency	50Hz/60Hz	
Grid frequency range	47~53Hz/57~ 63Hz	
THD	< 3 % (nominal power)	
DC current injection	<0.5 %In	
Power factor	>0.99@default value at nominal power, adj. 0.8 overexcited~0.8 underexcited	
Protection		
Anti-islanding protection	Yes	
LVRT	Yes	
DC reverse connection protection	Yes	
AC short circuit protection	Yes	
Leakage current protection	Yes	
DC switch	Yes	
DC fuse	Yes	
Overvoltage protection	Type II DIN rail surge arrester	Type II DIN rail surge arrester (40KA)
System Data		
Max. efficiency	98.30%	
Max. European efficiency	98.00%	
Isolation method	Transformerless	
Ingress protection rating	IP65 (Fan IP55)	
Night power consumption	<1W	
Operating ambient temperature range	-25~60℃ (>45℃ derating)	
Allowable relative humidity range	0~100%, no condensing	
Cooling method	Smart forced air cooling	
Max. operating altitude	4000m (>3000m derating)	
Display	Graphic LCD	
Communication	RS485 (RJ45 connector)	
DC connection type	MC4	
AC connection type	Clamping yoke connector	
Certification	VDE0126-1-1, EN62109-1, EN62109-2, G59/2, CEI-021, AS/NZS 3100, AS4777.2, AS4777.3, VDE-AR-N-4105, BDEW	
Mechanical Data		
Dimensions (W*H*D)	634*820*257mm	
Mounting method	Wall bracket	
Weight	65kg	

Circuit Diagram

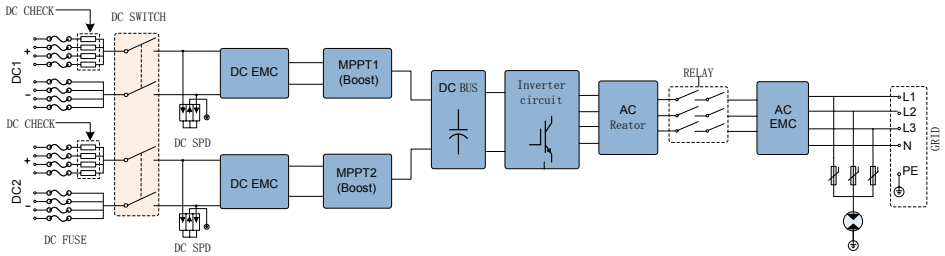

Figure A.7: The Sungrow 30KTL inverter - page 2

IBC SOLAR

CABLES FOR PHOTOVOLTAICS

FlexiSun® 2.5, 4, 6, 10, 16 mm² PV1-F

PRODUCT ADVANTAGES:

For use indoors, outdoors, in explosive areas, and in industrial, commercial, and agricultural applications

Can also be installed:
- underground
- in electrical installation pipes
- on, inside, and under plaster
- in electrical installation ducts
- in equipment

Suitable for use inside and connected to insulated equipment (protection class II)

VDE-tested (VDE reg. no. 8026)

TÜV 2 PfG 1169/08.2007, cert. no. R 60014271

For moveable, suspended or fixed installation in photovoltaic systems at temperatures ranging from −40 °C to +120 °C

Max. ambient temperature up to +120 °C (moveable and fixed)
Designed according to IEC 60216: constant temperature 120 °C = 20,000 h (= 2.3 years), constant temperature max. 90 °C = 30 years

Pollution- and halogen-free

Improved fire-resistant performance

Ammonia resistance

UV and ozone resistant

Protected against short circuits and ground leakages

VDE
REG.-Nr. 8026

www.tuv.com TÜV TÜV Rheinland Group ID: 0000007806

Figure A.8: Cable characteristics. Page 1

TECHNICAL DATA

Electrical parameters	
Nominal voltage (AC)	U0/U 0.6/1.0 kV
Max. PV system voltage (DC)	1.8 kV
Max. permitted operating voltage (AC)	0.7/1.2 kV conductor-ground/conductor-conductor
Max. permitted operating voltage (DC)	0.9/1.8 kV conductor-ground/conductor-conductor
Test voltage (AC/DC)	6 kV/10 kV (test duration 15 min.)
Current carrying capacity	According to requirements for cables for PV systems DKE/VDE AK 411.2.3
Tests	According to DIN VDE 0282 part 2, HD 22.2 and EN 50395 conductor resistance, AC and DC voltage test, dielectric strength, surface resistance, spark test, leakage resistance at 20 °C and 90 °C in water and at 120 °C in air. EN 50305 section 6, DC resistance (10 days, 85 °C in saltwater, 1.5 kV DC)
Thermal parameters	
Ambient temperature	−40 °C to +120 °C (moveable and fixed), designed according to IEC 60216: constant temperature 120 °C = 20,000 h (2.3 years), constant temperature max. 90 °C = 30 years
Short circuit temperature	+250 °C (max. 5 sec on conductor)
Low-temperature resistance	Cold bending and elongation according to EN 60811-1-4, cold impact according to EN 50305
Damp / heat test	According to EN 60068-2-78, 1,000 h at 90 °C and 85 % humidity
Mechanical parameters	
Tensile load	15 N/mm² in use, 50 N/mm² during installation
Bending radius	See table
Abrasion	Emery paper (int. test according to DIN 53516), sheath to sheath (int. test), sheath to metal (int. test), sheath to plastic (int. test)
Shore hardness	85 (int. test according to DIN 53505)
Rodent resistant (martens)	For absolute safety, use protective hoses or cables with metallic sheathing such as web covering or braided sleeving
Resistance to external influences	
Resistance to petroleum	24 h, 100 °C (int. test according to DIN VDE 0473 811-2-1, DIN EN 60811-2-1)
Ozone resistance	Test according to DIN EN 50396, HD 22.2 test type B
UV resistance	Test according to UL 1581 (xeno-Test), ISO 4892-2 (meth. 1), HD 605/A1-2.4.20
Acid and base resistance	According to EN 60811-2-1, 7 days, 23 °C (N oxalic acid, N sodium hydroxide solution)
Ammonia resistance	30 days saturated ammonia atmosphere (int. test)
Water absorption (gravimetric)	Int. test according to DIN EN 60811-1-3 and DIN VDE 0473-811-1-3
Reaction to fire	
Flame spread, individual cable	DIN EN 60332-1-2 and DIN VDE 0482 part 332-1-2
Flame spread, bundle of cables	Int. test according to DIN EN 50305-9 and DIN VDE 0482 part 266-2-5
Smoke emission, light transmission >70 %	Int. test according to DIN EN 50268-2 and DIN VDE 0482 part 268-2
Low corrosiveness	DIN EN 50264-1
Low toxicity	Int. test according to DIN EN 50305 (ITC index less than 3)
Ecological safety measures	Have been taken concerning recycling and disposal as well as energy-saving production (free of pollutants and halogen; no environmentally harmful pollutants are released during thermal recycling)
Design criteria	
Conductor	Electrolytic copper, tin-plated, class 5 according to IEC 60228 (DIN VDE 0295)
Insulation	Halogen-free, heat- and ozone-resistant, special mixture of cross-linked hard ethylene propylene rubber-based elastomer (HEPR) 120 °C according to IEC 60502-1, (mixture type EI6/EI8)
Sheath	Halogen-free, heat- and cold-resistant, special mixture of cross-linked ethylene vinyl acetate-based elastomer (EVA). Ozone-, UV-, oil-, and chemical-resistant. According to HD 22.1 (mixture type EM4/EM8)
Labeling	IBC FlexiSun® (cross section) PV1-F 0.6/1 kV, VDE reg. no. 8026/TÜV cert. R 60014271

Nominal cross section	mm²	**2.5**	**4**	**6**	**10**	**16**
Conductor diameter	mm	1.9	2.4	2.9	4.0	5.5
Outer diameter (minimum)	mm	4.9	5.2	5.7	6.8	8.3
Outer diameter (maximum)	mm	5.1	5.6	6.1	7.2	9.0
Net cable weight. approximate	kg/km	43	58	77	120	178
Min. bending radius	mm	15	17	18	22	36
Max. permissible tensile load	N	38	60	90	150	240
Max. current load at 60 °C	A	41	55	70	98	132
Permitted short circuit current (1 sec)	kA	0.32	0.50	0.76	1.26	2.01
Item numbers		7000202003	7000202004	7000202006	7000202010	7000202016

Subject to technical changes for further improvements.

www.ibc-solar.com IBC SOLAR AG • Am Hochgericht 10 • 96231 Bad Staffelstein, Germany • Phone +49 (0)9573-92 24 0

Figure A.9: Cable characteristics. Page 2

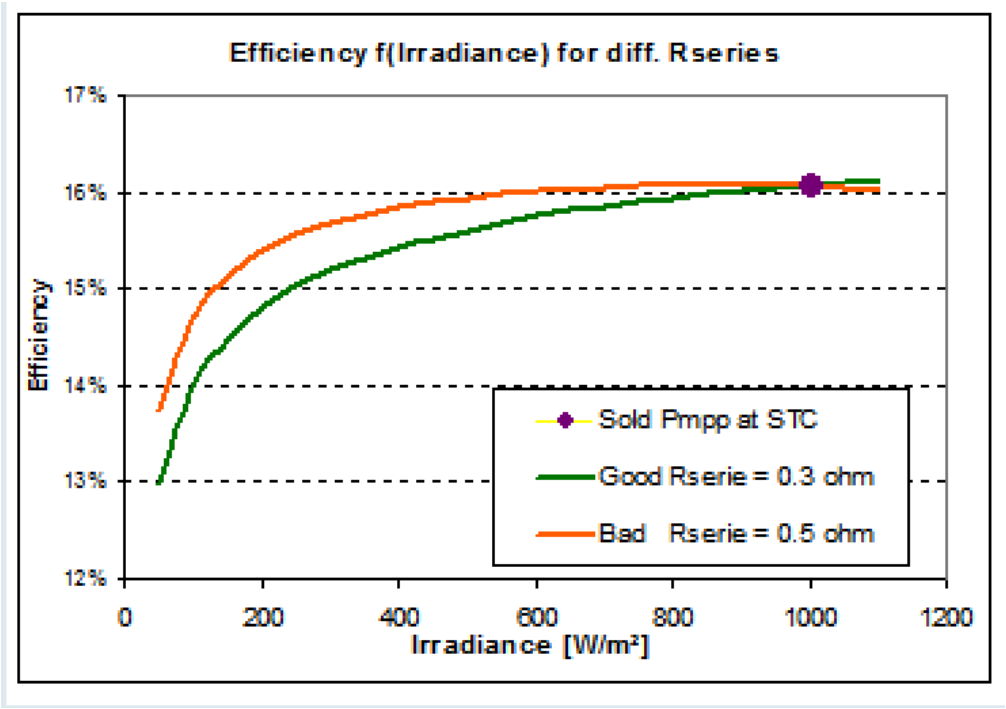

(a) Series resistance as a function of irradiation

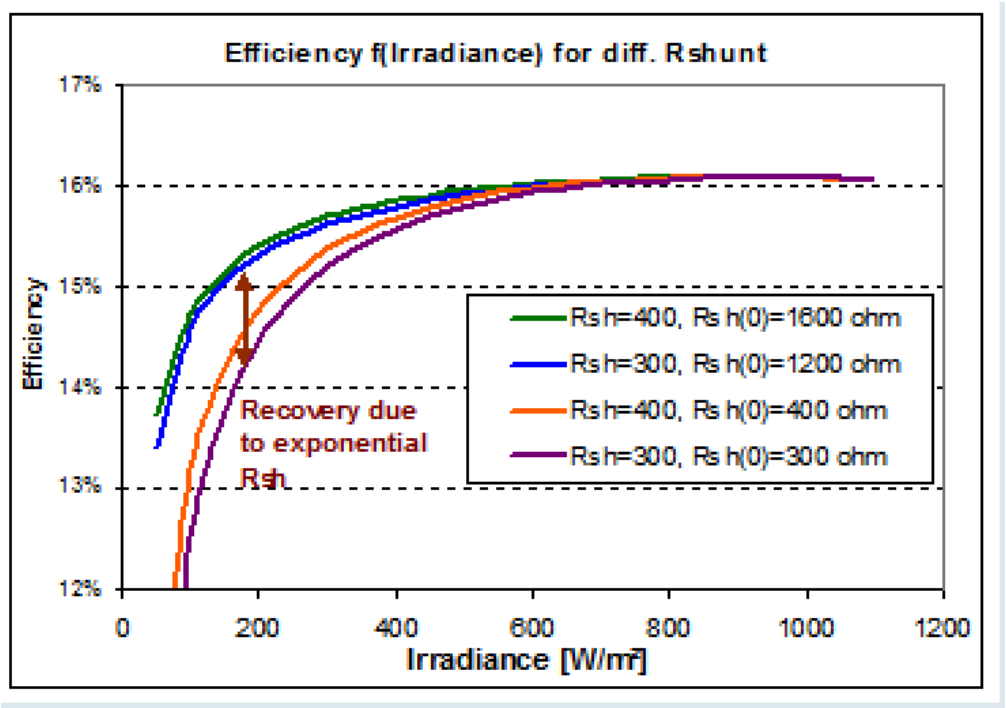

(b) Shunt resistance as a function of irradiation

Figure A.10: Module efficiency as function of irradiation. Low light performance is increased with decreasing irradiation for higher series resistance and lower shunt resistance.

Appendix B

Simulation Results

B.1 Scenario 1 and 2 Simulation Results

Monthly simulation results from PVsyst.

Table B.1: Scenario 1 results

Scenario 1	**Actual data**		**Meteonrom**		**Meteocontrol**		**ASKO**		**Ås**	
Date	Energy (kWh)	Irradiation (kWh/m²)	Energy (kWh)	GHI (kWh/m²)	Energy (kWh)	GHI (kWh/m²)	Energy (kWh)	GHI (kWh/m²)	Energy (kWh)	GHI (kWh/m²)
Jan	968	8,98	2926	10,30	2357	8,40	2380	8,30	2790	9,80
Feb	4267	21,19	8618	27,20	5927	19,30	6290	20,70	6920	22,60
Mar	17979	65,43	22846	70,50	19141	59,50	20520	65,00	21720	67,90
Apr	41077	129,22	32545	102,40	36837	115,20	40260	128,90	41370	130,40
May	45853	142,29	48957	157,30	40817	131,60	43260	142,00	43790	141,80
June	56183	180,03	50583	165,70	52459	171,70	54140	179,90	54730	179,90
Jul	51627	164,69	49235	163,10	48565	161,60	48770	164,50	50470	168,30
Aug	41875	135,17	38730	127,50	40469	134,60	40070	134,80	41780	139,00
Sept	23486	74,87	23636	77,40	23369	76,60	22460	74,40	23510	76,90
Oct	12440	41,59	10446	34,30	13514	43,80	12440	41,10	13090	42,90
Nov	3100	13,77	3318	11,70	4414	15,20	3720	13,00	4230	14,90
Dec	1099	5,57	1576	6,10	1663	6,40	1290	4,70	1600	6,40

Table B.2: Scenario 2 results

Scenario 2	Actual data		Meteonrom		Meteocontrol		ASKO		Ås	
Date	Energy (kWh)	Irradiation (kWh/m²)	Energy (kWh)	GHI (kWh/m²)	Energy (kWh)	GHI (kWh/m²)	Energy (kWh)	GHI (kWh/m²)	Energy (kWh)	GHI (kWh/m²)
Jan	968	8,98	2933	10,30	2357	8,40	2500	8,30	2760	9,80
Feb	4267	21,19	8620	27,20	5927	19,30	6430	20,70	6870	22,60
Mar	17979	65,43	22850	70,50	19141	59,50	20790	65,00	21440	67,90
Apr	41077	129,22	32548	102,40	36837	115,20	40820	128,90	41150	130,40
May	45853	142,29	48960	157,30	40817	131,60	43680	142,00	44620	141,80
June	56183	180,03	50585	165,70	52459	171,70	54270	179,90	55120	179,90
Jul	51627	164,69	49237	163,10	48565	161,60	49230	164,50	51060	168,30
Aug	41875	135,17	38732	127,50	40469	134,60	40410	134,80	41950	139,00
Sept	23486	74,87	23639	77,40	23369	76,60	22730	74,40	23610	76,90
Oct	12440	41,59	10449	34,30	13514	43,80	12660	41,10	12860	42,90
Nov	3100	13,77	3324	11,70	4414	15,20	3870	13,00	4080	14,90
Dec	1099	5,57	1586	6,10	1663	6,40	1380	4,70	1480	6,40

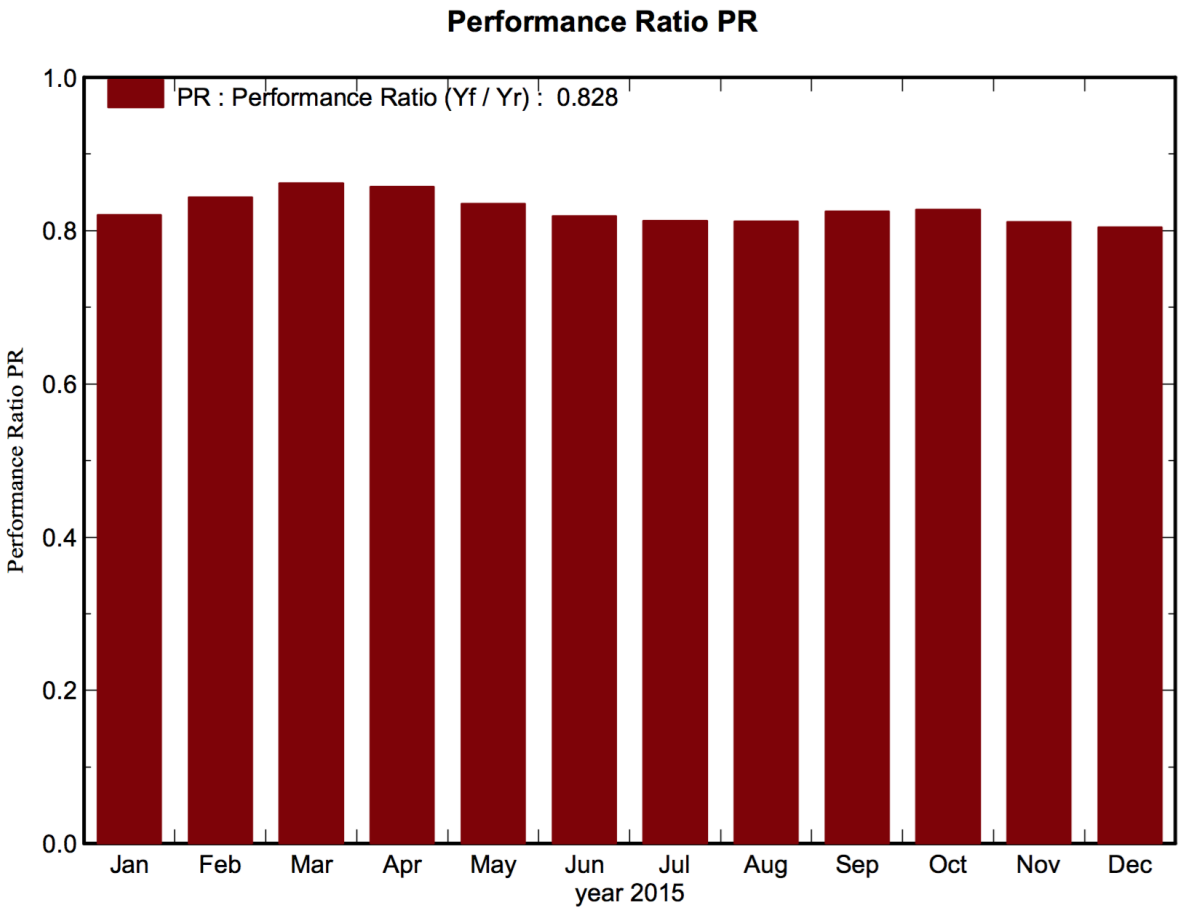

Figure B.1: Excerpt from PVsyst presenting monthly performance ratio with ASKO meteo data for scenario 2.

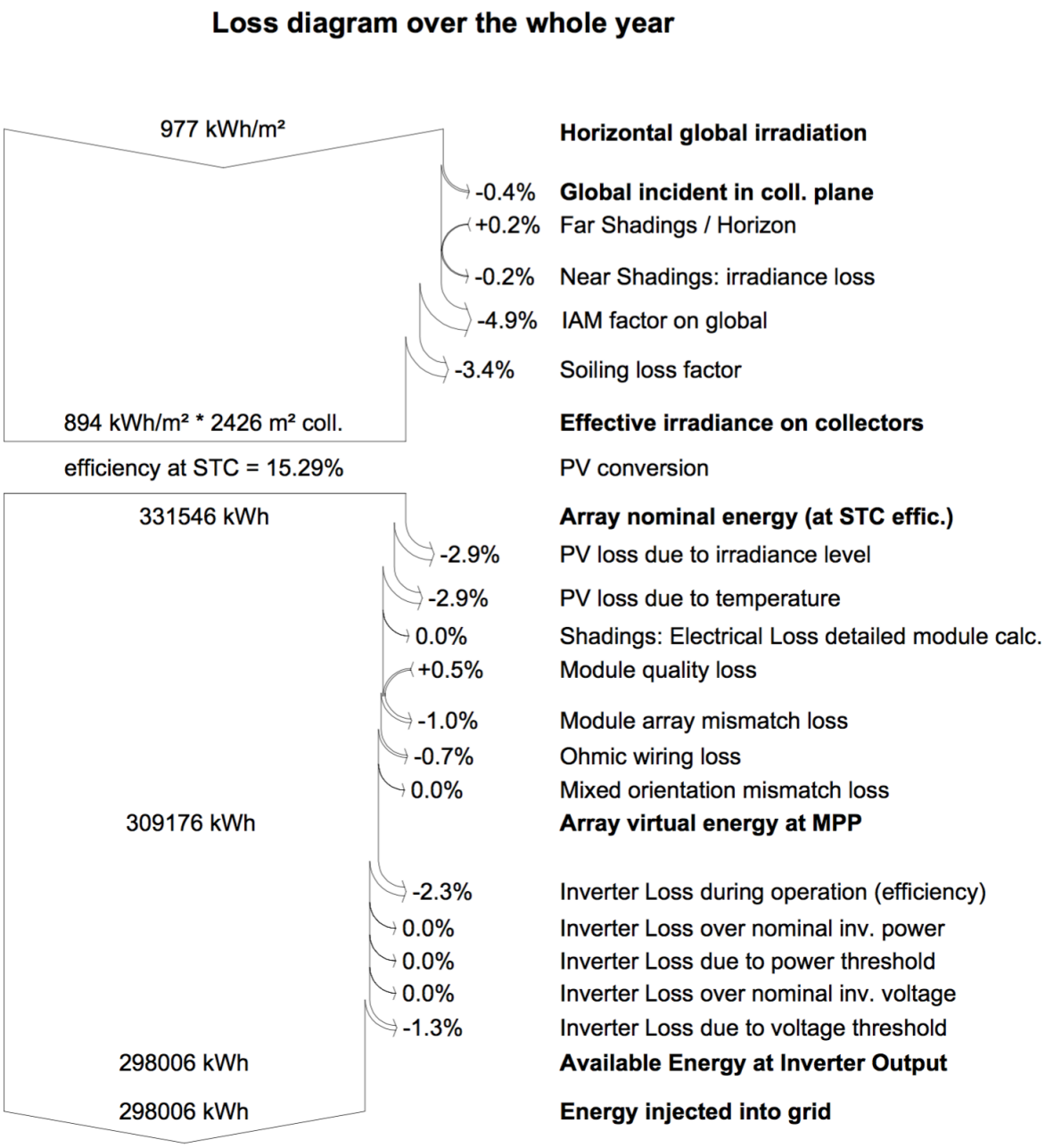

Figure B.2: Loss diagram for the experimental soiling levels based upon scenario 2 with ASKO meteo.

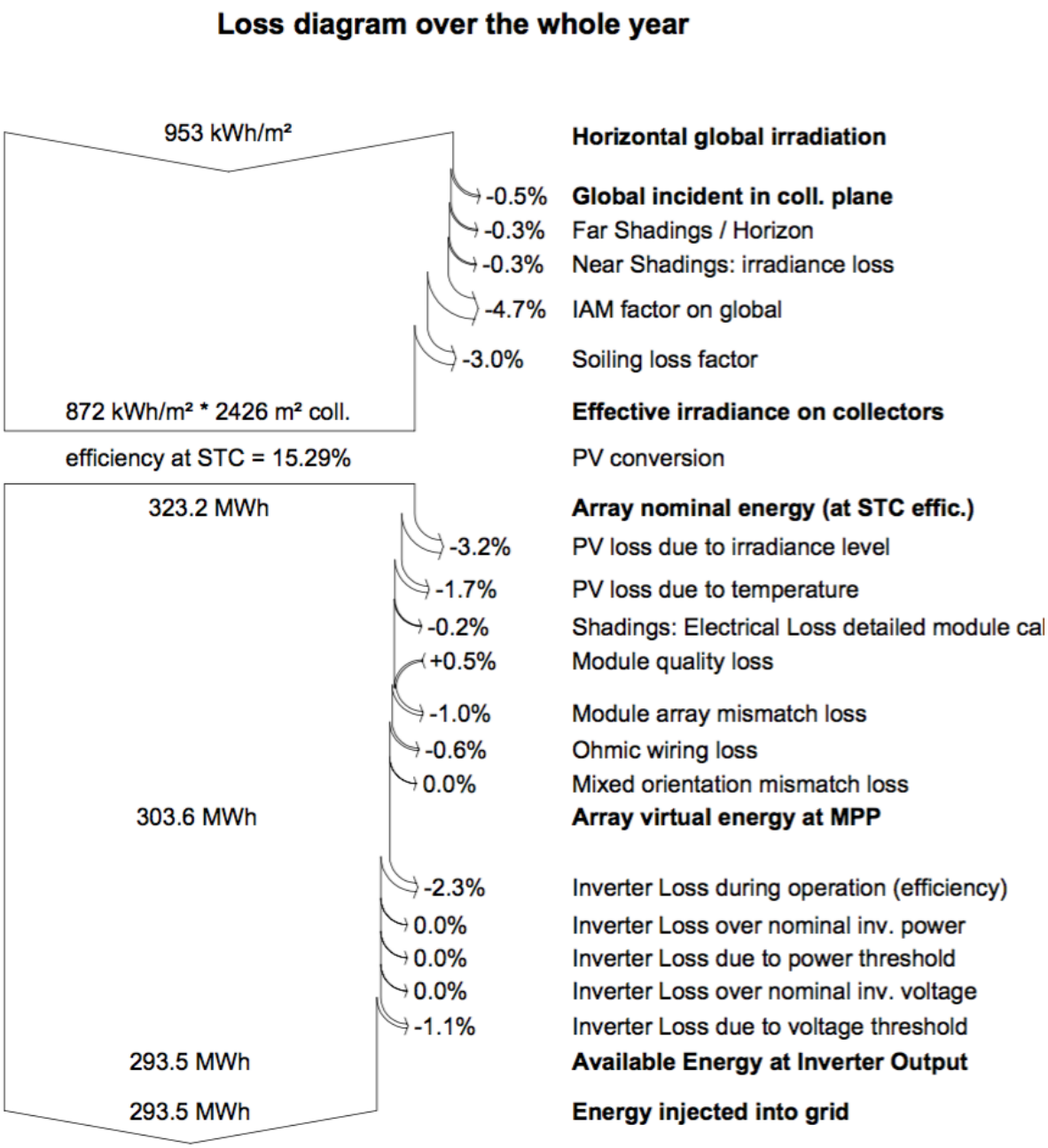

Figure B.3: Excerpt of the loss diagram from a scenario 2 simulation with Meteonorm meteo data.

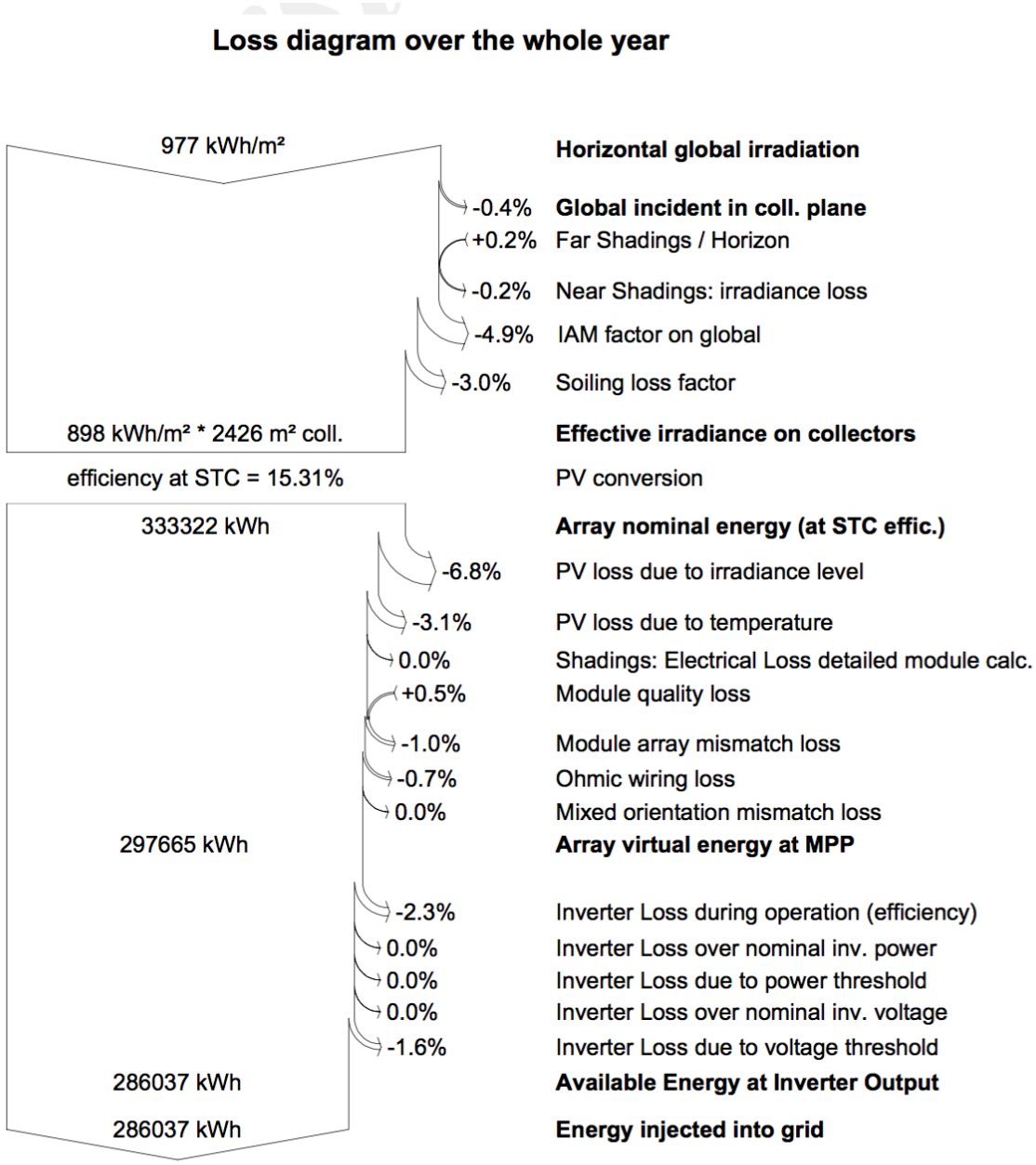

Figure B.4: Loss diagram for scenario 2 with ASKO meteo data and the new module resistance and short circuit current information. The loss factor that emerges compared to the other loss diagrams presented is the high PV loss due to irradiation level.

B.2 Other Simulation Parameters and Results

Table B.3: Experimental soiling values derived from snow data and the results presented in the combined scenarios based upon the alternative module characteristics. The decrease in predicted energy with new information due to higher losses, resulted in an underestimate during winter months. The experimental soiling values were experimentally derived to account for snow losses and can thus be be adjusted.

Date	Jan	Feb	Mar	Apr	May	Jun	Jul	Aug	Sep	Okt	Nov	Dec
Soiling: snow fraction (%)	50	29	14	3	1	1	1	1	1	3	16	16

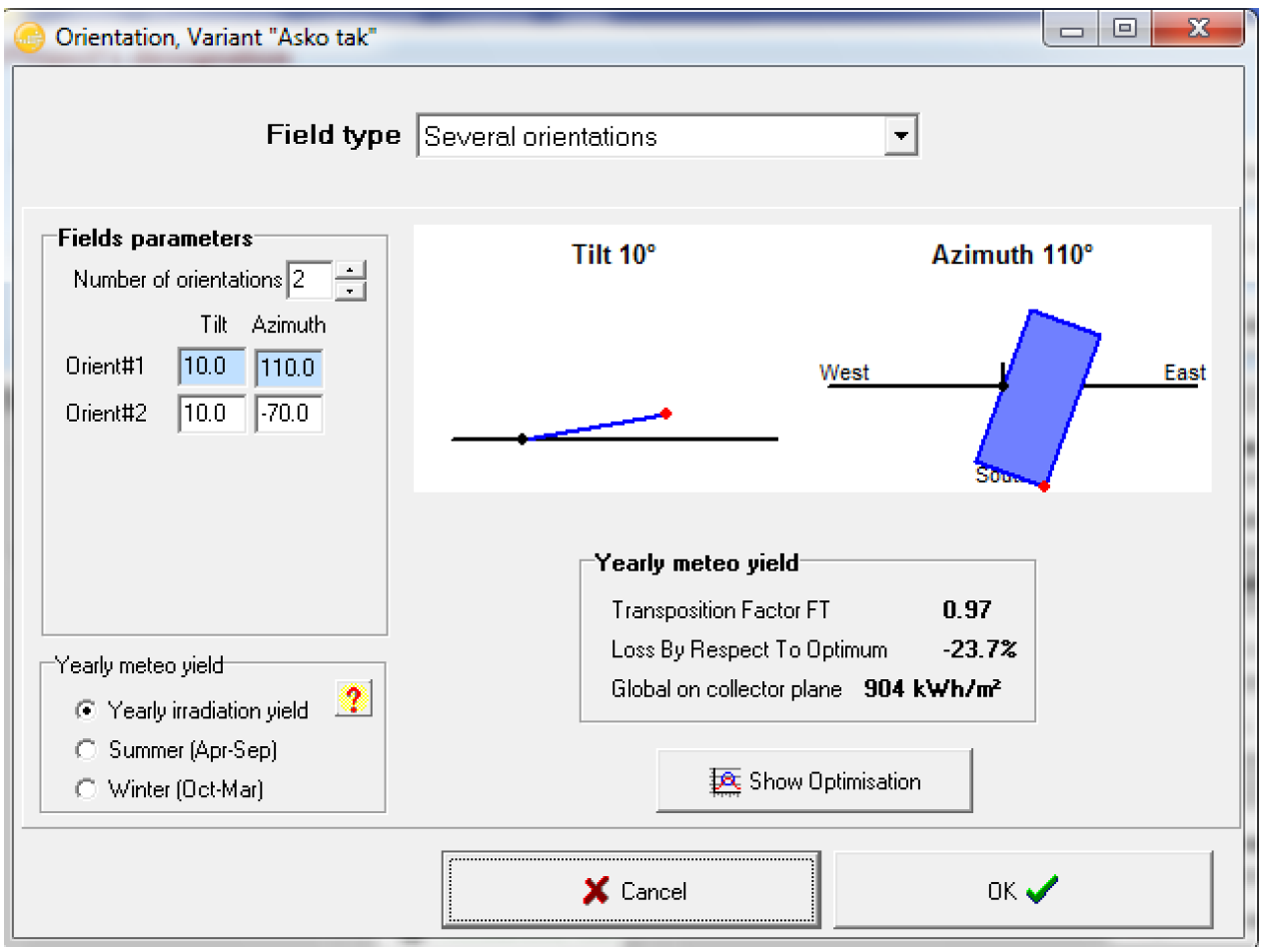

Figure B.5: Excerpt from PVsyst displaying the tilt and orientation of the modules.

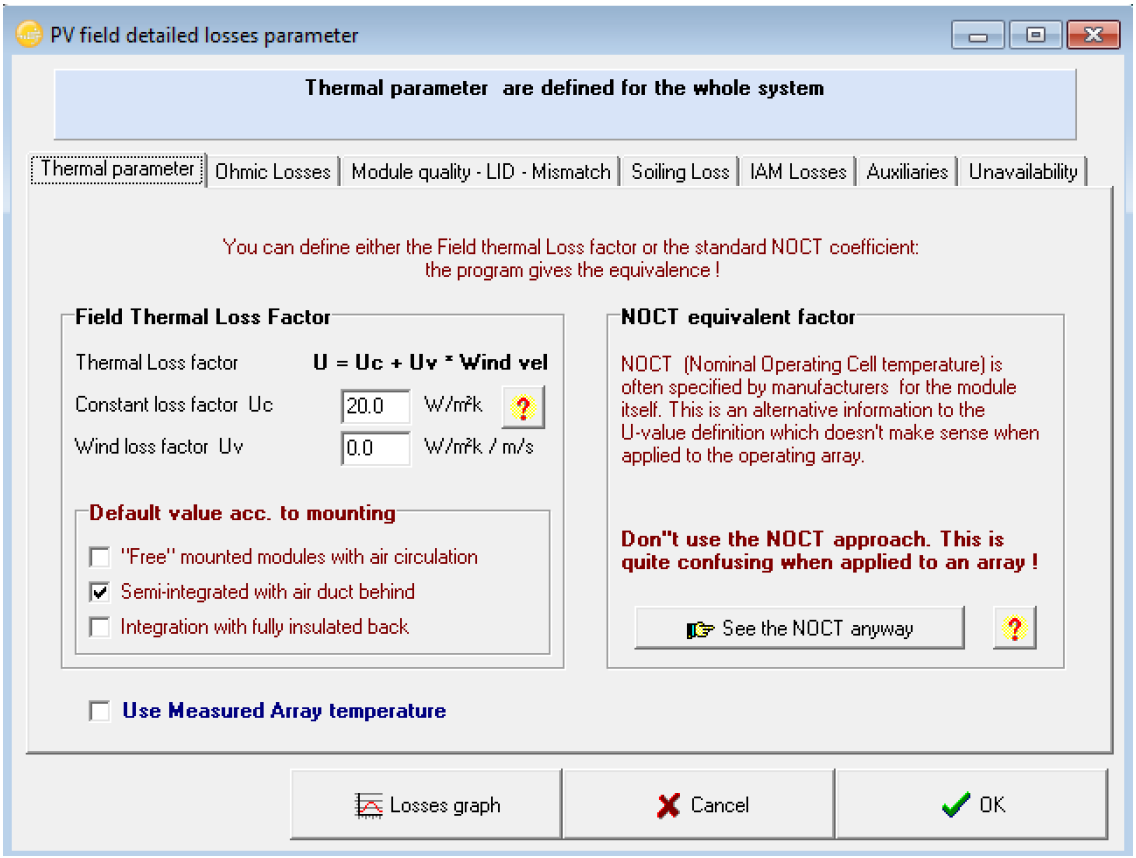

Figure B.6: Excerpt from PVsyst that shows the detailed losses window. The window includes several tabs, each related to a loss parameter that can be adjusted.

Appendix C

Further Information

meteo control
Energy & Weather Services

meteocontrol GmbH | Spicherer Straße 48 | D-86157 Augsburg

phone +49-(0)-821-34666-23 fax +49-(0)-821-34666-11
e-mail data-order@meteocontrol.de web www.meteocontrol.de

Order sheet meteo data

Valid from: August 2015

Insolation data for any chosen point worldwide

Very accurate insolation data is essential for planning and review of solar plants. meteocontrol provides you with quarter-hourly[1], hourly, daily, monthly or annual values for almost any chosen point worldwide with the utmost precision.

The temporal availability of our data depends upon the corresponding weather satellite. Thus, the starting point of our time series varies from continent to continent.

Europe: 1995 – today
Africa: 1994 – today
America: 2000 – today
Asia: 1999 – today
Other regions: availability will be provided upon request

Depending on the specific site, meteocontrol generates the requested data in cooperation with scientists of *Universität Oldenburg* (sites within Europe) or in collaboration with specialists from *Ciemat* (sites outside of Europe) without utilization of statistical procedures that depend on random values. Basis are always highly resolved satellite images originating from the corresponding weather-satellites.

State-of-the-art scientific models (Heliosat-Method) allow for already defining diffuse insolation through the insolation model itself. meteocontrol is therefore able to provide exact values of diffuse and direct insolation as well as horizontal insolation data. If needed, we do also calculate the insolation on any given module plane or values of direct normal insolation (DNI).

As we provide insolation data on the point, we just need the exact geographic coordinates of your site. Alternatively you can send us the corresponding address or postal code.

Insolation data combined with temperature data for precise site analyses

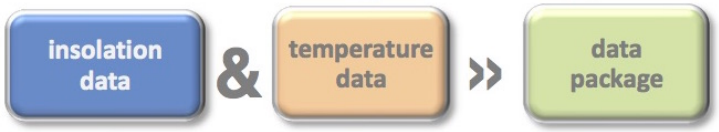

Sometimes reliable temperature data is necessary to evaluate a certain site in detail. For this purpose we offer high quality temperature data. The values are created for any given point worldwide using NCEP reanalysis (CFSR / CFSV2).

Figure C.1: The order sheet available at Meteocontrol.com

meteo control
Energy & Weather Services

Proven Reliability

Satellite data of meteocontrol were compared with numerous scientific analyses of chosen reference ground measurement stations. All of them achieve the same result: the exact coordinate data retrieval ensures a continual precision of data without losses by statistical interpolations.

- rRMSE hourly values[2]: 14.5%
- rRMSE daily values[2]: 7.5%
- rRMSE monthly values[2]: 3.6%
- rBIAS[2]: 1.5%

[2] *Values referring to sites within Europe. Reference: Kemper et. Al. 2008*

Flexible price structure for maximised customer satisfaction

Our clear price structure allows for easy comprehension of prices for the customer at each step. Changes of orders can be implemented fast and easy without much time and effort. Highest flexibility is provided by the possibility of data orders down to the month[2]. Thus, only the necessary data has to be ordered.

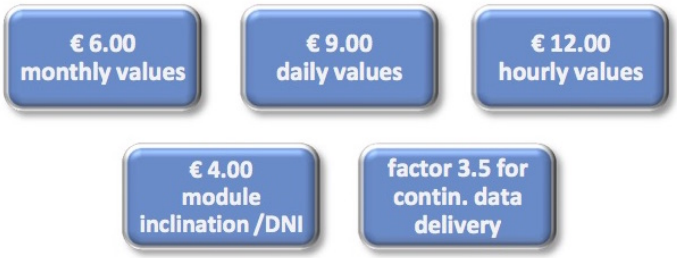

Scope of services

- Global, diffuse, and direct insolation data
- Historical time series of data
- Different temporal resolutions (quarter-hourly[1], hourly, daily, monthly or annual values)
- Conversion of data to module inclination, calculation of direct normal insolation (DNI)
- Long-time mean values
- Insolation maps with long-time mean values for Europe as well as separate European countries

Your benefits

- High-resolution regional satellite data for almost any possible point worldwide
- No data gaps
- Retrieveable for any possible coordinate – irrespective of ground measurement stations
- Actual (quarter-[1])hourly values from satellite data
- Easy order and fast delivery of data

Figure C.2: The order sheet available at Meteocontrol.com

Norwegian University
of Life Sciences

Postboks 5003
NO-1432 Ås, Norway
+47 67 23 00 00
www.nmbu.no